University of Stavanger

Faculty of Science and Technology

MASTER'S THESIS

Study program/ Specialization: Petroleum Geosciences Engineering	Spring semester, 2019 Open
Writer: Sofie Knutdatter Arntzen	Sofie K. Arntzen ………………………………………… (Writer's signature)
Faculty supervisor: Nestor Cardozo, University of Stavanger External supervisor: Tore Skar, Suncor Energy A/S	
Thesis title: Tectonic evolution of the Marulk Basin and adjacent highs, northern North Sea	
Credits (ECTS): 30	
Key words: *Marulk Basin* *Tampen Spur* *Structural evolution* *Rift evolution*	Pages: 86 Stavanger, 14th June 2019

Tectonic evolution of the Marulk Basin and adjacent highs, northern North Sea

By

Sofie Knutdatter Arntzen

MSc Thesis

Presented to the Faculty of Science and Technology
University of Stavanger

University of Stavanger
June 2019

Acknowledgement

Firstly, I want to thank my thesis advisor at Suncor Energy Norge A/S, Tore Skar, for his guidance, sharing of ideas and support throughout this thesis study. I would also like express my gratitude to Professor Nestor Cardozo, for valuable feedback and comments.

Secondly, I want to thank Suncor Energy Norge A/S for providing me the data, facilities and guidance making this thesis possible. A special thanks also goes to colleagues in Suncor Energy, for the knowledge and discussions you have shared with me the past two years.

Abstract

The Marulk Basin is located in the northern North Sea, at the boarder towards the Mid-Norwegian Margin. The geological evolution of the Marulk Basin has received limited attention in the literature, and thus, the main motivation of this thesis study is to improve the geological understanding of this marginal area of the northern North Sea. Interpretation of 3D seismic data combined with regional 2D seismic lines and exploration wells are used to assess the tectonic evolution of the Marulk Basin with adjacent highs and put it into a regional context with regards to the northernmost propagation of the North Sea rift system. The northern part of the North Sea rift system (Viking Graben) was affected by two main extensional events; the Permo - Triassic and the middle Jurassic-early Cretaceous event with continued fault activity into the early Cretaceous. Interpretation of geological cross-sections and analysis of thickness maps shows thickness variations of the pre-rift, syn-rift and post-rift successions between the Viking Graben basins and the north-westerly basins. Basin-bounding faults become progressively younger towards the northwest thereby reflecting a northwestward shift in depocenter development from Jurassic to Cretaceous times. The Marulk Basin and the adjacent highs are bounded by large (first-order) normal faults having geometries varying from steeply dipping planar faults to listric and ramp-flat-ramp fault plane geometries. The NNE-SSW first-order faults are interpreted to be of Permo-Triassic origin, while the NE-SW trending faults are more likely to originate from the middle Jurassic-early Cretaceous rift event. The Marulk Basin and adjacent highs are further separated by smaller (second-order) normal faults showing greater variation in trend and origin. Faults related to the Jurassic extensional event are divided into two fault populations that are related to a middle Bathonian-early Oxfordian rift stage and a late Oxfordian-early Cretaceous rift stage. The southern end of the Marulk Basin and the Tampen Spur show a clear multiphase rift evolution, while the central and northern areas area of the Marulk Basin is mostly affected by late Jurassic- early Cretaceous extension.

Table of Content

List of Figures

List of Tables

1. Introduction

The Marulk Basin is located in the northern North Sea and is bounded by the Tampen Spur to the southeast, the Penguin Ridge and Magnus Basin to the west, and the Møre-Trøndelag Fault Complex to the north (Figure 1). The structural evolution of the northern North Sea is generally well documented (e.g., Badley et al., 1988; Ziegler, 1975; Færseth, 1996; Odinsen et al., 2000; Fazlikhani et al., 2017), and significant effort has been put into understanding the tectonostratigraphic evolution of syn-rift and post-rift (inter-rift) sedimentary architectures (Nøttvedt et al., 1995; Ravnås et al., 2000).

Petroleum exploration in the northern North Sea initiated in the early 1970s and resulted in several discoveries both in the Norwegian and British sectors. These include the major Statfjord, Snorre, Gullfaks and Troll fields in the Norwegian sector, and the Brent, Magnus and Penguin fields in the British sector (Figure 1). Due to the high density of fields, the structural configuration and evolution of the Tampen Spur area have received significant attention in the literature (e.g., Fossen and Rørnes, 1996; Dahl and Solli, 1993; Berger and Roberts, 1999; Hesthammer et al., 1999). However, published descriptions and interpretations from the adjacent Marulk Basin are limited, and its relation to the general structural development of the northern North Sea has yet to be discussed. The motivation of this thesis is to gain understanding of the structural setting and evolution of the Marulk Basin and adjacent highs

1.1 Objectives

Analysing the structural evolution of the Marulk Basin is important as it lays the foundation to further explain the spatio-temporal distribution of erosion versus deposition, rates of faulting and subsidence, paleo-topography, and paleo-depositional environments in the northern North Sea. This information can be further analysed to predict reservoir distribution, source rock maturation, trap configuration, and assess the petroleum potential in the area.

The aim of this thesis is to investigate and propose a model(s) for the structural evolution of the Marulk Basin and adjacent structural highs by performing regional 3D seismic interpretation and detailed descriptions of key seismic sections. In order to accomplish these objectives, four key objectives are defined:

- Understand how the Marulk Basin relates to the rift evolution in the northern North Sea.
- Address the structural configuration of intrabasinal highs (Mort High, Makrell Horst and Penguin Ridge).
- Compare the structural development of the Marulk Basin and intrabasinal highs with the well-studied basins and highs in the Tampen Spur area to the south.
- Propose a model(s) for the structural evolution of the Marulk Basin.

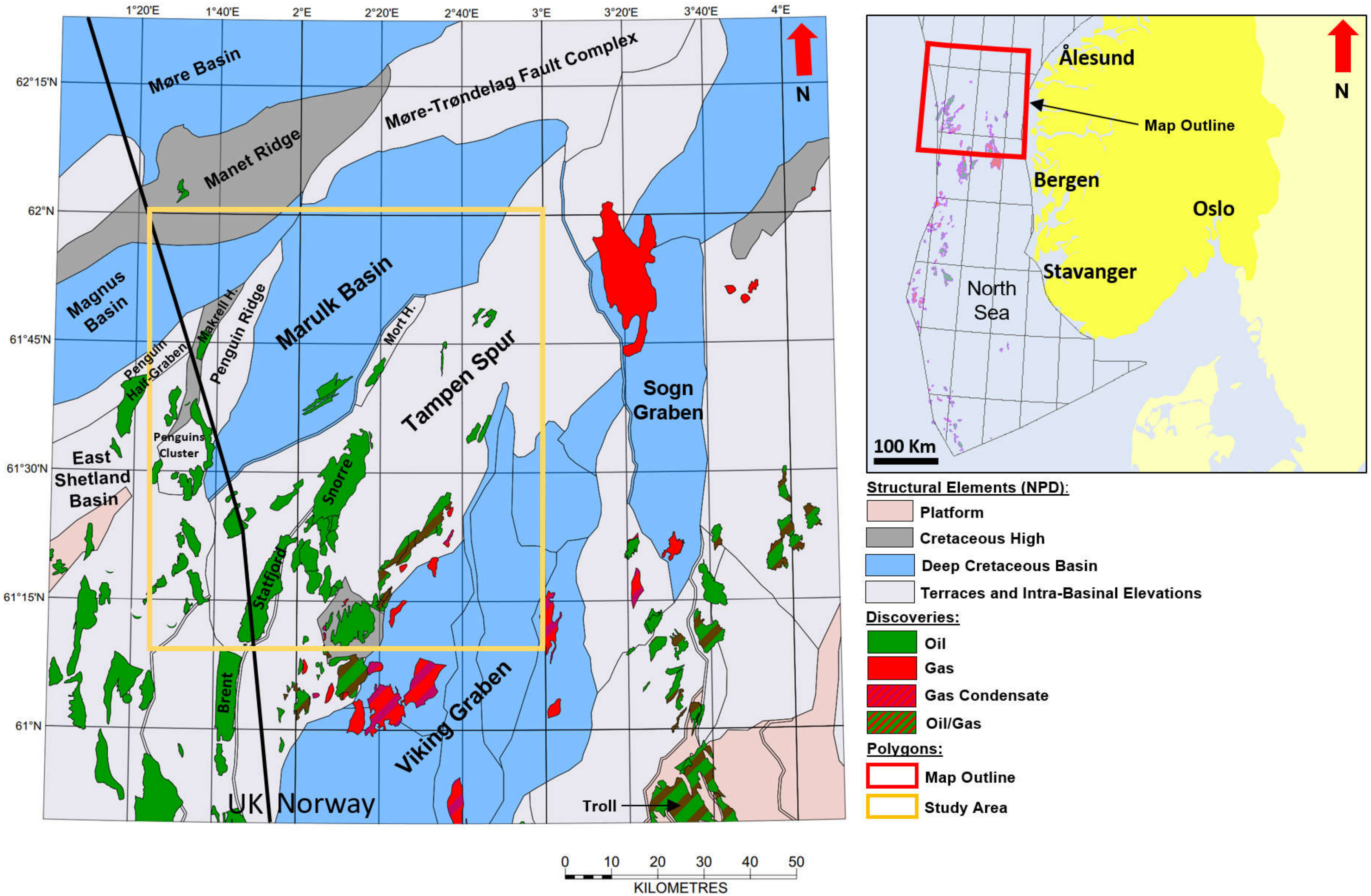

Figure 1: Outline of study area within the northern North Sea.

2. Geological Setting

The northern North Sea basin consists of a post-Caledonian graben system dominated by north and northeast oriented normal faults with large displacements (Færseth, 1996). The present day structural configuration of the area is the result of a long and complex tectonic history resulting in various tectonic provinces and sedimentary basins (Ziegler, 1975). Two main episodes of rifting are generally recognized: the Permo-Triassic rifting and the mid-Jurassic to early Cretaceous rifting, followed by subsequent thermal cooling and subsidence (Badley et al., 1988; Færseth, 1996; Odinsen et al., 2000). The northern North Sea basin is bounded by the Permo-Triassic Øygarden Fault Complex to the east, and normal faults of mainly Jurassic age to the west, separating the area from the East Shetland platform (Figure 2) (Færseth, 1996). Figure 3 shows the asymmetry in the deepest part of the basin within the Viking Graben (Odinsen et al., 2000).

The structural configuration of the two rifting periods differs significantly (Færseth, 1996). The interaction between Triassic and Jurassic rifting and the pre-rift basement structural configuration is a subject of debate (Fazlikhani et al., 2017; Odinsen et al., 2000). Due to compressional deformation during the Caledonian orogeny, the pre-rift basement shows heterogeneity both in terms of composition and structural trends (Færseth, 1996). A recent study of pre-rift basement seismic facies indicates that Devonian extensional shear zones, as recorded onshore western Norway, can be traced across the northern North Sea (Fazlikhani et al., 2017). These authors suggest that these shear zones influenced the fault trends during the Permo-Triassic rifting event. Færseth (1996) suggests that extension was relayed from the Sogn Graben to the central segment of the Viking Graben during the Jurassic, due to the presence of the Devonian Nordfjord-Sogn detachment (Figure 2).

Jurassic rifting reactivated some of the Permo-Triassic faults, which led to the formation of a second generation of tilted fault-blocks (Færseth, 1996). Fault activity was, however, mainly localized along the graben margins during maximum extension (Odinsen et al., 2000). Simultaneously, sets of smaller tilted fault blocks evolved, increasing the compartmentalization of the basin (Færseth, 1996). As a result, the structural style of the Viking Graben consists of smaller tilted fault blocks that are bounded by larger normal faults (e.g. Gullfaks Fault Block in Figure 3).

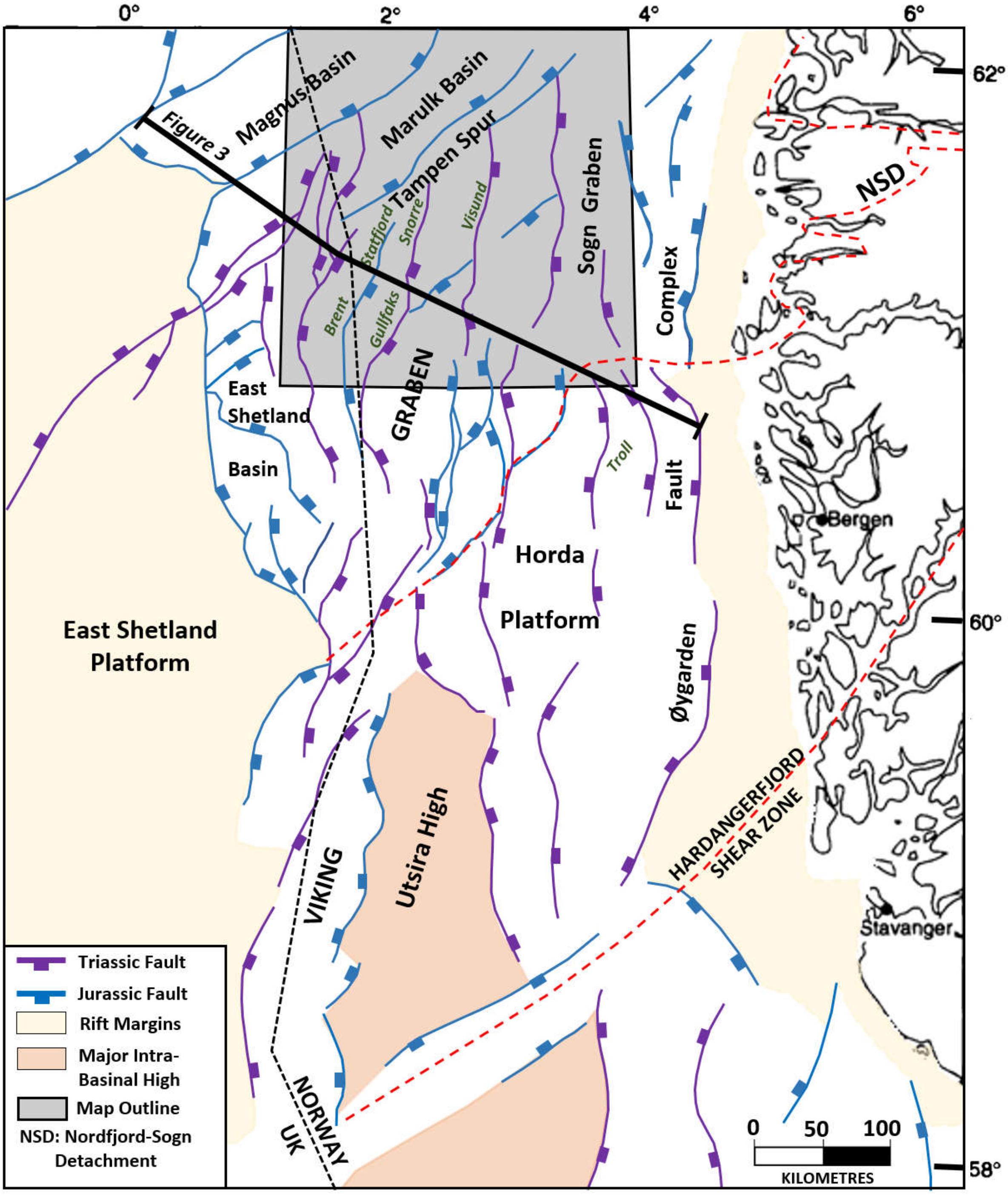

Figure 2: Fault map of the North Sea. Purple faults are of Permo-Triassic origin, while blue faults were formed during the Jurassic extensional phase. The black polygon defines the outline of Figure 2. Modified from Færseth (1996).

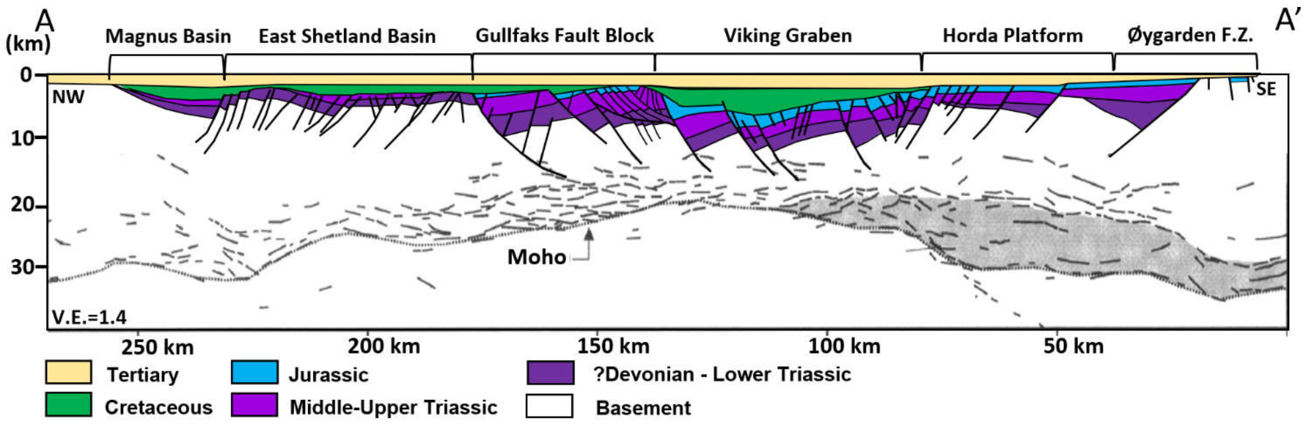

Figure 3: Depth converted crustal transect from the Magnus Basin in the west to Øygarden Fault Zone in the east, suggesting how crustal geometries relate to the Permo-Triassic and Jurassic fault systems. Transect line is displayed in figure 2. Modified from Odinsen et al. (2000).

In response to the multiphase rifting, the rate of accommodation space exceeded the rate of sediment supply. As a result, the depositional environments changed from mainly continental in the Permian-early Triassic, to marine during the late Jurassic-early Cretaceous (Nøttvedt et al., 1995). Ravnås et al. (2000) divide the Permian to Lower Cretaceous stratigraphy into three main sequences: the Permian-early Triassic syn-rift sequence, the middle Triassic-middle Jurassic inter-rift sequence, and the middle-late Jurassic syn-rift sequence (Figure 4). In general, information about the Lower Triassic sedimentary record in the northern North Sea is limited. However, incorporating well data and stratal geometries with the inferred tectonic history and outcrop analogues, non-marine, arid to semi-arid environments are inferred for this period. Therefore, the stratal record of this period is believed to be dominated by aeolian, sabkha, alluvial, and lacustrine facies (Ravnås et al., 2000).

Outbuilding and retreat of several large-scale alluvial and shallow marine clastic wedges are recorded for the middle Triassic to middle Jurassic period. It is believed that this period consisted of several stages of subsidence accompanied by climate changes and sediment supply variations (Ravnås et al., 2000; Steel and Ryseth, 1990). This period is generally referred to as a post-rift episode with relative tectonic quiescence. However, block rotation in relation to periods of increased subsidence indicates minor extension, which is confirmed by the presence of syn-rift sedimentary architectures (Ravnås et al., 2000). Increased subsidence during the middle Sinemurian (Lower Jurassic) represents the establishment of marine conditions and the initiation of mixed marine and non-marine depositional environments (Nøttvedt et al., 1995; Ravnås et al., 2000).

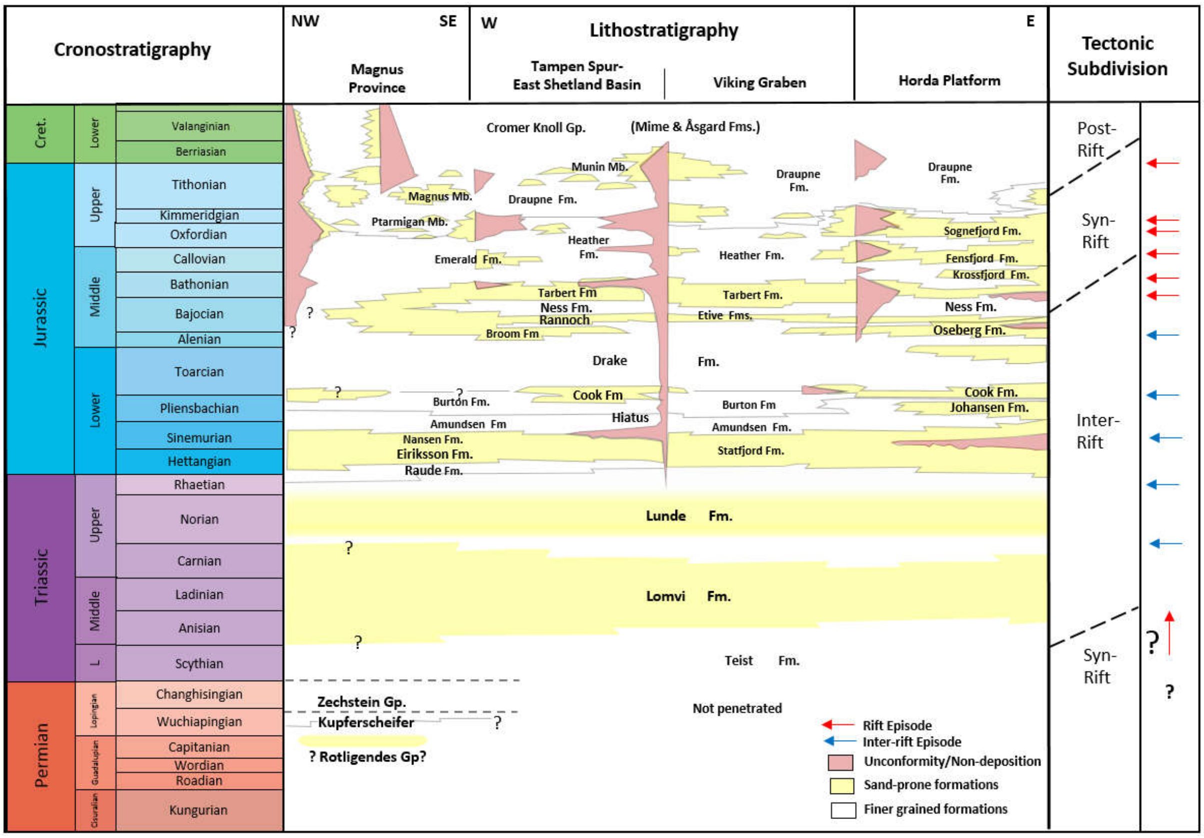

Figure 4: Lithostratigraphic chart with related tectonic subdivision modified from Ravnås et al. (2000)

The middle Jurassic to early Cretaceous rift phase represents a change from fluvial and shallow marine to deep marine depositional environments (Nøttvedt et al., 1995). The rift episode period is characterised by a series of rift events interrupted by periods of relative tectonic quiescence. Shallow marine sand-prone intervals developed along basin margins and footwalls developec uplifted islands. Deep marine sand-prone intervals developed as aprons and fans along fault-scarps or relay ramps, or as gravity flows (Ravnås et al., 2000). Figure 5 illustrates the relationship in the Penguin half graben between a late Oxfordian-Kimmeridgian syn-rift wedge, and a Kimmeridgian-Tithonian basin infill during relative tectonic quiescence.

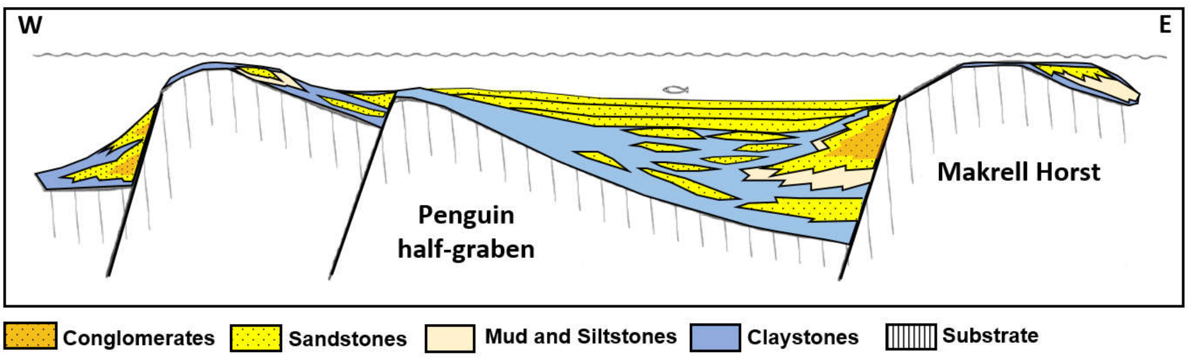

Figure 5: Schematic illustration of syn-rift wedge development within the Penguin Half-Graben, showing progressive shoreline advance and retreat at the western margin of the Makrell Horst, followed by the subsequent phase of tectonic quiescence as indicated by the parallel layered gravity flow deposits. Modified from (Ravnås et al., 2000).

Following the middle-late Jurassic rifting episode, lithospheric cooling and subsidence led to Cretaceous-early Cenozoic post-rift infill (Wood and Barton, 1983). Deep marine depositional environments dominated along the basin axis, onlapping towards the basin margins and intrabasinal highs. Variations in rate of subsidence resulted from uplift along the eastern Norwegian margin (Nøttvedt et al., 1995).

2.1 Main structural elements in the study area

The Marulk Basin is surrounded by several large structural elements of different age and configuration. The main structural elements to be described in this thesis are the Makrell Horst and Penguin Ridge to the west, and the Mort Horst and Snorre Fault Block in the east. To understand the tectonic setting of the Marulk Basin, also the Magnus Basin and the Møre Basin must be taken into consideration.

2.1.1 Makrell Horst

The Makrell Horst, which is also referred to as the Penguin Horst, is a NNE-SSW trending structural high. Together with the Penguin Ridge this horst limits the Marulk Basin to the west (Figure 1). The Makrell Horst continues into the British sector and terminates in the northern part of the East Shetland Basin. The southern end of the structure is also the location of the Penguins field, which is an assembly of four oil and gas accumulations. Several studies try to explain the structural evolution of the Makrell Horst. A study by Domínguez (2007) interprets the Makrell Horst as an extensional feature of Triassic age, with reactivation of Triassic structures during the late Jurassic extensional phase. Thomas and Coward (1995) suggest the Makrell Horst to be the result of fault reactivation due to late Jurassic to early Cretaceous basin inversion, as inferred from their interpretation of compressional flower structures. The inversion theory is also discussed by Booth et al. (1992), which interpreted the horst as a large-scale flower-structure. Grunnaleite and Gabrielsen (1995), on the other hand, explains the evolution of Makrell Horst in relation to the development of the Manet Ridge and Magnus Basin, suggesting a mid-Cretaceous age for the Makrell Horst with final rotation in late Cretaceous times.

2.1.2 Penguin Ridge

The Penguin Ridge is located along the eastern downthrown side of the Makrell Horst and follows the same structural trend (Figure 1). The ridge terminates towards the Magnus Fault in the north, while continuing into the East Shetland Basin in the south (Domínguez, 2007).

Compared to the adjacent horst, the Penguin Ridge shows much less structural relief. Similar to the Makrell Horst, evolution of the Penguin Ridge was initiated during the Permo-Triassic rift phase, with reactivation of Triassic faults and development of younger faults during the late Jurassic rift phase (Domínguez, 2007). To the south, local flower-structures have been interpreted and are believed to result from oblique-slip reactivation during the late Jurassic rift event (Domínguez, 2007).

2.1.3 Magnus Basin

The Magnus Basin limits the Penguin Half-Graben and the Penguin Ridge to the west of the study area, and Marulk Basin to the north (Figure 1). The Manet Ridge separates the Magnus Basin from the deeper Møre Basin to the north. The axis of the basin has a NE-SW trend, similar to the Møre Basin. Grunnaleite and Gabrielsen (1995) suggests that the Magnus Basin developed during the middle Cretaceous with increased subsidence into the late Cretaceous.

2.1.4 Snorre Fault Block

The Tampen Spur marks the southeastern boundary of the Marulk Basin with the Mort Horst to the north and the Snorre Fault Block to the south (Figure 1; Figure 2). The Tampen Spur area comprises an assemblage of westerly tilted fault blocks with Triassic and Jurassic reservoirs at their crest, making it one of the most prolific hydrocarbon provinces in the North Sea. The Permo-Triassic rifting phase developed west dipping faults of mainly N-S and NW-SE trend in the area of the Snorre Fault Block (Dahl and Solli, 1993) and the following period of subsidence led to large accumulations of Triassic to Middle Jurassic deposits (Lervik et al., 1989). Uplift and rotation of the Snorre Fault Block occurred during the middle to late Jurassic extensional phase and resulted in erosion of up to 1500 meters of Jurassic and uppermost Triassic rocks (Berger and Roberts, 1999; Dahl and Solli, 1993).

2.1.5 Mort Horst

The Mort Horst (also referred to as the Zeta Structure) is a NNE-SSW trending structural high, located north of the Snorre Fault Block (Figure 1). The geometry of the horst differs significantly from the typical rotated fault blocks in the Tampen Spur area, bounded by two major opposing fault complexes (Berger and Roberts, 1999). The Mort Horst is suggested to originate from the late Jurassic to early Cretaceous rift event, and shows a complex internal structure which is discussed in detail by Berger and Roberts (1999).

2.1.6 Møre Basin

The Møre Basin is separated from the Marulk Basin by the Møre-Trøndelag Fault Complex (Figure 1). The Møre-Trøndelag Fault Complex can be traced from the Magnus Basin towards the northeast onto mainland Norway (Gabrielsen et al., 1984) and is assumed to be related to a weak zone inherited from Caledonian deformation (Grunnaleite and Gabrielsen, 1995). The axis of the Møre Basin trends NE-SW (Grunnaleite and Gabrielsen, 1995), and the present structural configuration is attributed mainly to the late Jurassic to early Cretaceous extensional phase. NW-SE extension is suggested for this period (Bukovics and Ziegler, 1985; Gabrielsen et al., 1999) . Extension is interpreted to have continued episodically in the mid-Cretaceous and Paleocene, and two episodes of inversion are interpreted during the late early Cretaceous and during Oligocene to Miocene times (Grunnaleite and Gabrielsen, 1995).

2.2 Stratigraphy

2.2.1 Triassic

Hegre Group

The Triassic succession in the northern North Sea basin is subdivided into the Teist, Lomvi and Lunde formations (Figure 4). The Teist Formation is recognized by alternating sandstones and mudstones of continental origin (Steel and Ryseth, 1990). The sandstones are generally assigned to fluvial and eolian environments, while finer-grained intervals are related to overbank deposits and lacustrine environments (Steel and Ryseth, 1990; Vollset and Doré, 1984). The Teist Formation is assigned an age from early Triassic to Carnian (Vollset and Doré, 1984). The lower boundary is uncertain due to sparse well control. The Teist Formation coarsen upwards into the sandy unit of the Lomvi Formation (Steel and Ryseth, 1990). The Lomvi Formation is characterized by coarse grained fluvial sandstones with occasional evaporitic influence (Lervik et al., 1989; Vollset and Doré, 1984). Lacustrine and fluvial environments are also dominant in the Lunde Formation of Carnian to Rhaetian age, with interbedded sandstones, claystones, shales and marls.

Statfjord Group

The Statfjord Group is subdivided into the Raude, Eiriksson and Nansen formations (Figure 4). It represents the transition from Triassic to Jurassic (Rhaetian to Sinemurian), and is generally recognized by an upward coarsening sequence of alternating fine grained and coarse-grained sediments (Røe and Steel, 1985; Vollset and Doré, 1984). The stratigraphic record reflects a change from continental to shallow marine environments (Vollset and Doré, 1984). The Raude and Eiriksson formations consists of alternating sandstone and mudstones, deposited in alluvial braided river systems (Kirk, 1980; Nystuen and Fält, 1995; Nystuen et al., 1989). The origin of the Nansen Formation has been a subject of debate, fluvial to shallow marine depositional environments are suggested (Nystuen et al., 1989; Røe and Steel, 1985). Nystuen and Fält (1995) also suggest lateral variations from continental to marine facies as a response to the Sinemurian to Pliensbachian transgression.

2.2.2 Jurassic

Dunlin Group

Following the Triassic, a transgression led to the final drowning of the continental basin, with deposition of sediments of the Dunlin Group (Røe and Steel, 1985). The Dunlin Group is of Hettangian to Bajocian in age and consists of dark marine shales, with occasional development of sandy units along basin margins (Vollset and Doré, 1984). The lower boundary of the Dunlin Group is often a marked break in the gamma ray, contrasting to the underlying sandstones of the Statfjord Group (Røe and Steel, 1985; Vollset and Doré, 1984). The group is further subdivided into the Amundsen, Johansen, Burton, Cook and Drake formations (Figure 4).

Brent Group

The Brent Group represents the lithological subdivision resulting from the northward progradation and retreat of a large deltaic system (Helland-Hansen et al., 1992; Johannessen et al., 1995). From oldest to youngest the Brent Group includes the Broom, Rannoch, Etive, Ness and Tarbert formations with ages ranging from Bajocian to early Bathonian (Figure 4) (Vollset and Doré, 1984). The Broom Formation is recognized as the precursor of the regressive Rannoch Formation, marked by shallow marine deposition and lateral basin infill (Helland-Hansen et al., 1992; Vollset and Doré, 1984). The northward advance of the delta is represented by the Rannoch, Etive and lower part of the Ness formations. The Rannoch and Etive formations are generally recognized by a coarsening upward sequence represented by delta-front/shoreface facies, overlain by continental delta-plain deposits of the Ness Formation (Helland-Hansen et al., 1992). The Rannoch-Etive transition is as both conformable and erosive (Domínguez, 2007; Helland-Hansen et al., 1992). The Upper Ness and Tarbert formations represents a transgression and the final southward retreat of the delta, as a response to pre-rift fault activity (Fjellanger et al., 1996). The Tarbert Formation is recognized as a delta front/shoreface facies that developed above the continental Ness Formation (Helland-Hansen et al., 1992).

Viking Group

The Viking Group is represented by the Heather and Draupne formations with ages ranging from Bathonian to Berriasian (Figure 4). The Heather Formation is dominated by silty mudstones deposited during the marine transgression that led to retreat and final drowning of the Brent Delta (Fjellanger et al., 1996; Nøttvedt et al., 2000). The Heather Formation was deposited during the middle Bathonian to early Oxfordian rift stage, with only minor block tilting and without development of major footwall islands (Nøttvedt et al., 2000). Færseth et al. (1995) reports small amounts of resedimented sands within this succession on the Visund Fault Block.

The Draupne Formation consists of claystones deposited in marine environments (Vollset and Doré, 1984). Deposition of the Draupne Formation started in the late Oxfordian and continued into the early Cretaceous. This period is characterised by increased extension and fault block rotation with development of major footwall islands (Nøttvedt et al., 2000). Increased syn-rift sand deposition from gravity flows and shore line progradation was significant (Færseth et al., 1995; Nøttvedt et al., 2000; Ravnås et al., 2000).

2.2.3 Cretaceous

Cromer Knoll Group

On the Tampen Spur the Cromer Knoll Group consists of the Åsgard, Sola, Rødby and Mime formations, with an age of Ryazanian to Albian/early Cenomanian. The Åsgård, Sola and Rødby formations are dominated by marine fine-grained sediments with variation in amount of calcareous material (Isaksen and Tonstad, 1989). Locally, the Åsgård and Sola formations are absent above the structural highs. The Mime Formation is diachronously deposited in shallow marine environments as primarily limestones and marls (Isaksen and Tonstad, 1989). On the Snorre Fault Block, the Mime Formation is present on top of a west-dipping Triassic substratum. Above the Mime Formation, a hiatus is recognized, followed by a thin Rødby Formation (Dahl and Solli, 1993).

In general terms, the Cromer Knoll group is assigned to the post-rift period with rapidly subsiding basins. However, fault movements in the northern Viking Graben and on the Tampen Spur has been recorded into the early Cretaceous (Dahl and Solli, 1993; Gabrielsen et al., 1999). Whether these movements are the result of subsidence due to differential loading or continued extension is subject of debate.

Shetland Group

Within the Viking Graben and on the Tampen Spur the Shetland Group is divided into the Svarte, Blodøks, Trygvason, Kyrre and Jorsafare formations and represent the Upper Cretaceous. The Shetland group was deposited in an open marine environment, and deposition was dominated by siliciclastic facies of argillaceous sediments (Isaksen and Tonstad, 1989; Nybakken and Bäckstrøm, 1989). The thickness of the Shetland Group is determined by continued subsidence following the middle Jurassic to early Cretaceous rifting phase, most prominent along the old graben axis (Nybakken and Bäckstrøm, 1989). On the Tampen Spur the Shetland Group is locally absent (Nybakken and Bäckstrøm, 1989).

3. Data and Methodology

The dataset used for this thesis study is provided by Suncor Energy Norge and consists of 3D seismic cubes, regional 2D seismic lines, and key wells (Figure 6).

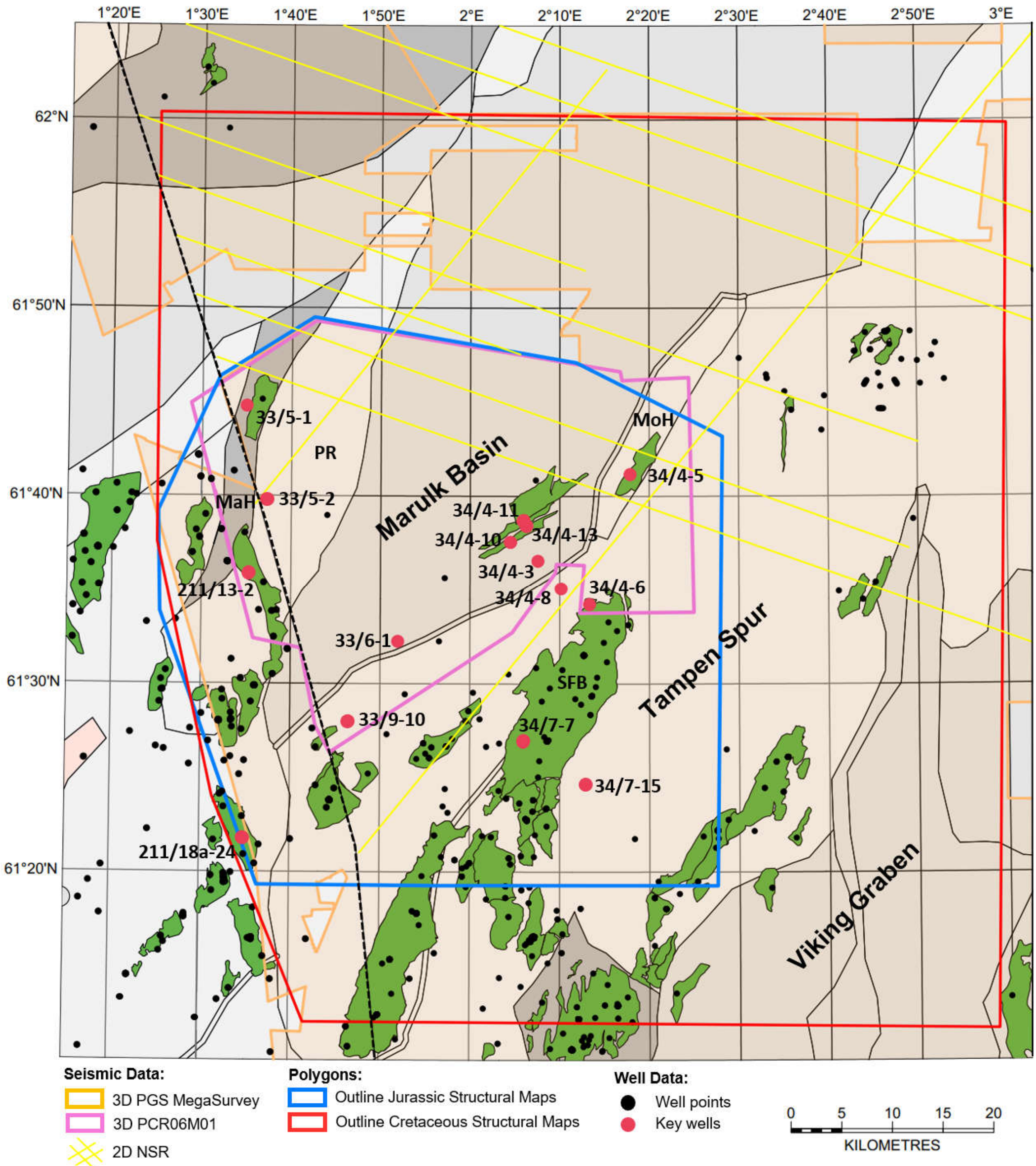

Figure 6: Map illustrating the seismic 3D cubes, 2D lines and key wells used in this study. In addition, the map displays the extension of the Jurassic structure maps (blue polygon) and the Cretaceous structure maps (red polygon). MaH, Makrell Horst; MoH, Mort Horst; SFB, Snorre Fault Block.

3.1 Well Data

The main well control within the study area is from the basin margins, in particular the Snorre Fault Block, the Penguin Ridge and the Makrell Horst (Figure 6). Only a few wells were drilled in the basinal areas. Key wells (Table 1) were picked based on location, stratal record, and the access to well-logs and checkshots for generation of synthetic seismograms and seismic to well tie. The remaining wells were used as supplement to understand the spatial distribution of stratigraphic intervals, for example to identify missing sections above structural highs which is also important in seismic correlation. Information about the public Norwegian wells was provided by well completion reports and NPD fact pages. Limited information was available for the UK wells, resulting in some uncertainty surrounding the well top picks. However, pseudo checkshots based on a regional velocity model enabled the generation of synthetic seismograms for the UK wells used for seismic correlation.

Table 1: Key wells used for seismic correlation within the study area. N, Norwegian; UK, United Kingdom; MS, MegaSurvey.

Well	Depth (MD)	Oldest Rock	Oldest Formation	Structural element	Checkshot	Well-tie	Bulk Shift (ms)
N 33/5-1	3829	Early Triassic	Teist Fm	Makrell Horst	x	MS	5
N 33/5-2	4520	Late Triassic	Lunde Fm	Penguin Ridge	x	MS	-8
N 33/6-1	3900	Late Triassic	Lunde Fm	Marulk Basin	x	MS	12
N 33/9-10	3715	Late Triassic	Statfjord Gp	Tampen Spur	x	MS	15
N 34/4-3	4460	Late Triassic	Lunde Fm	Marulk Basin	x	MS	0
N 34/4-5	3917	Late Triassic	Lunde Fm	Mort Horst	x	MS	10
N 34/4-6	3282	Late Triassic	Teist Fm	Snorre Fault Block	x	MS	-10
N 34/4-8	3110	Late Triassic	Lunde Fm	Snorre West	x	MS	-15
N 34/4-10 R	2380	Early Jurassic	Statfjord Gp	Marulk Basin	x	MS	-3
N 34/4-11	4327	Late Triassic	Lunde Fm	Marulk Basin	x	MS	-8
N 34/4-13 S	5010	Late Triassic	Lunde Fm	Marulk Basin	x	MS	15
N 34/7-7	3526	Late Triassic	Lunde Fm	Snorre Fault Block	x	MS	-12
N 34/7-15 S	4646	Early Jurassic	Drake Fm	Pancake Basin	x	MS	10
UK 211/18a-24	4381	Late Triassic	Cormorant Fm	East Shetland Basin	Pseudo	MS	5
UK 211/13-2	4041	Late Triassic	Cormorant Fm	Penguin Ridge	Pseudo	MS	7

3.2 Seismic Data

Regional 3D seismic interpretation was done using primarily the PGS North Sea MegaSurvey V2.1. The MegaSurvey is a post stack merge of public and PGS proprietary seismic 3D cubes resulting in one dataset with extensive coverage. This enables regional seismic interpretation on one large 3D cube, contrary to the interpretation of individual cubes with final merge of the interpreted surfaces. Within the area of interest, the MegaSurvey consists of 34 individual public 3D cubes of different quality and vintages, acquired from 1986 to 2011 (Table 2). As a result, the merged dataset shows great variation in seismic quality. In addition, the PCR06M1 3D cube (Table 1) covering the southern Marulk Basin was used. To supplement the 3D seismic towards the north, 2D seismic lines of the NSR (North Sea Renaissance) TGS surveys were used (Figure 6).

Originally, the MegaSurvey has reversed polarity compared to SEG polarity convention. In this thesis, however, the seismic phase spectrum is multiplied by -1, flipping the polarity 180 degrees. The resultant 3D data have normal polarity (SEG polarity convention), where an increase in acoustic impedance is represented by a red peak in the seismic. Similarly, a decrease in acoustic impedance is shown as a blue trough (Figure 7) (Sheriff, 2002). Statistical wavelet extraction was performed for well 34/4-10 (Figure 8A), corresponding to a zero-phase wavelet. The wavelet was extracted in the time interval between -1550 and -3600 ms, corresponding to the main interval of interest. The dominant frequency of the extracted wavelet lies within 15-25Hz (Figure 8B). The information obtained by wavelet extraction was used to construct the wavelet for the generation of synthetic seismograms.

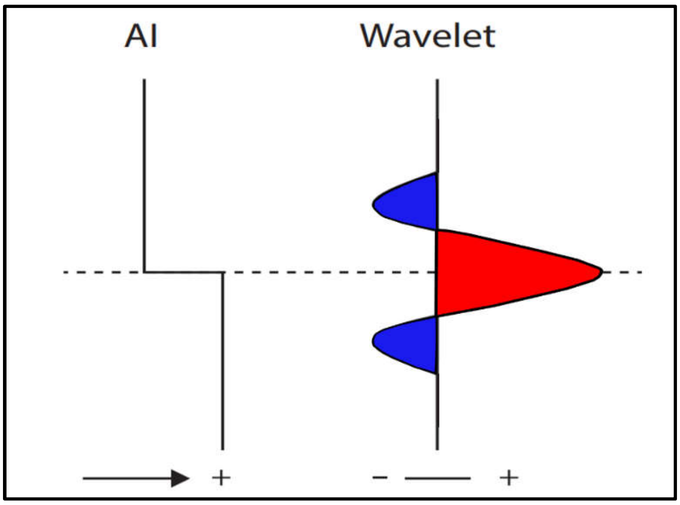

Figure 7: The MegaSurvey has normal polarity according to the SEG polarity convention, where increase in acoustic impedance is represented by a red peak.

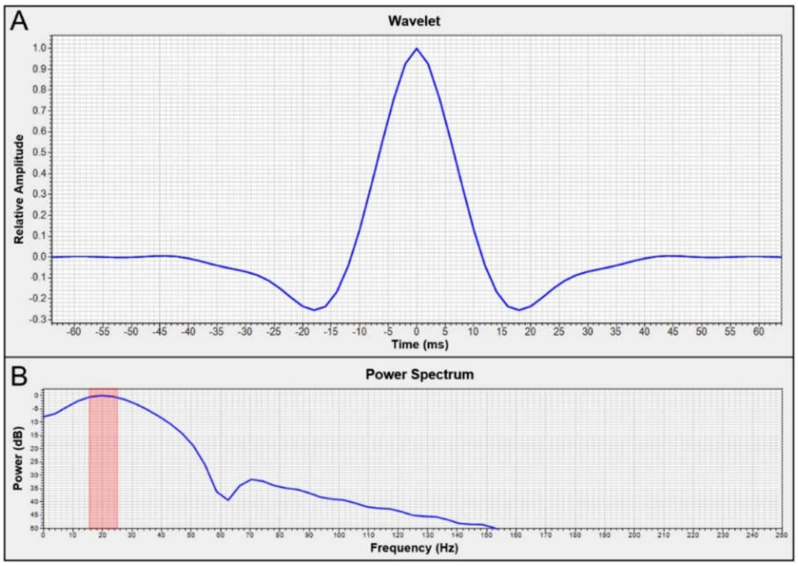

Figure 8: Example of extracted wavelet from well 34/4-10 (A). Dominant frequency is in the range between 15-25 Hz as indicated by the red band in (B).

Table 2: List of 3D seismic surveys contained within the PGS North Sea MegaSurvey V2.1 within the area of study. GB, Great Britain; BL., Block.

Seismic survey	Area	Survey Year	Seismic Dimension
BG1102	BL. 34/2, 34/5	2011	3D
BP_MAGNUS	GB	?	3D
DON_211_83	GB	?	3D
DON_RAW	GB	?	3D
E86	BL. 33/9	1986	3D
LU07021118	GB	?	3D
MC3D-34-6	34/6	1994	3D
MN9401	BL. 34/4-5	1994	3D
MN9601M	BL.35/1	1996	3D
MS97MR01	BL. 34/8	2001	3D
NH02M2	BL. 34/8	2002	3D
NH9106	BL.34/8	1991	3D
NVG2000	BL.34/9	2000	3D
NX0701	BL. 33/2, 33/3	2007	3D
NX0801	BL. 34/8,9,11,12	2008	3D
P87200	GB	?	3D
P88201	GB	?	3D
PC07N023	BL. 33/3, 34/1, 34/2	2007	3D
PCR06M1	BL. 33/6, 34/4	2007	3D
SG9701	BL. 34/4,7	1997	3D
ST03M01	BL. 33/9, 33/12	2003	3D
ST05M05	Statfjord	2005	3D
ST05M08	Visund	2005	3D
ST0110	BL. 33/9-6	2001	3D
ST0412	BL. 34/7	2004	3D
ST0503-2	BL.6201/11	2005	3D
ST0503LNR10R11	BL. 33/2	2009	3D
ST9101	Statfjord	1991	3D
ST9406	33/6, 34/4	1994	3D
ST9607	BL. 34/10	1996	3D
ST9703	Statfjord	1997	3D
TGS_Q34	BL. 34/1,2,3	1996	3D
TQ_34_12	BL. 34/12	1998	3D
WIN0901	BL. 33/12	2009	3D

3.3 Seismic Well-Tie

A detailed seismic interpretation requires seismic to well-ties in order to relate key stratigraphic units in depth to the seismic reflection data in time. As listed in Table 1, seismic well-ties were constructed for 15 wells in the area of interest, including basinal areas and structural highs (Figure 6). Impedance and reflectivity of the different layers in the wells was calculated using the sonic and density logs. Checkshot data was used as time-depth reference. Based on information given by the extracted wavelets, a zero phase Ricker Wavelet was created and convolved with the computed reflectivity to get the synthetic seismograms representing the well data. Some variability was observed in the frequency content at the different well locations. For well 34/4-10, a Ricker wavelet of 25Hz was used to calculate the synthetic seismogram (Figure 9). To correlate with the seismic, a bulk shift of -3 ms was applied, resulting in a good tie for the key reflectors. Seismic well ties enable confident seismic correlation across the area of interest. Higher uncertainties are related to the deepest part of the Marulk Basin and the northernmost areas, due to lack of well control. The well-ties constructed for this study are not good for field-scale projects, but they are detailed enough to construct a stratigraphic framework for regional seismic interpretation.

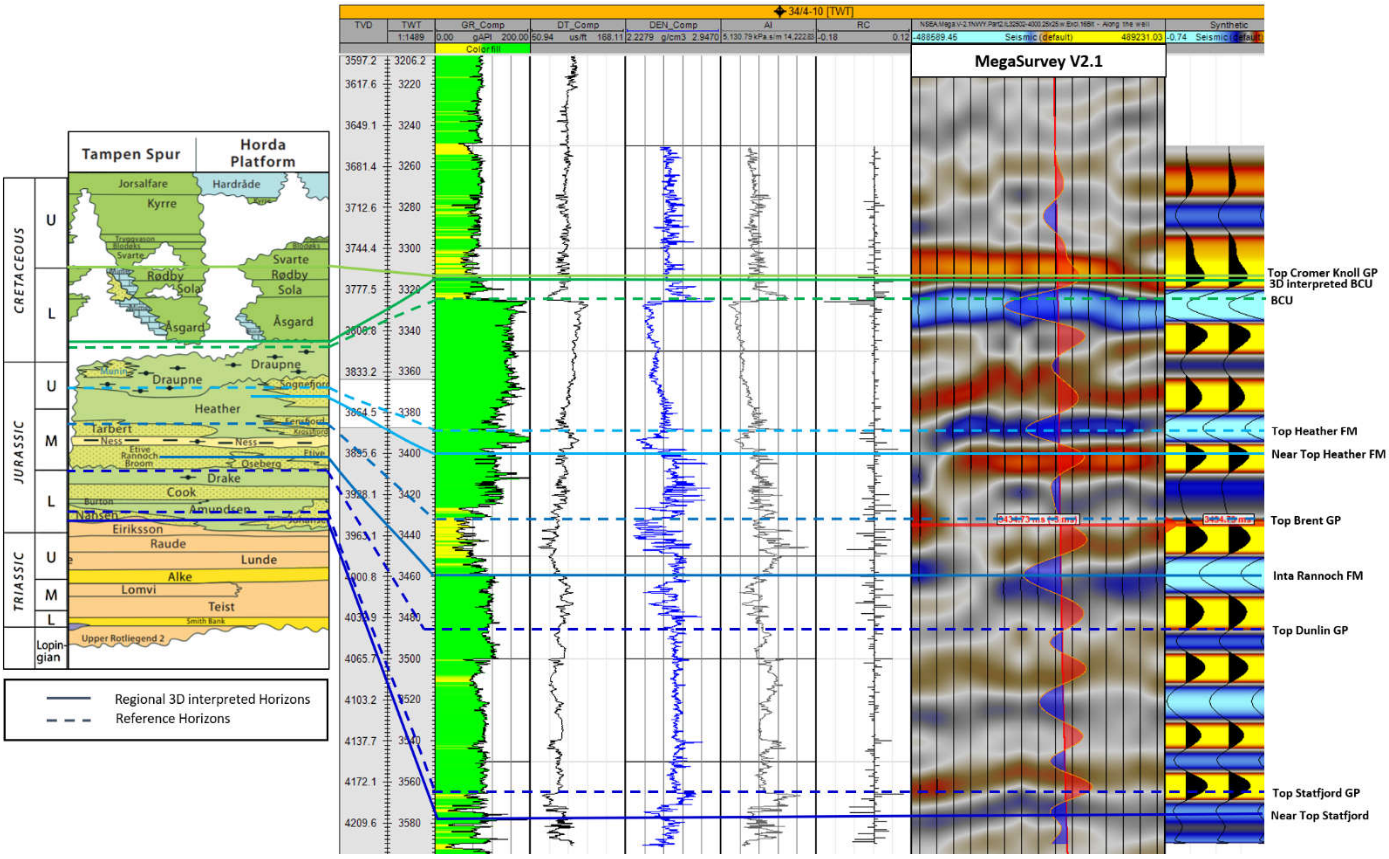

Figure 9: Synthetic seismogram and well-tie from well 34/4-10, and chronostratigraphic chart (modified from NPD). Continuous lines represent horizons in which regional 3D interpretation is performed, while stippled lines represent additional horizons used as reference. Note that this well-tie only covers the Mesozoic section.

3.4 Seismic Interpretation

Regional 3D seismic interpretation was carried out for six horizons of early Jurassic to late Cretaceous age (Table 3). Two criteria were key in determining what horizons to pick for the seismic interpretation: (1) The horizons must be able to represent key stratigraphic markers based on the established tectonostratigraphic framework of the area, and (2) the horizons must show reflection continuity on a regional scale. As a basis for defining the horizons, the stratigraphic framework of Ravnås et al. (2000) was used (Figure 4). The interpreted horizons and their relation to the rift evolution is explained in Figure 10.

Table 3: List of interpreted horizons with corresponding seismic character using SEG normal polarity.

Horizon	Age	Acoustic Impedance	Peak/Trough
Top Shetland GP	Top Upper Cretaceous	Decrease	Through
Top Cromer Knoll GP	Top Lower Cretaceous	Increase	Peak
BCU	Base Cretaceous	Increase	Peak
Near Top Heather FM	Near Top Middle Jurassic	Increase	Peak
Intra Rannoch FM	Near Top Lower Jurassic	Decrease	Trough
Near Top Statfjord GP	Intra Lower Jurassic	Decrease	Trough

3.4.1 Interpretation Strategy

Initial screening of the available 3D seismic data was done to get a general overview of the seismic quality and structural complexities within the area of interest. Furthermore, seismic sections were selected through well locations with established seismic well-ties, enabling seismic correlation between the key wells in the study area. This seismic correlation established a reference grid, ensuring correct interpretation ("picking") of reflections in the areas between the wells.

The 3D seismic interpretation was divided into two main steps. First, faults were mapped to establish the fault framework within the study area. Secondly, horizon interpretation was initiated. As an important reference, the BCU marker horizon was interpreted first. The 3D interpretation was performed using the seismic interpretation tools of the Petrel software (Schlumberger, 2017). Horizon picking was done every 25th line creating a grid of inlines and crosslines. The PGS MegaSurvey is a collection of several seismic cubes, and the quality of the seismic data varies. Therefore, 2D auto tracking was only performed in areas with moderate to good seismic quality, while manual picking was necessary in areas with less continuous reflectors.

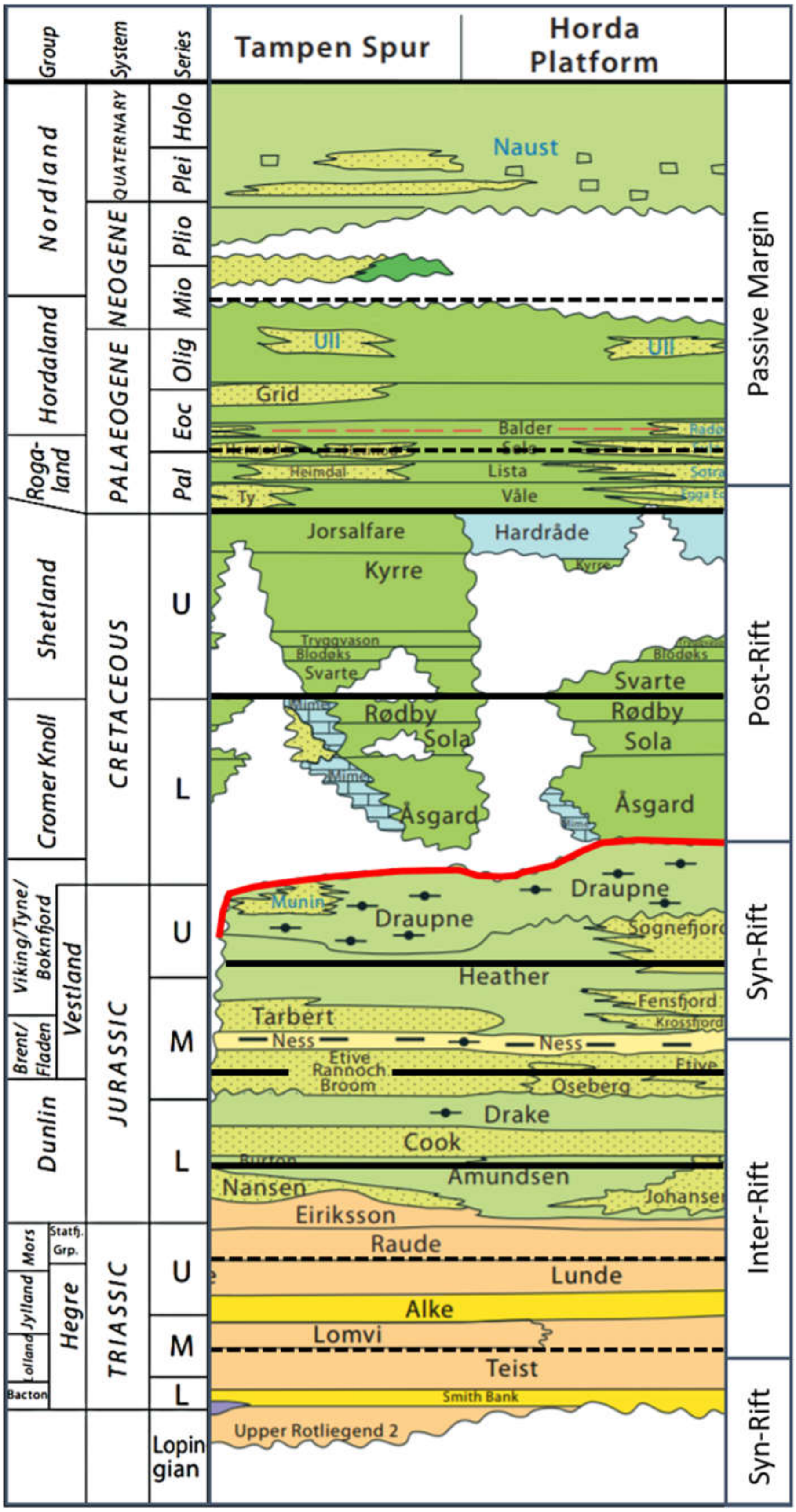

Figure 10: Stratigraphic column with related tectonic subdivision. The thick black solid lines represent 3D interpreted horizons, while stippled lines represent horizons interpreted on individual 2D lines. The red line marks the BCU.

Interpolation of the interpreted 3D grid produced surfaces and time structural maps for the different horizons, and polygons were made to represent the fault separation. Subtraction of the structural maps gave isochore maps representing the intervals' thickness in time. In the case where a surface is truncated by another, the two surfaces are merged in order to get complete structural maps. These areas are highlighted with zero thickness on the thickness maps. The structural and thickness maps were further used to assess the structural evolution of the area, including timing of faulting, different fault families, and fault evolution. In addition, thickness maps facilitate the analysis of depocenters through time and the type of basin infill (e.g. pre-rift, syn-rift, or post-rift). The thickness maps also indicate which areas underwent the highest rate of accommodation space generation in a given time period, and thus, how the rift evolved through time.

Poor quality 3D seismic below the BCU and lack of well control in the northernmost areas limits northward interpretation of pre-Cretaceous horizons. However, interpretation of the BCU, the Top Cromer Knoll Group, the Top Shetland Group was extended northwards by correlating the 3D seismic with regional 2D seismic lines. Interpretation of these horizons was also extended eastward to cover the eastern boundary of the northern Viking Graben, allowing discussion of the post-Jurassic evolution in these areas.

3.4.2 Seismic Character

Near Top Statfjord

The Near Top Statfjord reflector is picked at a soft event just beneath the top of the Statfjord sandstone, which is associated with a high response in the gamma ray log. The soft response is laterally continuous and was therefore used for the regional seismic interpretation. The seismic response is associated with a low acoustic impedance shale in the wells. In contrast, the Top Statfjord pick is a lithological boundary typically defined at the contact between the uppermost Statfjord sandstone and the shales and siltstones of the overlying Dunlin Group (Vollset and Doré, 1984), and is generally represented by a hard event in the seismic. This boundary does not represent a specific age, but rather a time span and does not give strong continuous reflectivity due to variations in the lateral distribution, quality and hydrocarbon saturation of the sandstones.

The Near Top Stafjord reflector is best developed across the Tampen Spur, on the Penguin Ridge and the shallower parts of the Marulk Basin (Beta Ridge). The reflector is less developed in the deepest part of the Marulk Basin, the Pancake Basin and west of Makrell Horst. The reflector is not present on the northern end of the Snorre Fault Block or the Makrell Horst. Complex structures make the 3D interpretation on the Mort Horst complicated. In relation to the tectono-stratigraphic framework, the Statfjord Group lies within the inter-rift sequence of relative tectonic quiescence (Ravnås et al., 2000).

Intra Rannoch

The Intra Rannoch reflector is characterised by a soft event which shows lateral continuity within the study area. The decrease in acoustic impedance is related to a shaly interval in the wells. The lateral extent of the reflection suggests that it may be a regional flooding surface, a condensed section or a rift-related unconformity as indicated by Domínguez (2007). As for the Near Top Statfjord reflector, the Intra Rannoch reflector is best developed across the Tampen Spur and the shallower parts of the Marulk Basin. The reflector is absent on the Makrell Horst and on the northern end of the Snorre Fault Block. On the Penguin Ridge, the reflector is truncated by the near top Heather reflector and the BCU and can only be interpreted in the central and southern areas of the ridge. The reflector is less developed in the deeper part of the Marulk Basin and the Pancake Basin. This may be due to the loss of resolution with depth, and/or deformation along the large basin bounding faults.

The Intra Rannoch reflector lies within the upper part of the inter-rift sequence. However, Domínguez (2007) suggests that Jurassic rifting was initiated as early as the middle Jurassic, resulting in the development of a Top Rannoch unconformity. In such case, the interpreted intra Rannoch reflector could represent the upper boundary of the inter-rift succession in some areas

Near Top Heather

The Near Top Heather reflector is picked on a hard event just beneath the Top Heather boundary. The top of the Heather Formation is observed as a distinct peak in the gamma ray, associated with a soft event in the seismic. The following decrease in the gamma ray readings results in a high amplitude hard kick, which shows very good lateral continuity within the area of interest. The highest uncertainty related to the Near Top Heather reflector is within the deepest part of Marulk Basin. The reflector is absent on the northern end of the Snorre Fault block and Makrell Horst.

The Near Top Heather reflector truncates older reflectors. This is most evident west of Mort Horst and on the Penguin ridge where this reflector truncates the Intra-Rannoch reflector. The latter suggests that the Near Top Heather reflector may be a rift-related unconformity, possibly the Top Heather unconformity/hiatus recognized by Nøttvedt et al. (2000). In relation to the rift evolution, the Near Top Heather reflector lies within the upper Jurassic syn-rift succession and is the approximate boundary between the early (middle Bathonian-early Oxfordian) and late (late Oxfordian-early Cretaceous) rift stages.

Base Cretaceous Unconformity (BCU)

The BCU is an unconformity between the Cromer Knoll Group and the Viking Group within the basinal areas and is generally represented by a blue through (Figure 9). The red peak immediately above shows very good lateral continuity which enables auto-tracking in most areas, and thus, this reflector was used for regional interpretation of the BCU. Above structural highs the Cromer Knoll Group unconformably overlays middle Jurassic and Triassic substratum. Polarity changes are evident in some areas of the structural highs due to variation in the truncated lithology and possibly hydrocarbon saturation of the pore space. Manual interpretation is necessary in those areas. The BCU belongs to the upper part of the late Jurassic rift phase, marking the lower boundary of the Cretaceous post-rift succession (Figure 6).

Top Cromer Knoll

The Top Cromer Knoll reflector is represented by a hard event (red peak) in the seismic and is associated with a decrease in gamma ray readings in the wells. In general, the reflector shows good lateral continuity and is best developed within the basinal areas. The reflector does not extend above structural highs, where the thickness of the Cromer Knoll Group is below seismic resolution. In relation to the generalized rift evolution, the Cromer Knoll Group belongs to the Cretaceous post-rift succession (Figure 6).

Top Shetland

The top of the Shetland Group is tied to a soft event (blue trough) in the seismic. A coarsening upward followed by a fining upward gamma ray log pattern, defines a moderate response, which corresponds to the soft event of Top Shetland. However, as this boundary is not defined by a distinct change in lithology, the resultant seismic amplitude is low. The seismic response of the Top Shetland is therefore highly variable. The reflector is best developed within the basinal areas, while it is less developed above structural highs. In relation to the rift evolution, the Top Shetland defines the boundary between the Upper Cretaceous and Paleocene within the post-rift succession (Figure 6).

3.4.3 Seismic Units

The interpreted reflectors define the top and base of individual stratigraphic successions, here referred to as "seismic units". The seismic units are used to describe the geological evolution within their respective time frame. Nine units are defined and listed in Table 4.

Table 4: Seismic units with associated top and base reflectors and corresponding time frame.

Unit	Base Reflector	Top Reflector	Age
0	-	Near Top Teist	~ Pre-Carnian-Carnian
1	Near Top Teist	Near Top Statfjord	~ Carnian-Sinnemurian
2	Near Top Statfjord	Intra Rannoch	~ Sinnemurian-Bajocian
3	Intra Rannoch	Near Top Heather	~ Bajocian-early Oxfordian
4	Near Top Heather	BCU	~ late Oxfordian – early Cretaceous
5	BCU	Top Cromer Knoll	early Cretaceous
6	Top Cromer Knoll	Top Shetland	late Cretaceous
7	Top Shetland	Top Rogaland	Paleocene-early Eocene
8	Top Rogaland	Top Hordaland	Eocene – early Miocene

4. Results

In this chapter, the results of the seismic interpretation are described and displayed through a series of structure maps, seismic sections and isochron maps. First, the large-scale structural geometries and trends are described to address the northwestwards evolution of the North Sea rift system (section 4.1). Second, the various fault systems are described and classified (section 4.2). Third, the main structural highs and basins in the greater Marulk Basin area are described to address their roles in the spatial and temporal evolution of the area (section 4.3). Finally, the structural evolution of the area is described through a series of isochron maps (section 4.4).

4.1 Large-scale structural geometries and trends

Four major basins align in a southeast-northwest direction: the Viking, the Pancake Basin, the Marulk Basin, and Magnus Basin (Figure 11). The axis of the Viking Graben and the Pancake Basin trends approximately NNE-SSW, while the axis of the Marulk and Magnus basins trends NE-SW (Figure 11). The basins are divided by structural highs with different geometries, dimensions, orientations and origins. The Viking Graben is separated from the Pancake Basin by the uplifted crest of the Visund Fault Block, which trends parallel to the axis of the basins. The Pancake Basin and the Marulk Basin are separated by the crest of the rotated Snorre Fault Block and the elongated Mort Horst to the north. The orientations of these highs align with the orientation of the Pancake Basin but deviates slightly from the main axis of the Marulk Basin. The Marulk Basin and the Magnus Basin are divided by the Makrell Horst and the Penguin Ridge, which strike obliquely to the basin axis of the adjacent basins. Based on these observations, a large-scale trend exists from southeast to the northwest where orientation of the inter-basinal highs gradually deviates from the adjacent basin axis in a northwesterly direction.

4.2 Fault geometries, interaction and linkage

The large-scale structural geometries are the result of the interplay between the large master faults separating the structural highs and lows. Geometry, trend, magnitude and age of these master faults vary, creating a complex structural framework. Fault geometries will be described using a selection of seismic sections (Figure 12) and Jurassic and Cretaceous structural maps (Figure 13). The important faults to be described are the bounding faults of the Snorre Fault Block, Mort Horst, Penguin Ridge and Makrell Horst (Figure 14; Figure 15) in addition to the Marulk North Fault and the Magnus Fault (Figure 11).

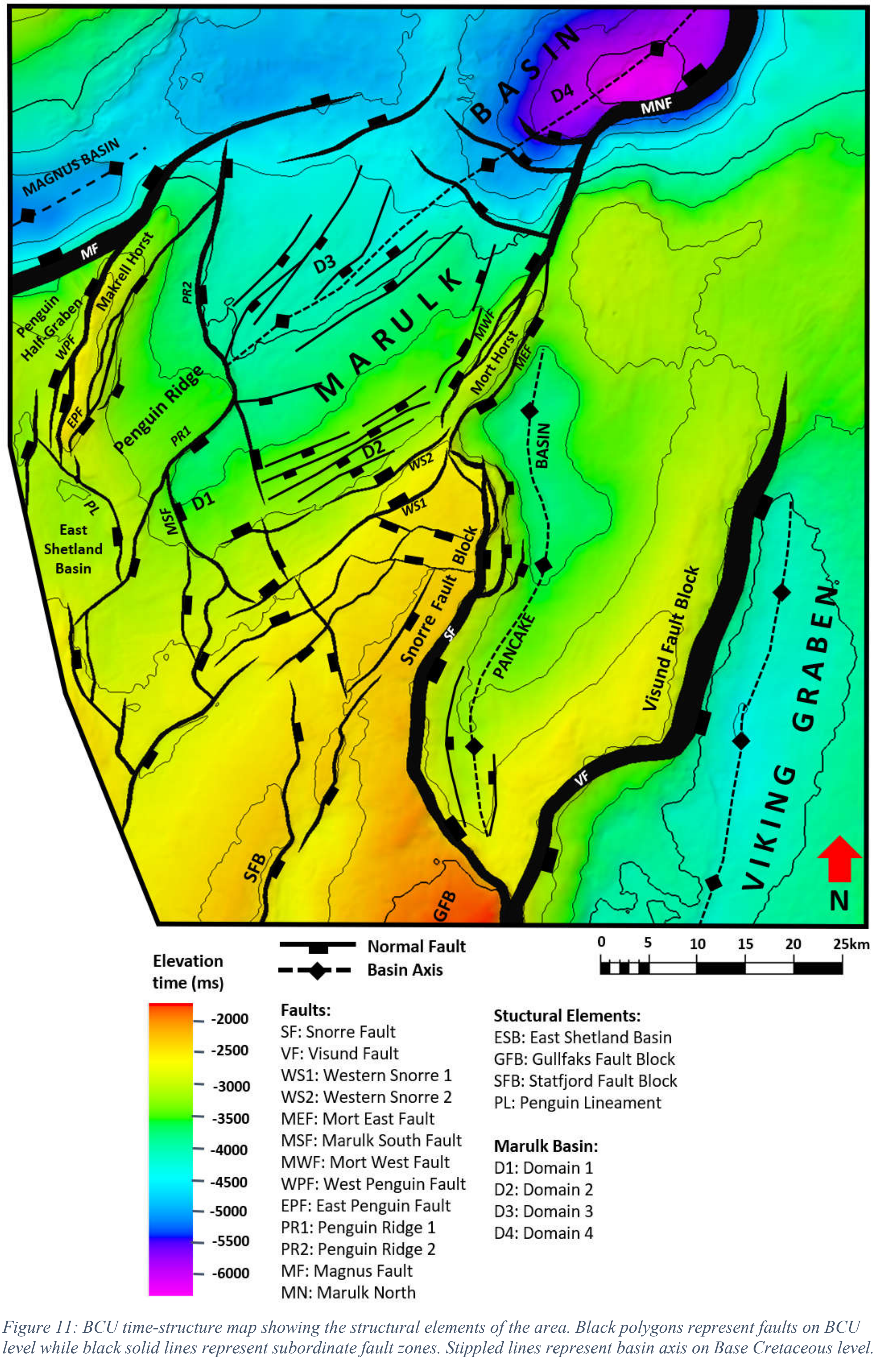

Figure 11: BCU time-structure map showing the structural elements of the area. Black polygons represent faults on BCU level while black solid lines represent subordinate fault zones. Stippled lines represent basin axis on Base Cretaceous level.

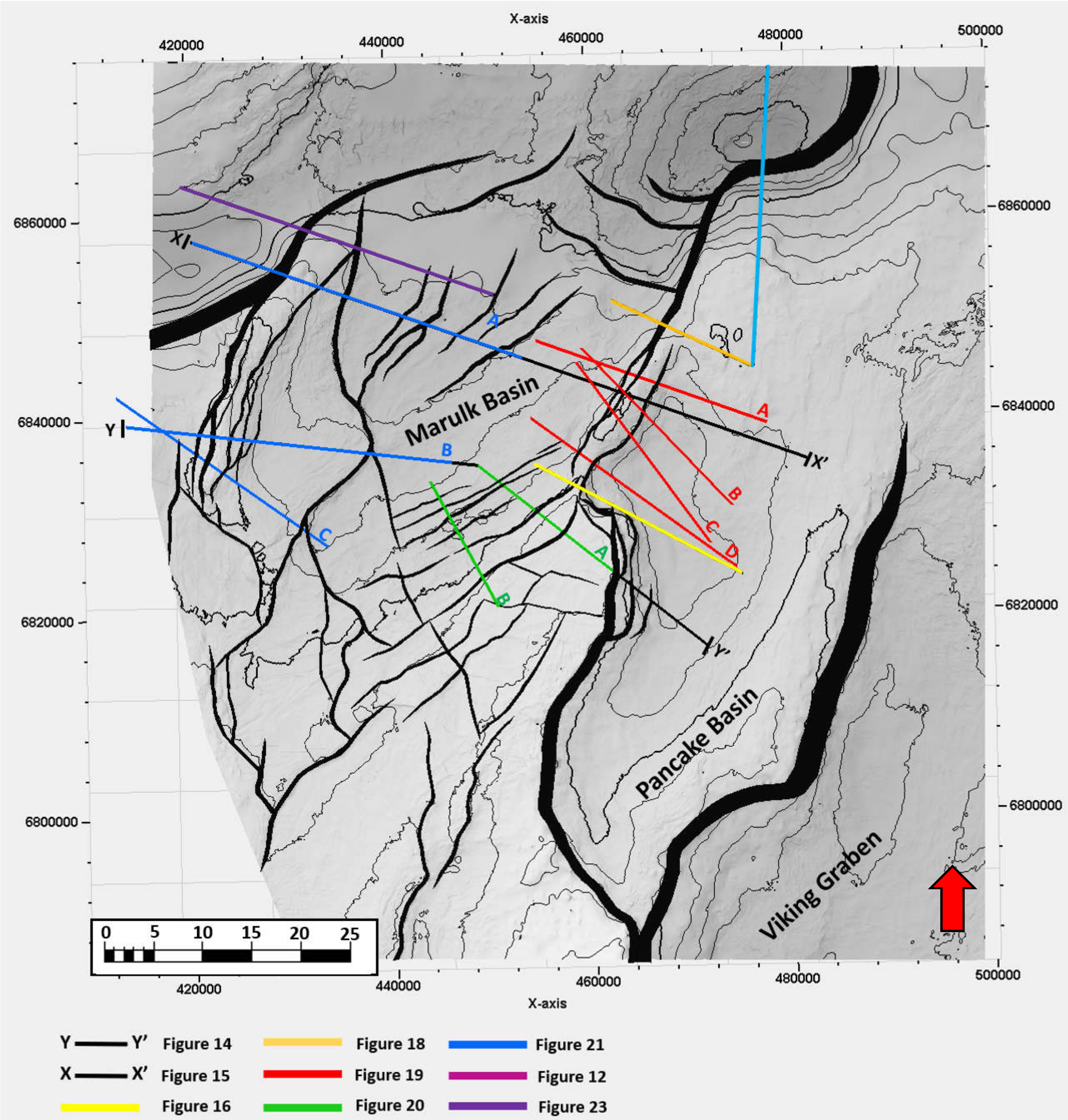

Figure 12: BCU structure map showing the location of the seismic sections described in section 4.2.

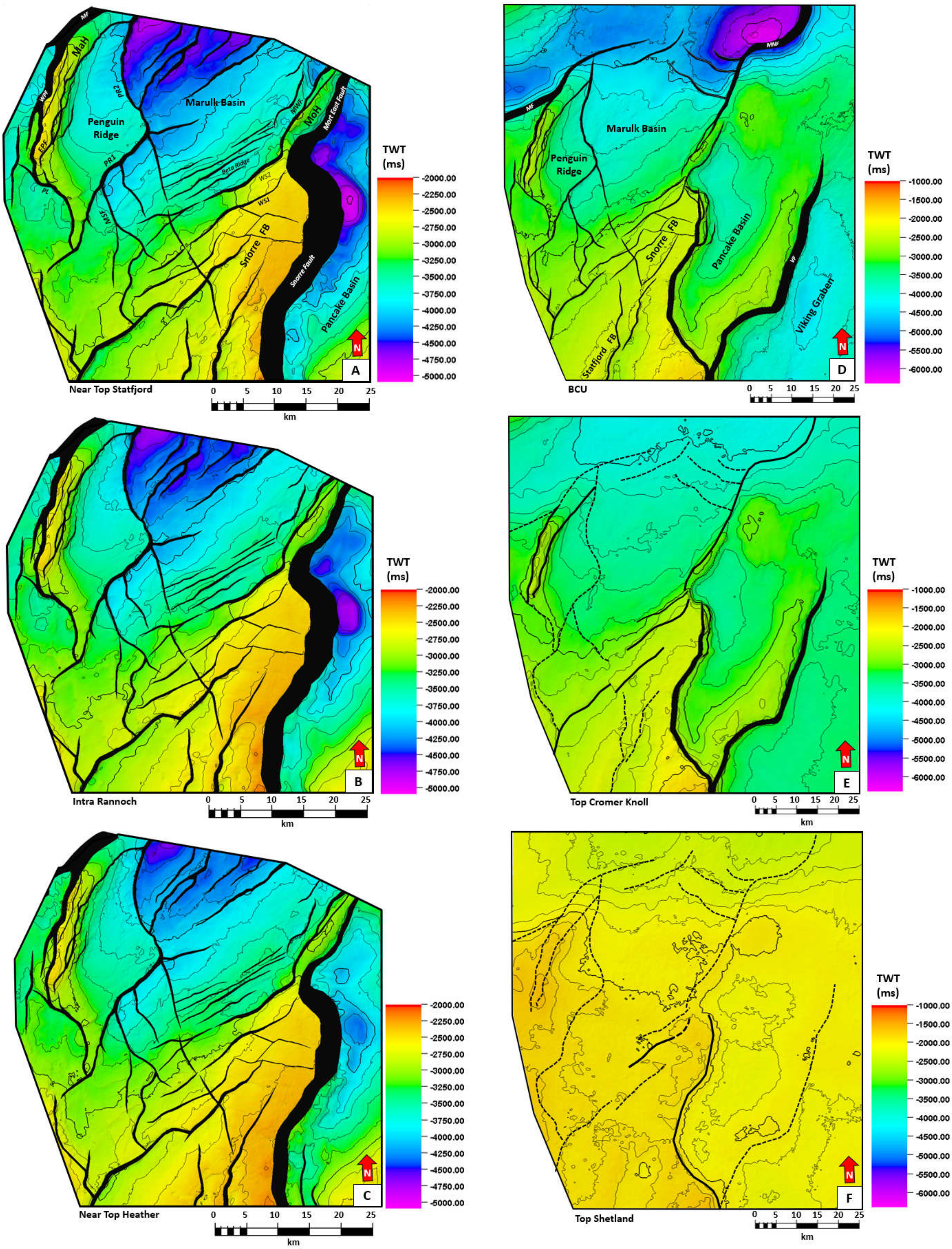

Figure 13: Time structural maps of the interpreted horizons. (A) Near Top Statfjord, (B) Intra Rannoch, (C) Near Top Heather, (D) BCU, (E) Top Cromer Knoll, and (F) Top Shetland. The pre-Creaceous maps (A, B and C) have same time-depth scale and contour interval of 200 ms. Similarly, the post-Cretaceous maps have the same time-depth scale with contour interval of 300, 200 and 100 ms respectively. Outline polygons of the structure maps are shown in Figure 6. Stippled lines indicate subordinate faults, included as reference.

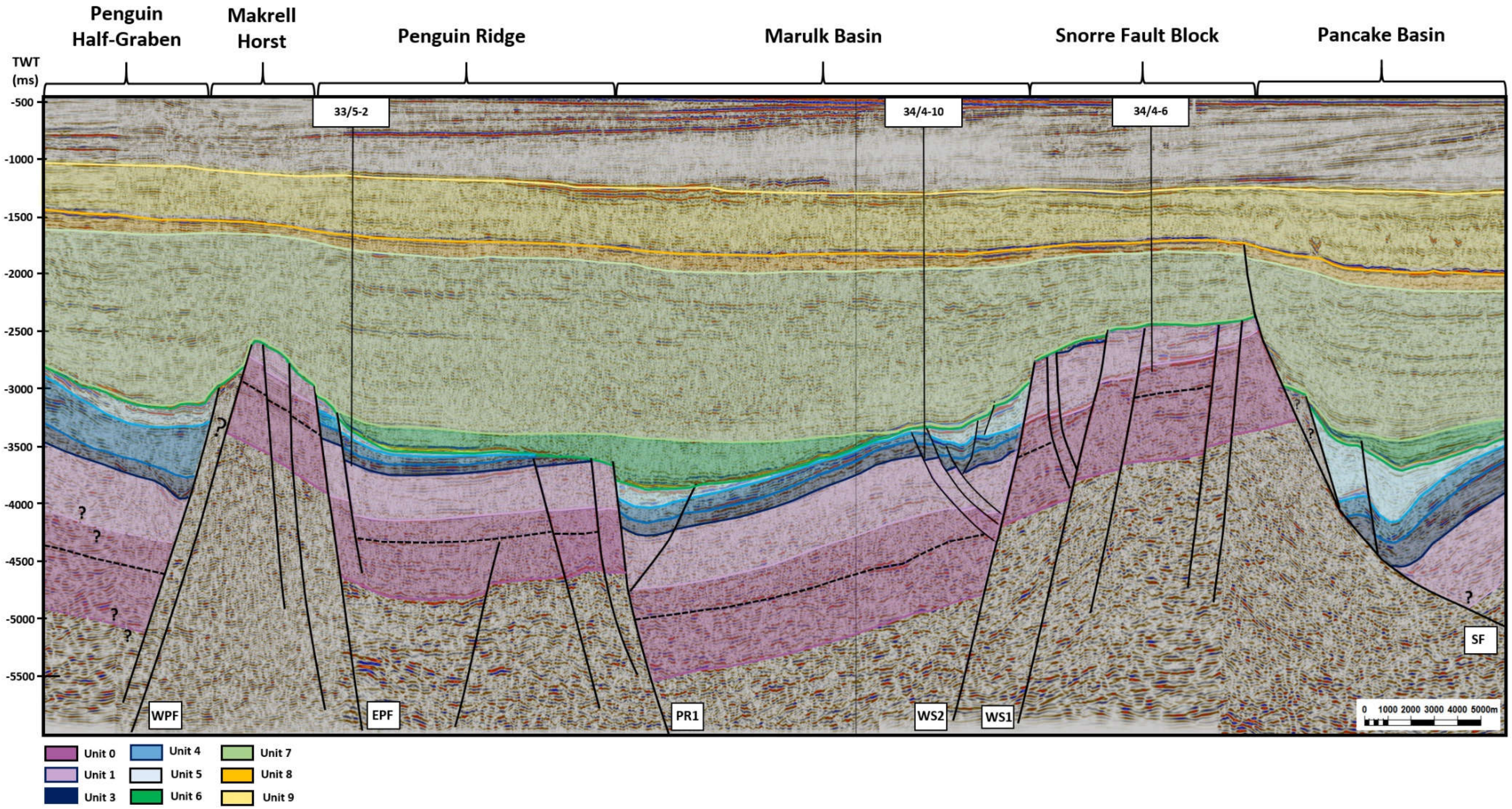

Figure 14: Interpreted seismic section from the Penguin Half-Graben in the west to the Pancake Basin in the East, crossing the southern end of the Marulk Basin. Location of seismic line is indicated in Figure 12. WPF, West Penguin Fault; EPF, East Penguin Fault; PR1, Penguin Ridge 1 Fault; WS2, Western Snorre 2 Fault; WS1, Western Snorre 1 Fault; SF, Snorre Fault.

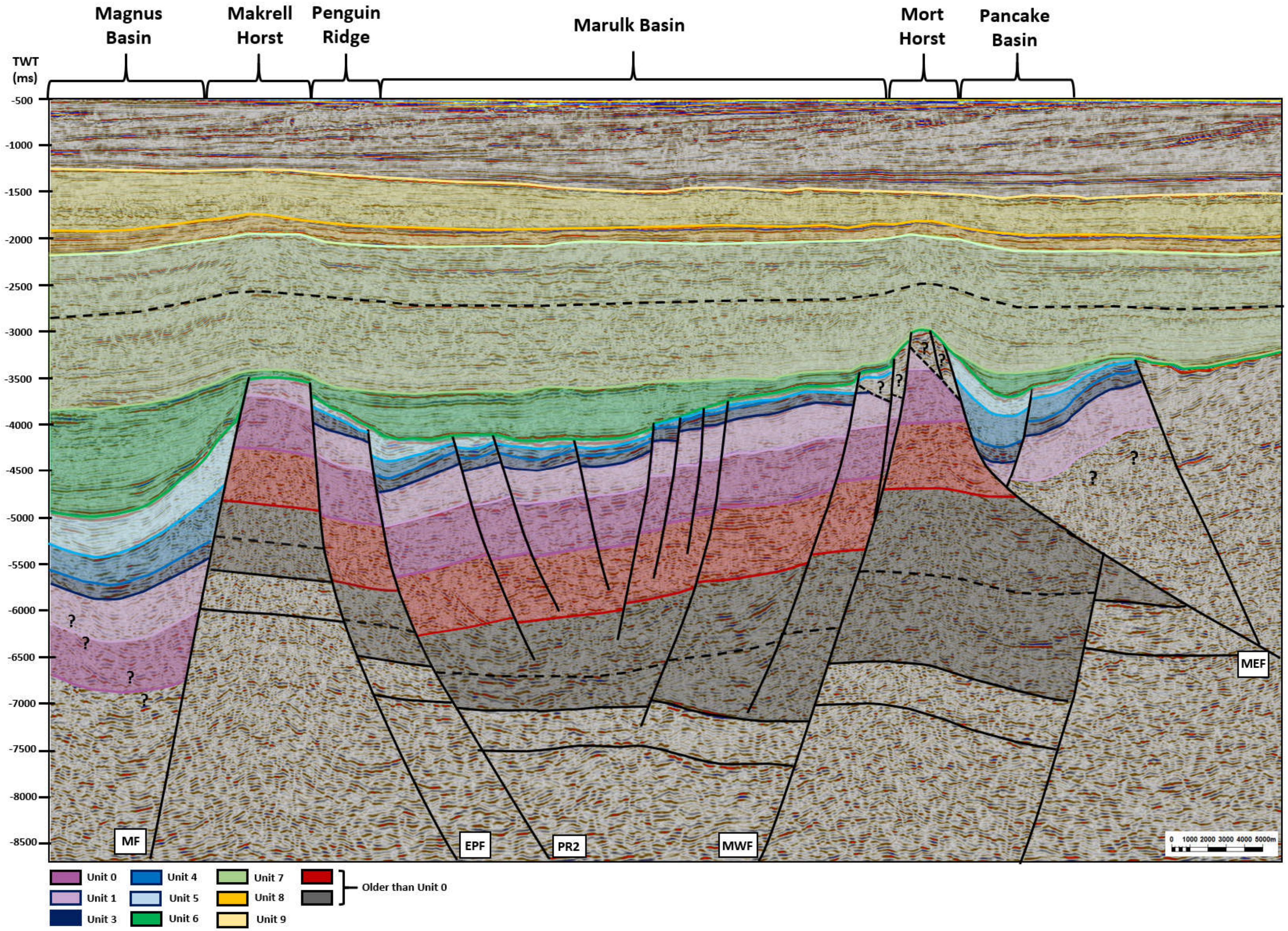

Figure 15: Interpreted 2D seismic line from the Magnus Basin in the west to the northernmost expression of the Pancake Basin in the east. Location of seismic line is indicated in Figure 12. MF, Magnus Fault; EPF, East Penguin Fault; PR2, Penguin Ridge 2 Fault; MWF, Mort West Fault; MEF, Mort East Fault.

Snorre Fault

One of the most prominent structural features in the study area is the major Snorre Fault, which extends from the Gullfaks Fault Block in the south to the Mort Horst in the north (Figure 11, SF). The Snorre Fault is approximately 50 km long and defines the eastern limit of the Snorre Fault Block, which is offset from the downthrown Pancake Basin (Figure 14). In the northern part of the fault, the trend is approximately NNE-SSW, but changes towards the south (NNW-SSE), before it links up with the Visund Fault. The seismic interpretation of the fault reveals steep fault plane geometry in the shallowest part, with a gradual decrease in dip with depth, resembling a listric normal fault (Figure 14).

The northern part of the Snorre Faults displays fault geometries that differ from farther south. Synthetic normal faults have developed in the hanging wall, linking up vertically with the main fault and creating secondary terrace structures (Figure 14). From this point and northward the fault terminates into an overlap zone defined by the northernmost part of the Snorre Fault and the southernmost part of the Mort East Fault (Figure 16A). The two faults are linked by WNW-ESE trending cross faults, defining the transition down to the basin (Figure 16B).

The Snorre Fault offset stratigraphy from the Top Rogaland reflector to the intra Triassic reflectors and deeper. Only minor throw is seen on the Top Shetland and Top Rogaland reflectors, but throw on the BCU is measured to around 600 ms. Throw at near Top Statfjord level along the Snorre Fault increases northwards to a maximum of ~3000 ms at the northeastern margin of the Snorre Fault Block (Figure 17). Fault throw decreases rapidly northwards before the fault dies out in the overlap zone (Figure 16B).

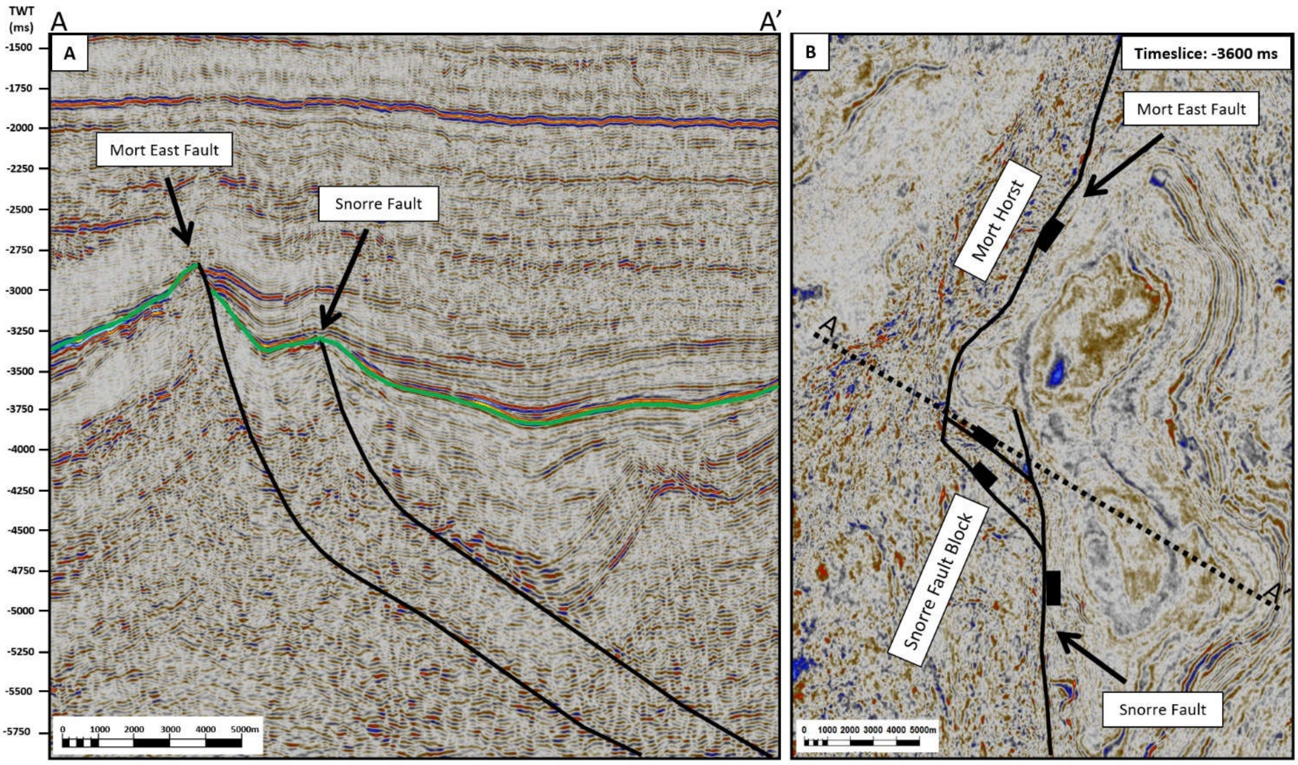

Figure 17: Transition zone between the Snorre Fault and the Mort East Fault. The seimic section (A) shows the relative overlapping of the two faults defining the Northern termination of the Snorre Fault Block and the southern termination of the Mort Horst. This can also be seen in the time slice (B) with related NNE dipping cross faults. Location of seismic line is indicated in Figure 12.

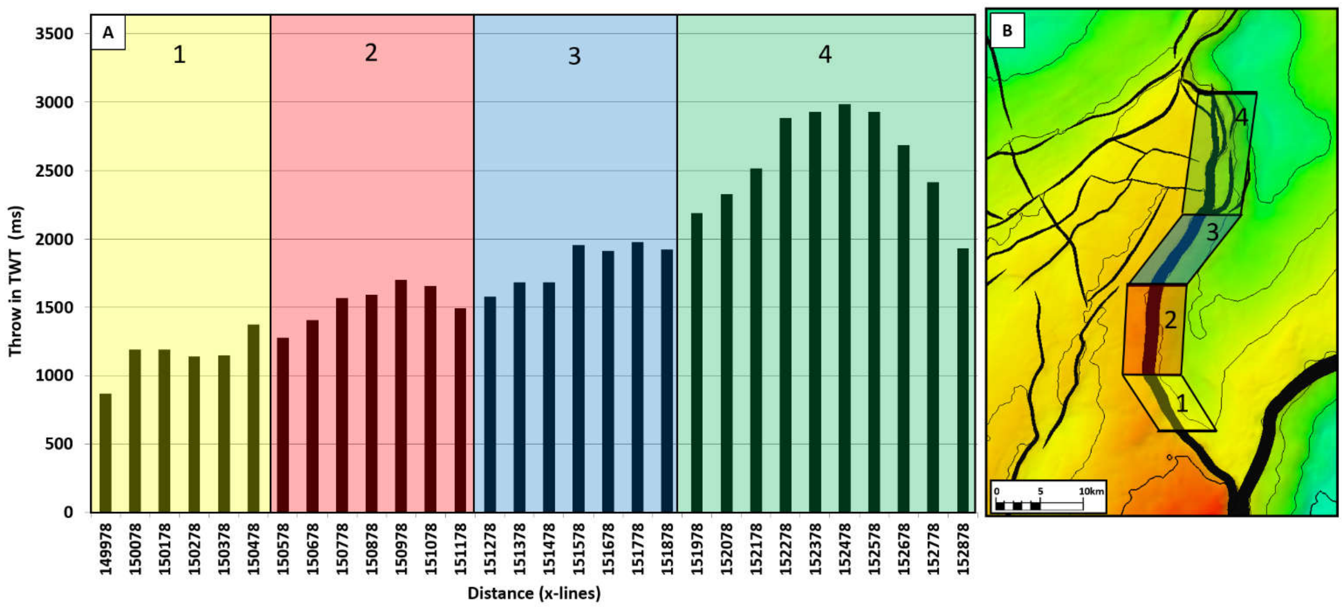

Figure 16: Measured TWT throw along the Snorre Fault. The Near Top Statfjord reflector is used as reference, projected in the northern areas. The diagram is divided into four segments (A) shown in map view (B).

Mort East Fault

The Mort East Fault defines the eastern margin of the Mort Horst (Figure 11; Figure 15). On the BCU level the Mort East Fault is 21 km long, trends approximately NNE-SSW, and dips ESE to SE. The southern extension of the fault defines the western boundary of the overlap zone with the Snorre Fault (Figure 16). To the north, the Mort East Fault is truncated by a younger fault system related to the Mort West Fault (Figure 18). The fault plane of the Mort East Fault is well developed as a continuous reflection in most seismic lines, enabling study of variations in fault-plane geometry along strike. The fault plane is interpreted in four seismic sections along the Mort Horst (Figure 19). In the northernmost area, the fault plane is recognized with a similar geometry as the Snorre Fault, steep in the shallowest part and gradual decrease in dip with depth (Figure 19A, B). The geometry of the fault changes into a ramp-flat-ramp geometry southwards (Figure 19C, D). Thus, a transition from a simple listric fault geometry to a more complex ramp-flat-ramp geometry is recognized near the northern tip of the Snorre Fault Block. However, in the overlap zone between the Mort East Fault and the Snorre Fault, both faults are purely listric (Figure 16).

Variations in hanging wall deformation styles are also recognized along the Mort East Fault. The northern part is characterised by a rollover anticline (Figure 19A, B) with local development of internal antithetic faults (Figure 19B). Farther south, the rollover anticline becomes more subtle (Figure 19C), whereas in the southernmost part, a more chaotic deformation pattern is observed, with possible development of synthetic accommodation faults connecting with the lower listric ramp (Figure 19D).

Offset of the Mort East Fault is observed at all stratigraphic levels from the BCU (only minor) to the Triassic and possibly basement level. Measuring throw along strike of Mort East Fault is difficult due to the complex internal structure of the horst, resulting in the lack of a confident reference reflector. However, the near Top Teist reflector is interpreted in two seismic sections along the fault (Figure 19B, C). Similar throw of approximately 1500 ms are measured for these sections into the downthrown Pancake Basin. Fault throw from the BCU to the Jurassic reflectors is largest in the southern end of the Mort Horst and decrease northwards (Figure 13).

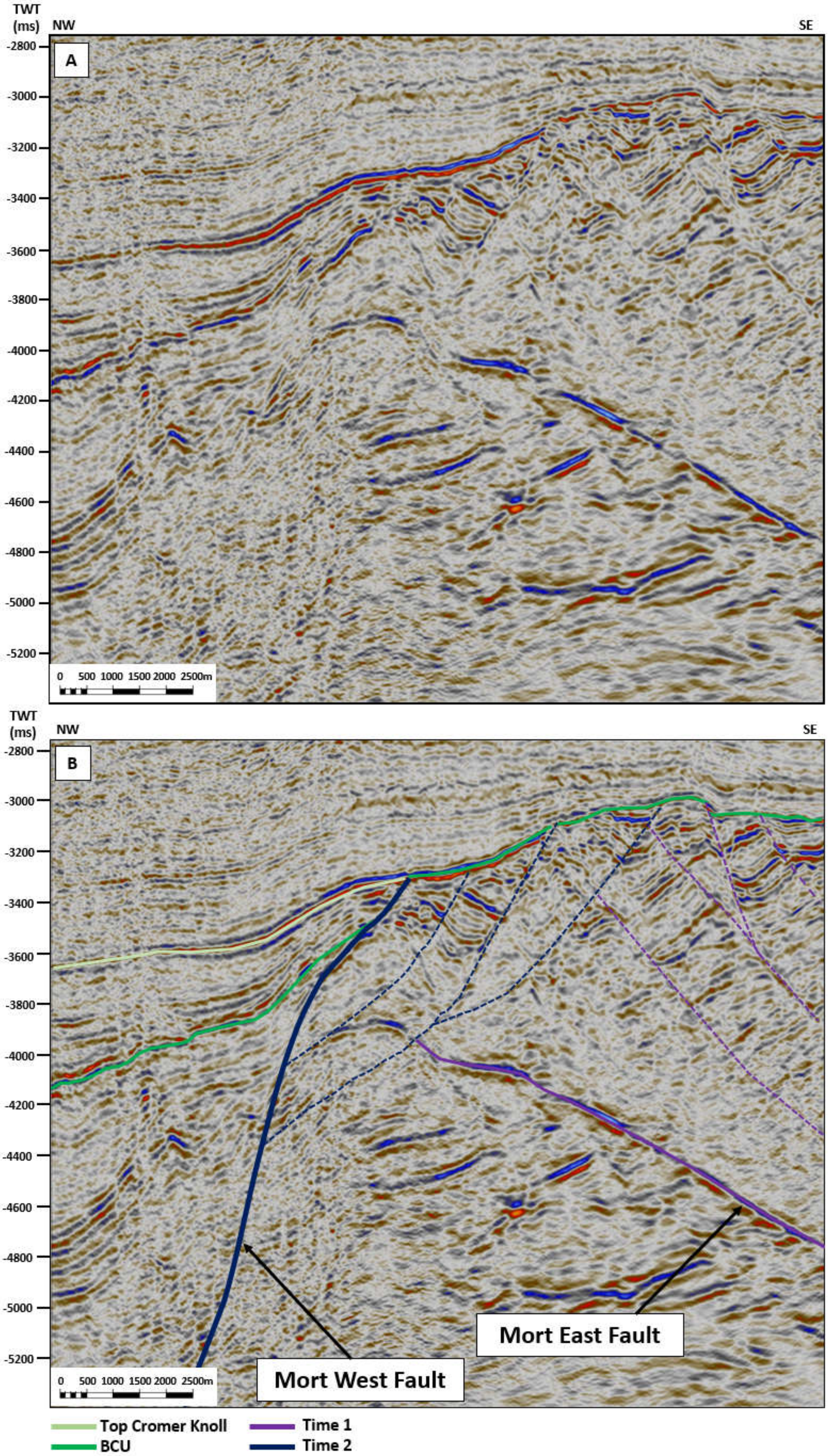

Figure 18: (A) NW-SE seismic section and (B) interpreted seismic section north of Mort Horst illustrating the relationship between the Mort East Fault and the Mort West Fault. Location of seismic line is indicated in Figure 12

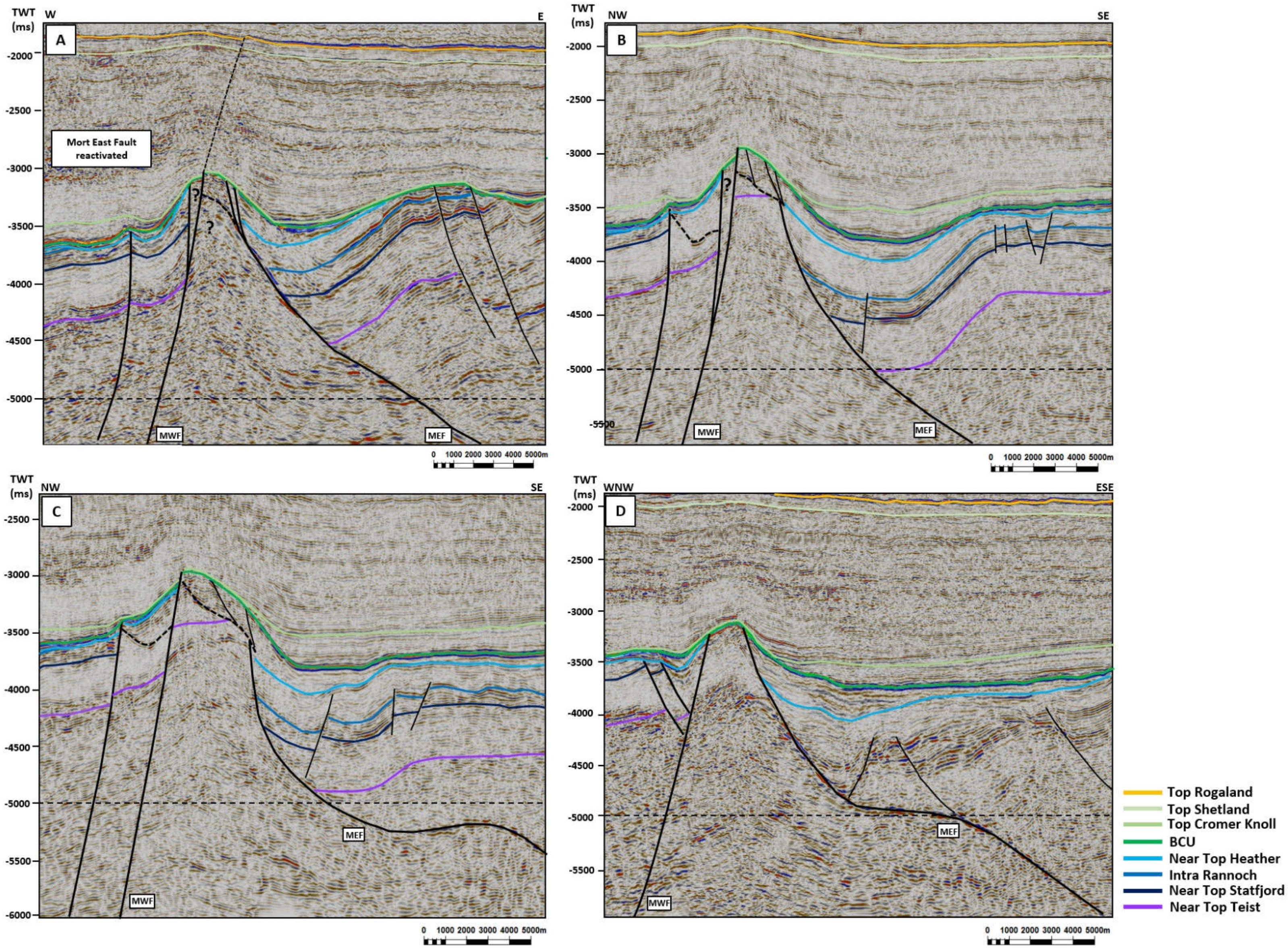

Figure 19: Seismic sections from north (A) and south (B, C and D) along the Mort Horst. The seismic sections display the progressive development of fault plane and hanging wall deformation along strike of the Mort East Fault and the Mort West Fault. Location of seismic line is indicated in Figure 12. MWF, Mort West Fault; MEF, Mort East Fault.

Mort West Fault

The Mort West Fault is approximately 50 km long and defines the western limit of the Mort Horst. The fault trends parallel to the Mort East Fault, and dips WNW to NW (Figure 11). In contrast to the Mort East Fault, the Mort West Fault is interpreted as a steeply dipping planar normal fault (Figure 19). The Mort West Fault continues northwards where it interferes with the major NW-dipping Marulk North Fault, generating the deepest part of the basin (Figure 11). Towards the south, the Mort West Fault terminates towards the NE-SW trending Western Snorre 2 Fault (Figure 11). The Mort West Fault offset stratigraphy from the Top Rogaland Group down to basement level (Figure 15). Offset on the Top Rogaland reflector is local and only minor. For the BCU, a general northward increase in displacement is recognized (Figure 11). Throw on the Near Top Teist reflector is measured on the same seismic sections as the Mort East Fault (Figure 19B, C). In the south (Figure 19C), throw on the Near Top Teist Reflector is measured to approximately 400 ms, increasing to ~490 ms further north (Figure 19B). Thus, fault displacement seems to increase northwards. The deeper layers and fault plane of the Mort West Fault is interpreted (Figure 15) and indicates similar throw for the deeper and shallower intra-Triassic reflectors.

Western Snorre Fault Zone

The northwestern limit of the Snorre structure is defined by several NE-SW trending faults, the largest of these are herein referred to as the Western Snorre 1 Fault (WS1) and the Western Snorre 2 Fault (WS2) (Figure 11). The WS1 fault extends for about 28 km and is interpreted as a steeply dipping normal fault (Figure 11; Figure 20). The WS1 fault offsets stratigraphy from Top Shetland down to Triassic and possibly deeper (Figure 20B). Only minor throw is seen on the Top Shetland reflector, while the BCU and Top Cromer Knoll reflectors show maximum throw between 100-200 ms. Throw along the WS1 increase southwards to a maximum in the range between 500-600 ms for the Near Top Teist reflector.

The WS2 fault shows similar length and runs parallel to the WS1 with similar geometry, trend and dip direction (Figure 11; Figure 20). Offset along the WS2 fault is observed from Top Cromer Knoll down to intra-Triassic reflectors. Maximum throw on the BCU and Top Cromer Knoll is similar to the WS1 fault (100-200 ms), while maximum throw of the Near Top Teist reflector exceeds the WS1 fault, with measurements in the range between 750-850 ms.

A dynamic relationship between the WS1 and WS2 is recognized. To the north, most of the throw has accumulated on the WS1 Fault (Figure 20A). This changes gradually in a southward direction, where more throw is picked up by the WS1 Fault (Figure 20B). As a result, the fault block bounded by the WS1 and WS2 faults deepens gradually towards SW as evident on the structural maps (Figure 13). Lack of deeper seismic data of good quality prevents interpretation of the deep layers and fault geometries. However, the large displacement of the Triassic reflectors suggests that these faults go all the way down to basement level

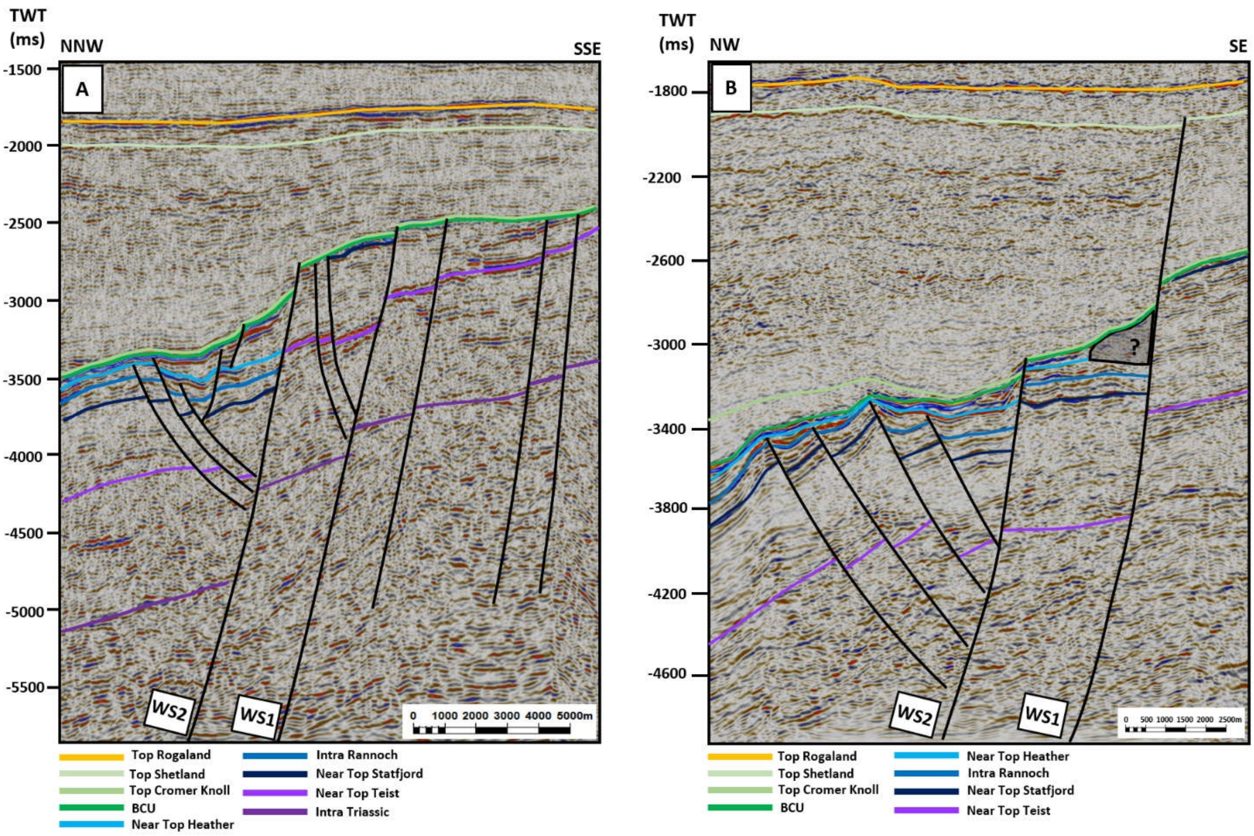

Figure 20: Two seismic lines crossing the Western Snorre Fault Zone. In the north (A) most throw is evident for the WS2 fault, changing gradually towards the southern section (B), where most throw is on the WS1 fault. Location of seismic lines is indicated in Figure 12.

West Penguin Fault

The West Penguin Fault is approximately 31 km long and bounds the Makrell Horst to the west (Figure 11; Figure 14). The fault is oriented approximately NNE-SSW, dipping in a northwesterly direction and is interpreted as a steeply dipping planar normal fault (Figure 21B and C). The West Penguin Fault interacts with the NE-SW trending Magnus Fault in the northern end of the Makrell Horst, which results in a slight change in structural trend (Figure 11). A marked change in structural trend is also seen at the southern end of the horst, where the West Penguing Fault deflects and is intersected by a southwest dipping fault zone. This change in trend at the southern end of Makrell Horst is discussed in detail by Domínguez (2007), who refers to the fault zone as the Penguin Lineament (Figure 11). The West Penguin Fault shows offset from Top Cromer Knoll down to basement level. The throw profile for the West Penguin Fault is poorly constrained due to low confidence in seismic mapping of intra-Triassic reflectors west of Penguin Horst, and poor well control for the deeper stratigraphy. The throw on Top Cromer Knoll and BCU is measured to be between 100-200 ms increasing northwards (Figure 13) and based on the Near Top Teist interpretation (Figure 21B, C), throw between 1600-1700 ms is estimated.

East Penguin Fault

The NNE-SSW trending, ESE-dipping East Penguin Fault is about 31 km long and separates the Makrell Horst from the Penguin Ridge to the east (Figure 11; Figure 14). Similar to the West Penguin Fault, the East Penguin Fault is interpreted as a steeply dipping, planar normal fault (Figure 21). The northern termination of the East Penguin Fault is uncertain due to lack of seismic data. However, based on interpretation of available 2D seismic lines, it is possible that the fault terminates against the northeastern bounding fault of the Penguin Ridge (described below). The southern termination is defined by a gradual reduce in displacement, before the fault dies out near the Penguin Lineament (Figure 11).

Offset on the East Penguin Fault is seen from the Top Cromer Knoll down to intra-Triassic reflectors and basement level (Figure 15). Throw on the East Penguin Fault is less compared to the West Penguin Fault as indicated by the difference in relief of intra-Triassic and Jurassic reflectors between the Penguin Ridge and the Penguin Half-Graben (Figure 21). Throw on the Near Top Teist reflector is estimated in three seismic sections along the fault. In the norther and southern transects (Figure 21A, C), throw is similar and measured to be approximately 500 ms. In the middle transect, the Top Teist reflector is measured with throw between 750-850 ms (Figure 21B).

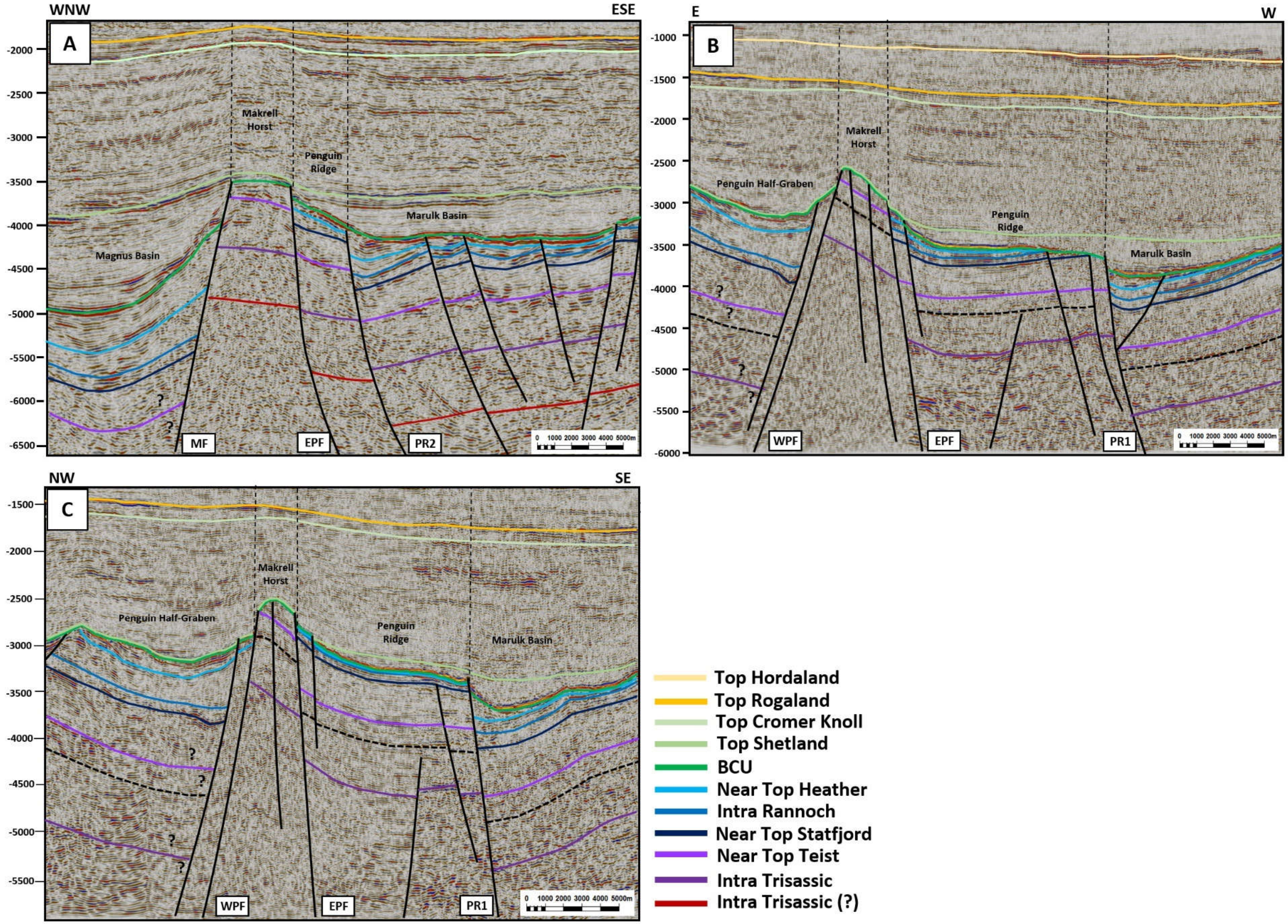

Figure 21: Seismic sections across (A) the northern end and (B,C) the southern end of the Makrell Horst. MF, Magnus Fault; WPF, West Penguin Fault; EPF, East Penguin Fault; PR1, Penguin Ridge 1 Fault; PR2, Penguin Ridge 2 Fault. Location of seismic lines is indicated in Figure 12

Eastern Penguin Ridge Fault zone

The Penguin Ridge is the downthrown half graben of the East Penguin Fault. The eastern boundary of the Penguin Ridge is defined by two faults with different trends. In the south the ridge is bounded by the Penguin Ridge 1 Fault (PR1), trending NE-SW with an SE oriented dip (Figure 11). The PR1 fault is approximately 28 km long and is interpreted to have steeply dipping, planar fault geometry (Figure 21B, C). Lack of deep seismic images of good quality inhibits interpretation of the deeper fault geometries, but rotation of the downthrown hanging wall block indicates a slight listric component in the deeper parts of the fault.

In the north, the PR1 fault terminates abruptly towards the Penguin Ridge 2 Fault (Figure 11). Southwards, a slight decrease in offset is seen along strike until fault branching occurs with offset partitioning between the PR1 fault and Marulk South Fault (Figure 11; Figure 13). The fault is interpreted southwards past the southern end of Penguin Ridge, with gradual decrease in displacement. Offset on the PR1 is seen from the BCU down to the Triassic and possibly deeper. Throw is largest in the northern end where it measures between ~700 ms, using the Near Top Teist reflector as reference (Figure 21B, C). However, an upward decrease in throw is seen along the fault plane in these seismic sections, with larger throw on the Intra-Triassic reflectors compared to the Jurassic reflectors, suggesting pre-Jurassic fault activity.

In the north, the eastern boundary of the Penguin Ridge is defined by the approximately 26 km long, ENE dipping Penguin Ridge 2 Fault (PR2) (Figure 11). The PR2 fault shows a trend markedly different from the main structural trend within in the area, striking approximately NNW-SSE. The trend of the PR2 fault can be traced through the Marulk Basin and into the Snorre Fault Block, with faults of opposite dips (Figure 11). The PR2 fault is interpreted as a steeply dipping normal fault with a slight listric component accounting for rotation in the downthrown hanging wall block (Figure 15).

The PR2 fault is interpreted to be the bounding fault of the Makrell Horst in the north (Figure 22), suggesting that the East Penguin Fault terminates into the PR2 fault south of this seismic section. The PR2 fault is not recognized in seismic further north, indicating possible termination towards the Magnus Fault. Offset on the PR2 fault is seen from the BCU down to basement level (Figure 15), and contrasting to the PR1 fault, the PR2 fault shows similar throw for the deep and shallower intra-Triassic reflectors. The Jurassic structural maps reveal northward increase in throw along the Penguin Ridge, reaching ~360 ms at Top Statfjord level at the northern end of the ridge (Figure 13A). In the northern seismic line (Figure 21A) the throw of the Near Top Statfjord and the Near Top Teist reflector is 500-550 ms.

Magnus Fault

The Magnus Fault trends approximately NE-SW and dips towards the NW (Figure 11). In the north the fault is depicted on 2D seismic (Figure 15: Figure 22) as a steeply dipping normal fault, bounding the upthrown Makrell Horst and the central Marulk Basin from the Magnus Basin. Offset is recognized from the BCU and deeper and throw on the BCU is measured to ~470 ms, decreasing northwards (Figure 15; Figure 22). Lack of seismic data extending into the British sector inhibits southward interpretation along strike of the Magnus Fault.

Marulk North Fault

The Marulk North Fault is a major fault defining the deepest part of the Marulk Basin on BCU level (Figure 11). The Marulk North Fault trends approximately NE-SW, but changes to NNE-SSW northwards. The fault is recognized by large throw (~860 ms) on the BCU marker horizon and its eroded footwall crest (Figure 23). Smalls offsets are recognized on reflectors within the Cromer Knoll Group, reaching up to the Top Rogaland reflector, suggesting fault reactivation. Detailed interpretation of the Marulk North Fault is hindered by variation in seismic quality and lack of well control.

Summary

The NNE-SSW trending Snorre Fault, Mort East Fault and Penguin West Fault are the major (first order) faults within the study area, with measured throw in the range of 1500-3000 ms. Large throw is also seen for the NE-SW trending Magnus and Marulk North faults. The first order normal faults show a variation from steeply dipping to listric and ramp-flat ramp fault plane geometries and acts as the main bounding faults of the large fault blocks and the deep basins in the study area. The study area is further subdivided by normal faults with maximum throw in the range from 500-850 ms (second order) including the Mort West Fault, East Penguin Fault, Western Snorre Fault Zone and the Eastern Penguin Ridge Fault Zone. The second order normal faults are steeply dipping and shows a greater variation in trend (NE-SW, NNE-SSW and NNW-SSE).

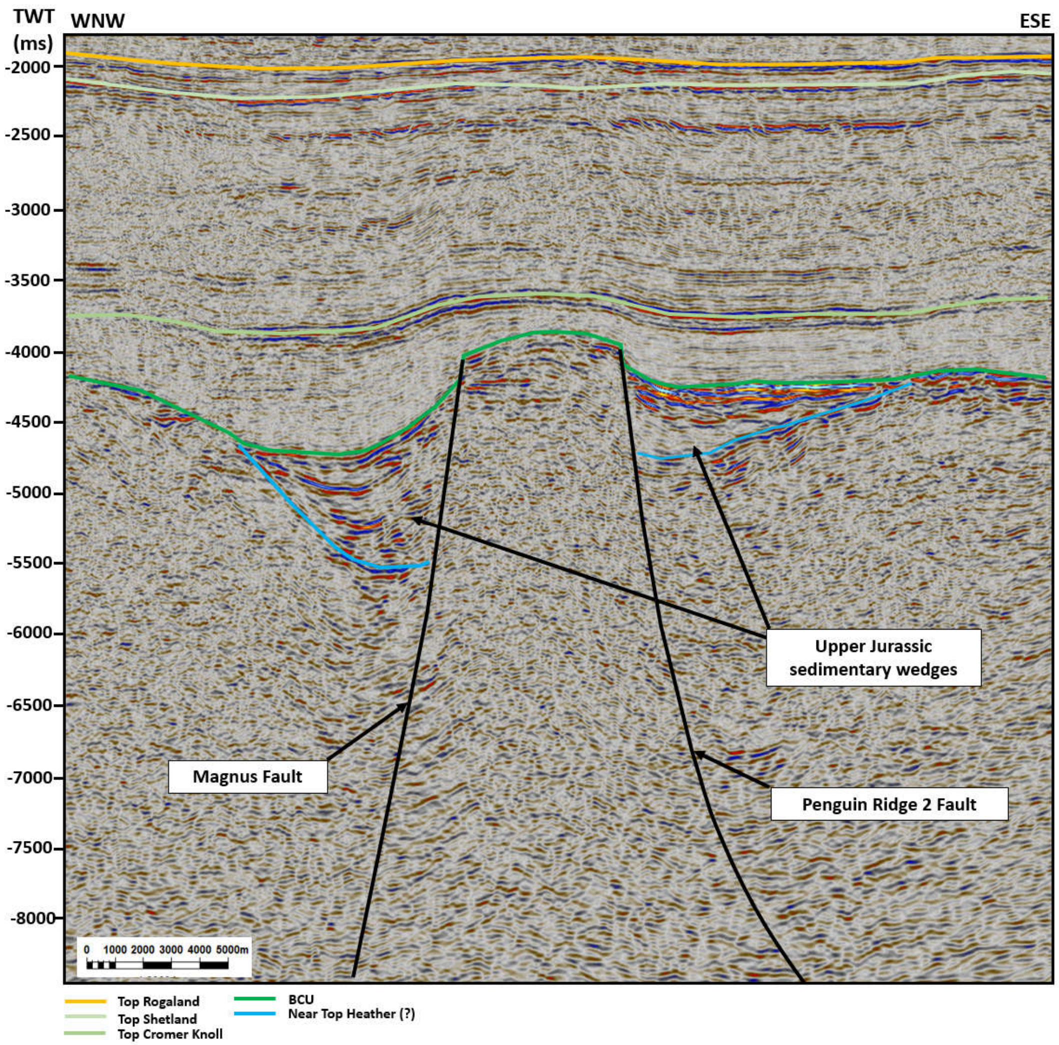

Figure 23: 2D seismic line across the northernmost expression of the Makrell Horst. Location of seismic line is indicated in Figure 12.

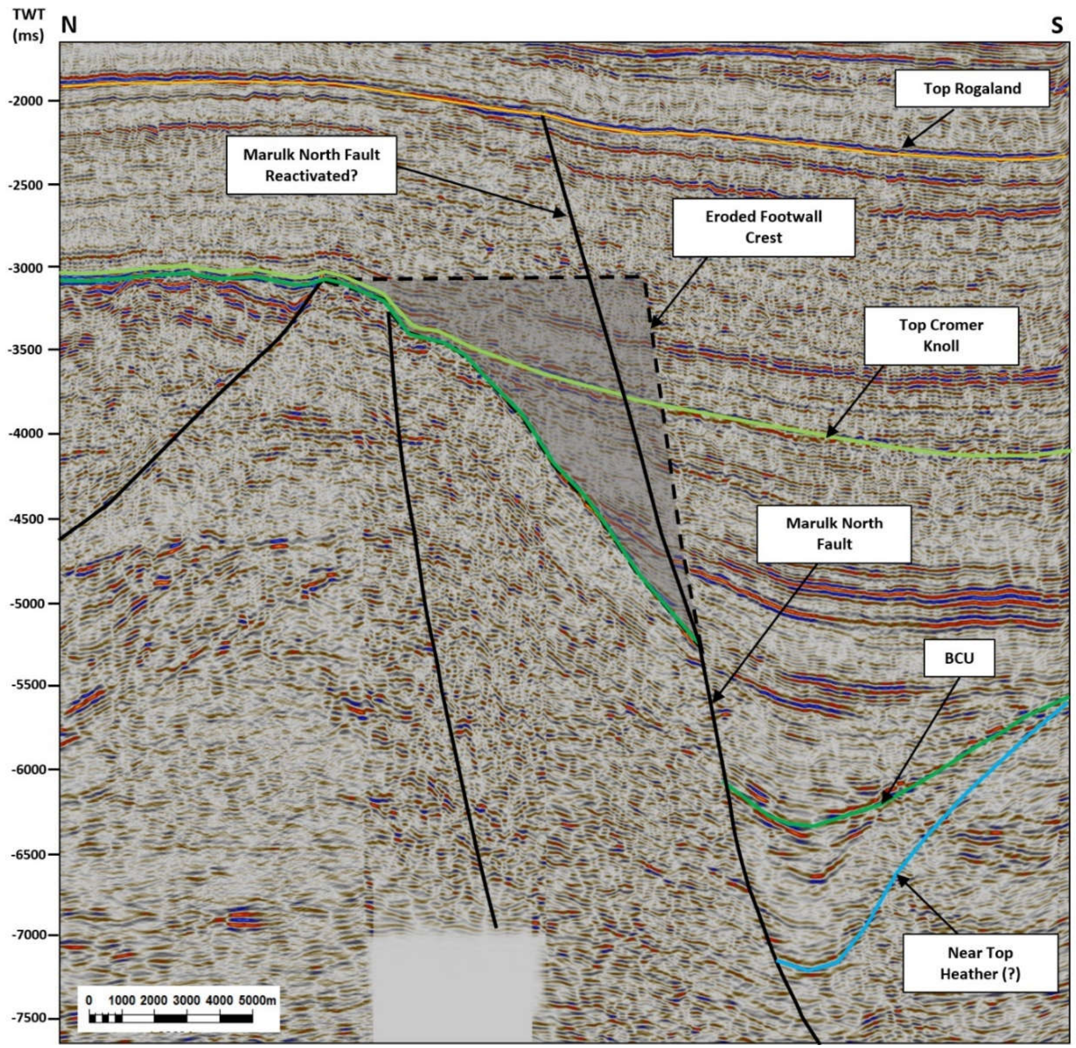

Figure 22: Seismic line crossing perpendicular to the NE-SW trending Marulk North Fault, generating the deepest part of the Marulk Basin. Location of seismic line is indicated in Figure 12.

4.3 Structural Styles

The faults described above defines the framework of the structural highs and lows with the study area. The following chapter aims to describe the structural elements within the area through a series of interpreted seismic sections (Figure 24). The important structural elements to be described are the Snorre Fault Block, the Mort Horst, the Makrell Horst, the Penguin Ridge and finally, the Marulk Basin (Figure 11).

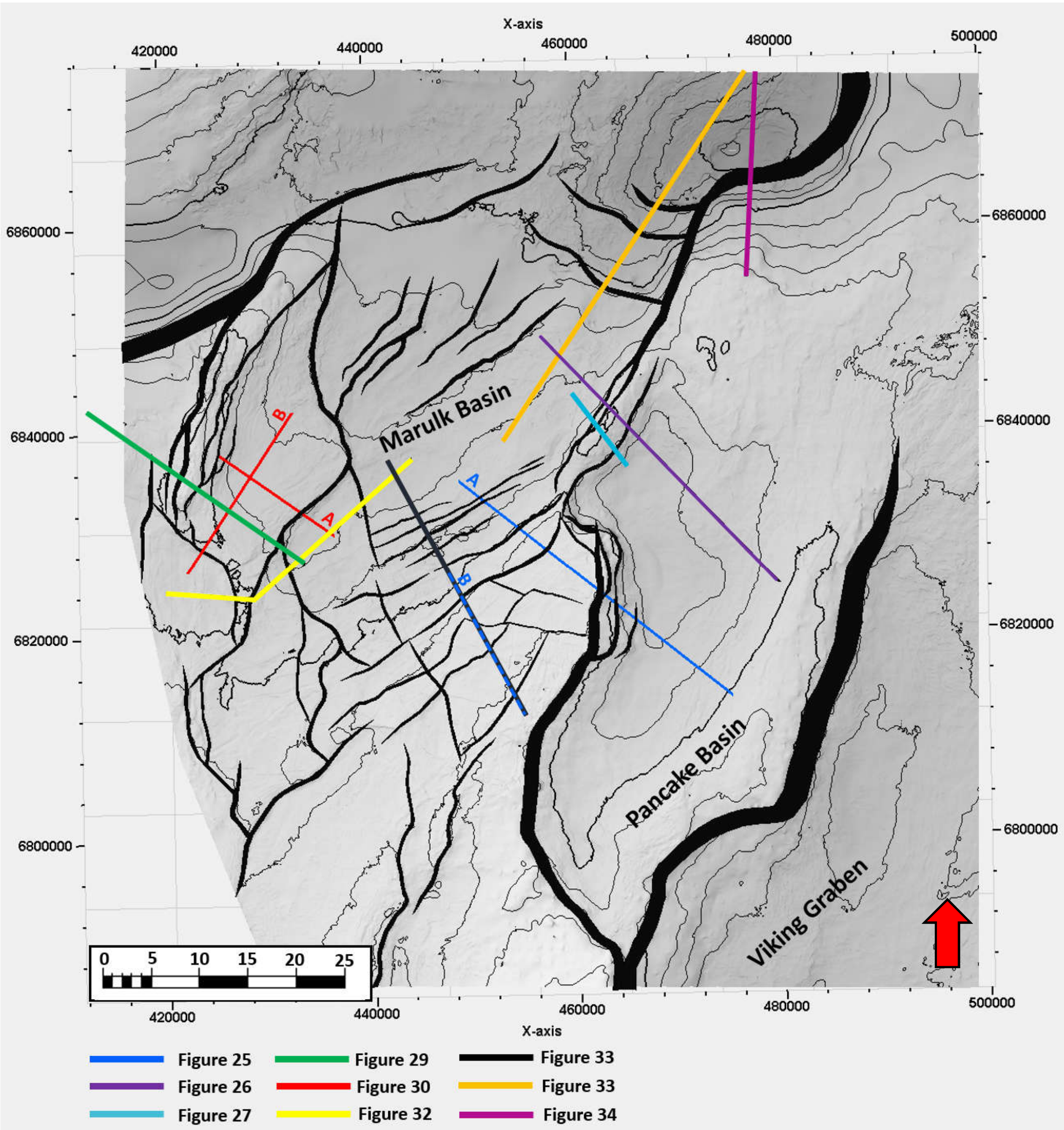

Figure 24: BCU structure map showing the location of the seismic sections described in section 4.3.

4.3.1 Snorre Fault Block

The Snorre Fault Block is the northernmost of the large westerly tilted fault blocks defining the Tampen Spur area. The fault block is a marked structural high, limited by the major Snorre Fault to the east and the Western Snorre Fault Zone (WS1 and WS2) to the NW (Figure 11). The fault block is shallowest in the eastern crestal areas, at ~2350 ms at BCU level. In the north, the fault block is recognized by an unconformable relation between the Lower Cretaceous Cromer Knoll Group and the Upper Triassic Lunde Formation. Both the eastern and western flank of the fault block is show offset into the Paleogene as observed on structural maps (Figure 13) and cross sections (Figure 25).

Internal Triassic reflectors are observed with a westerly dip that can be correlated into the southern Marulk Basin. The Triassic successions (Unit 0 and 1) show similar thickness from the Marulk Basin and into the Snorre Fault Block (Figure 14). However, within the fault block itself, eastward thickening is evident (Figure 25). Correlation of Unit 0 and Unit 1 into the SF hanging wall was not performed due to the high uncertainty in intra-Triassic reflection picks within the Pancake Basin. The Lower Jurassic succession (Unit 2) is preserved and interpreted both east and west of the Snorre Fault Block. Within the northern end of the fault block, however, this succession is not present as reflectors are truncated by the BCU further south (Figure 25B). The thickness of Unit 2 is observed to be larger in the Pancake Basin compared to the Marulk Basin. A similar trend is seen for the Middle-Upper Jurassic succession (Unit 3), although with a more pronounced thickness increase in the Pancake Basin.

The uppermost Jurassic unit (Unit 4) is a thick succession within the Pancake Basin, with rapid eastward thinning defining distinct sedimentary wedges. Unit 4 have also developed wedge geometries in the hanging wall of the WS2 fault, although less pronounced than in the Pancake Basin (Figure 25A). The Lower Cretaceous Cromer Knoll Group (Unit 5) is not seismically mappable across the Snorre Fault Block but is present in the adjacent Pancake and Marulk basins. A thin layer of the uppermost Cromer Knoll Group (Rødby Formation) is, however, encountered by the many wells drilled through the structure (e.g. 34/4-5) proving the presence of a thin veneer of the uppermost Lower Cretaceous across the structural high. The Snorre Fault Block is a pronounced structure showing thinning of the overburden for the Shetland, Rogaland and Hordaland groups (Units 6, 7 and 8) (Figure 14; Figure 25A).

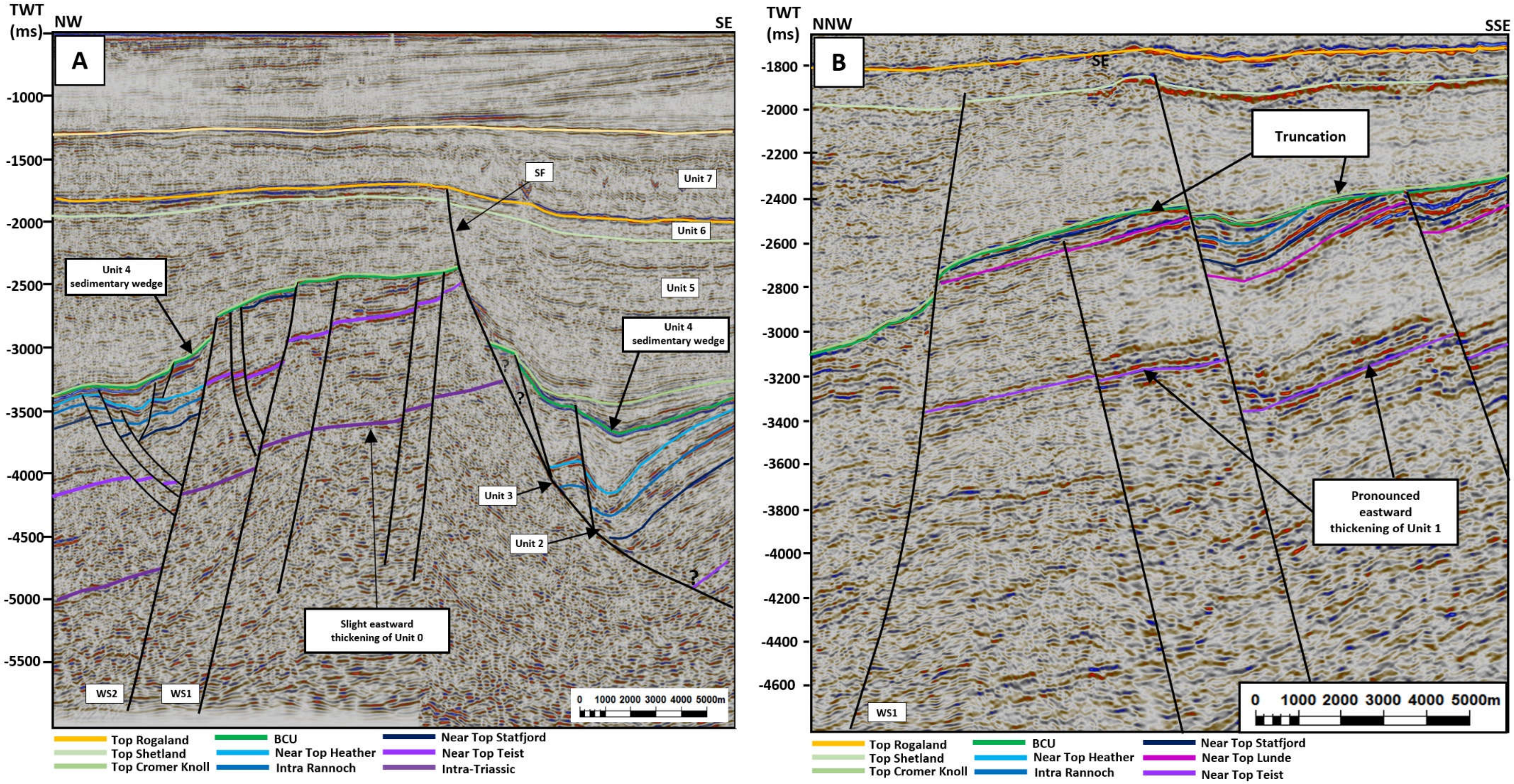

Figure 25: Seismic sections showing (A) NW-SE transect across the northern end of the Snorre Fault Block and (B) eastward thickening and truncation relations farther south. Location of the seismic lines is indicated in Figure 24. WS2, Western Snorre 2 Fault, WS1, Western Snorre 1 Fault; SF, Snorre Fault.

4.3.2 Mort Horst

The Mort Horst is a structural high confined by normal faults both to the east and west (Mort East Fault and Mort West Fault, respectively) as previously described. The structure is drilled by well 34/4-5, which encountered the horst at a depth of 3245 m (MD) at BCU level. The structure is a pronounced feature in the seismic, extending approximately 18 km northeast from the northern tip of the Snorre Fault Block. The horst is recognized with offset into post-Jurassic times as indicated by the structural maps (Figure 13). For the shallower Upper Cretaceous reflectors, the horst appears as an elongate low-relief anticline (Figure 13F; Figure 26).

An unconformable relation between the Lower Jurassic Statfjord Group and the Upper Triassic Lunde Formation is recorded in well 34/4-5 (Figure 27). The unconformable relation represents a gently east dipping fault plane, here referred to as the Intra Mort Fault, that can be mapped out from north to south along the horst. The fault plane is a detachment surface separating small fault blocks above from the sub-horizontal to slightly west-dipping Triassic seismic reflectors below. For the purpose of the regional interpretation, the fault surface was interpreted as the Top Statfjord Group and is therefore depicted in the time structure map of Top Statfjord (Figure 13A).

The seismic signature of the low angle fault plane can be correlated with similar seismic response and similar dip in the hanging wall of the Mort West Fault (Figure 26; Figure 27). The stratigraphy above the Intra Mort Fault plane in the downthrown block is unknown, as it has not been drilled by any wells. However, based on the stratigraphic intervals recorded above the fault plane in well 34/4-5, it is possible that Middle to Upper Jurassic intervals are preserved in this block. The observations above suggest that the Intra Mort Fault is cut by the Mort West Fault. The relation between the Intra Mort Fault and Mort East Fault is different. The detached fault block above the Intra Mort Fault is interpreted to carry across the Mort East Fault, thus, the Mort East Fault is cut by the Intra Mort Fault (Figure 26).

The intra-Triassic successions (Unit 0 and older) within the Marulk Basin have similar thickness within the Mort Horst (Figure 15), and no significant difference in thickness is observed between the Upper Triassic succession (Unit 1) in the eastern hanging wall of the Mort Horst, compared to the eastern Marulk Basin (Figure 26). The Lower Jurassic succession (Unit 2), on the other hand, shows more pronounced thickness increase within the Pancake

Basin than in the Marulk Basin. Establishing the thickness of Unit 2 within the horst is difficult, due to the level of deformation of this unit within the horst block itself.

The Middle to Upper Jurassic succession (Unit 3) thins to a thickness below seismic resolution west of the Mort Horst (Figure 26). The Intra-Rannoch reflector is interpreted to truncate against the Near Top Heather reflector, and thus, parts of the Heather Formation and upper part of the Brent Group are eroded west of the Mort West Fault (Figure 28). In the Pancake Basin, Unit 3 thickens towards the Mort East Fault, defining a distinct wedge geometry (Figure 26). Similarly, Unit 4 thickens towards the Mort East Fault, with maximum thickness at the southern the end of Mort Horst (Figure 16D). In the Marulk Basin, Unit 4 is very thin with a subtle increase in thickness towards the Mort West Fault.

Reflectors within the Cromer Knoll Group (Unit 5) onlap the BCU (Figure 26). In the Pancake Basin, Unit 5 reflectors onlap the BCU towards the Mort Horst. The reflectors also onlap the BCU farther to the east, defining a small Lower Cretaceous basin within the overall Pancake Basin. To the west, the BCU shows a westward deepening, with progressive eastward onlap of Unit 5 reflectors. The top Cromer Knoll reflector cannot be mapped above the Mort Horst, due to seismic resolution. However, a very thin layer of the lower and uppermost Cromer Knoll Group (Åsgard and Rødby Formation) is present above the BCU in well 34/4-4 (Figure 27). The Rødby Formation unconformably overlies the Åsgard Formation, suggesting either a period of erosion or possibly a hiatus. Reflectors of the lower Shetland Group (Unit 6) onlap the Cromer Knoll Group towards the Mort Horst. In the sediments above the horst, significant thinning is recognized throughout the Upper Cretaceous and Paleocene.

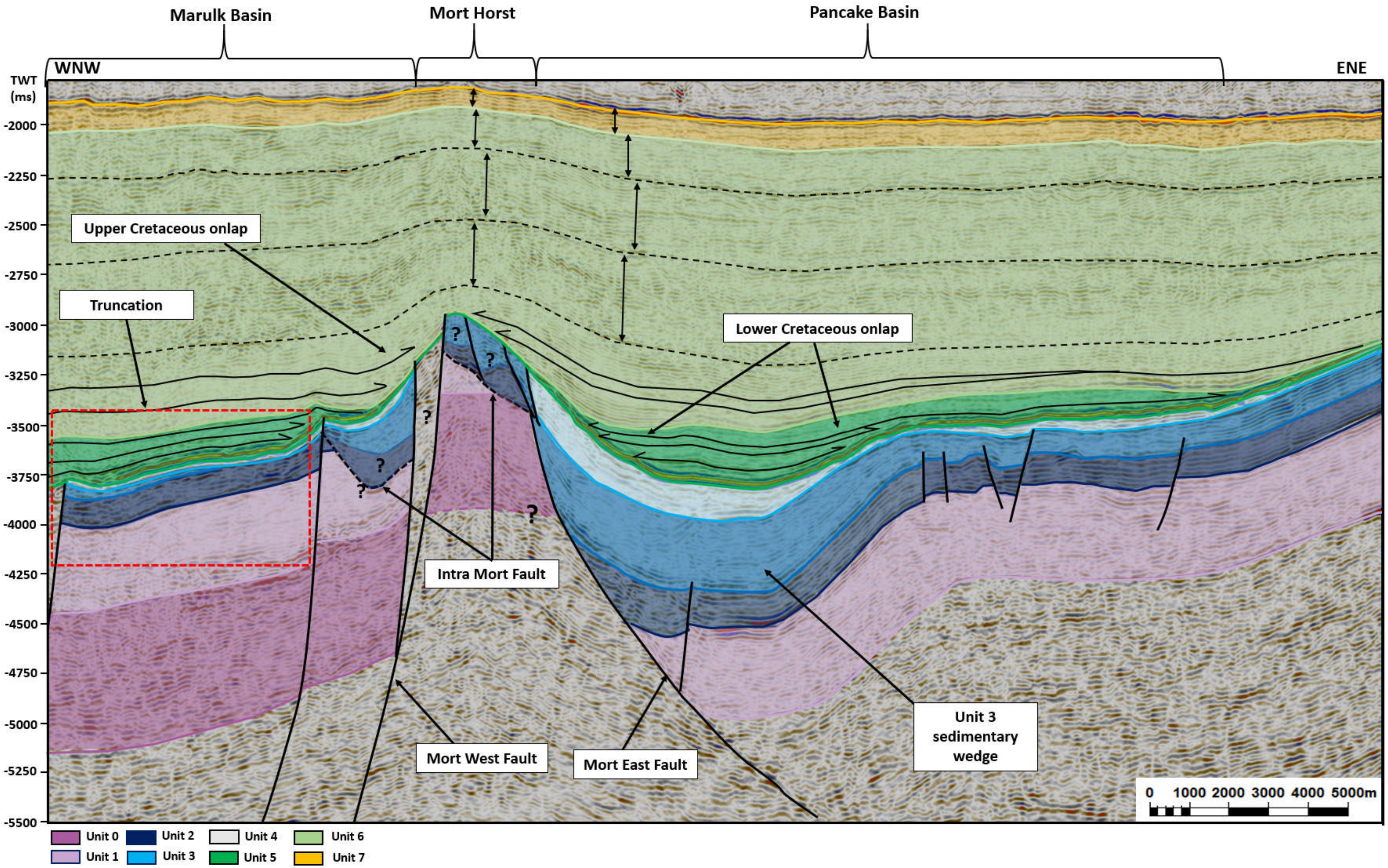

Figure 26: WNW to ENE seismic section across Mort Horst with interpreted stratigraphic units. The red box defines the outline of figure 28. Location of the seismic line is indicated in Figure 24.

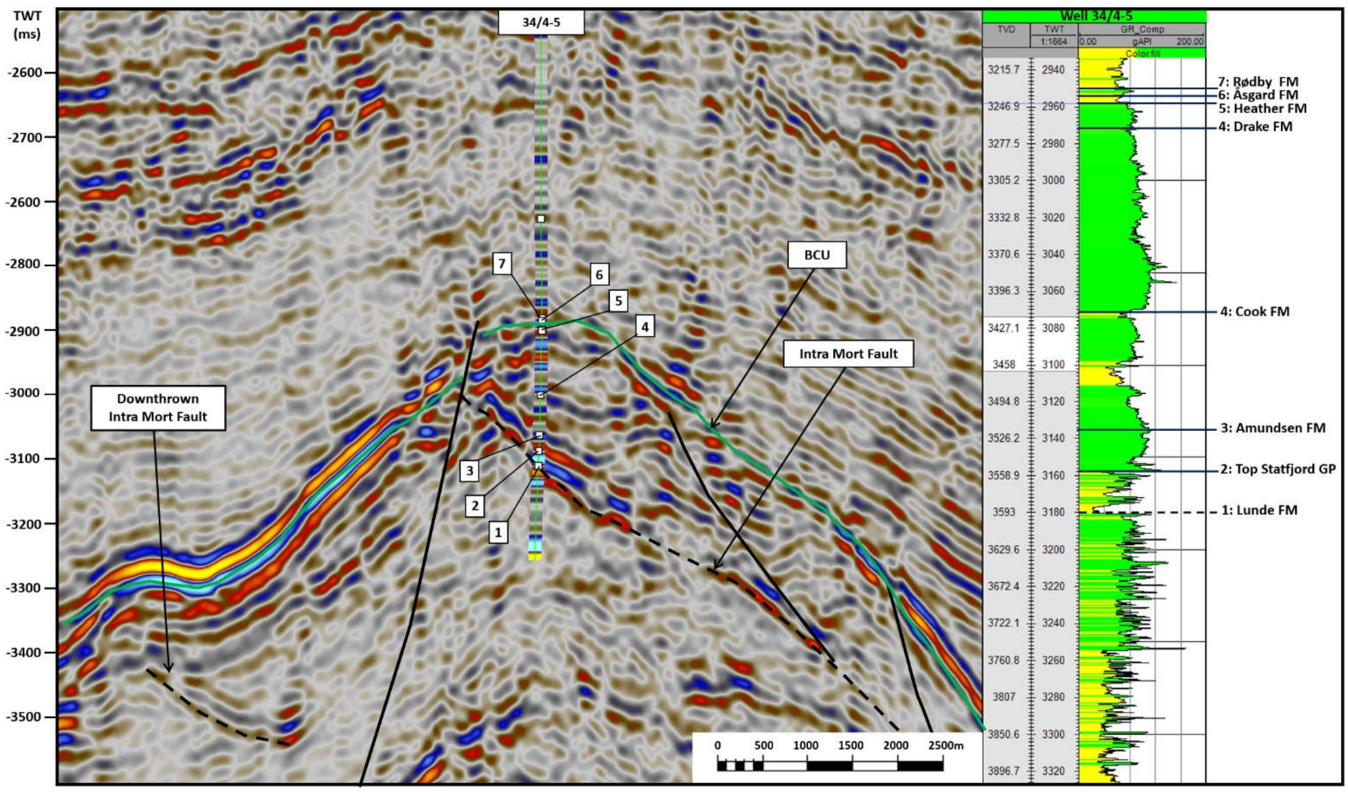

Figure 27: NW-SE seismic section across well 34/4-5 within the Mort Horst. Well-tops are displayed with related gamma-ray log readings. Location of the seismic line is indicated in Figure 24.

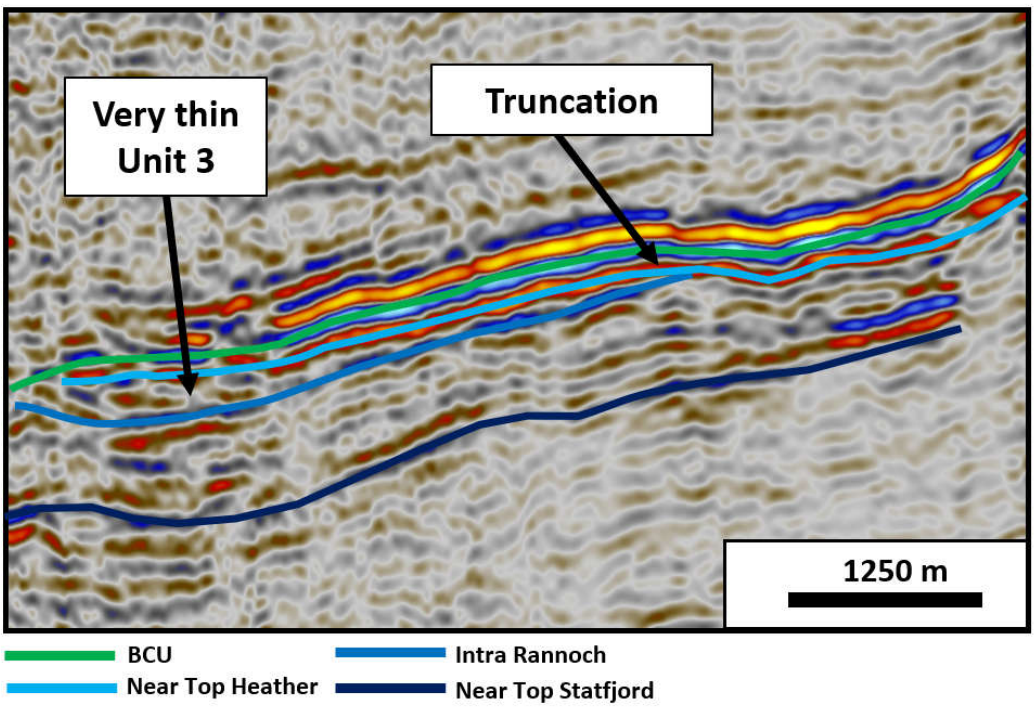

Figure 28: Zoom in of seismic west of the Mort Fault as indicated in figure 26, showing thinning of unit 3 and related truncation of the intra Rannoch reflector.

4.3.3 Makrell Horst

The Makrell Horst is a structural high trending SSW to NNE, bounded by the West Penguin Fault and the Magnus Fault to the west and the East Penguin Fault and Penguin Ridge (2) Fault to the east (Figure 11). Similar to the Mort Horst, the Makrell Horst is a pronounced feature in the seismic and can be traced approximately 35 kilometres from the East Shetland Basin in the south to the Magnus Basin in the north. At the shallowest BCU level, the horst is interpreted at approximately -2500 ms with gradual deepening towards the NNE. The structure is drilled by well 33/5-1 where the horst was encountered at 2692 m (MD) on BCU level.

At its crest, the horst is defined by an unconformable relation between the Lower Cretaceous Cromer Knoll Group and east dipping reflectors of the Upper Triassic Lunde Formation (Figure 29). However, the easterly dip of the internal reflectors is most prominent in the south, while in the northern areas, reflectors are gently west-dipping to sub-horizontal (Figure 15; Figure 22). Towards the south, the horst limits the Penguin Half-Graben to the west and Penguin Ridge to the east (Figure 29). In the north (Figure 15), the Makrell Horst is separated from the Magnus Basin to the west. Similar to the Mort Horst, the Makrell Horst offsets the post-Jurassic sediments as indicated by the structure maps (Figure 13), and the overburden is expressed by low relief, elongate anticlines that can be mapped into Paleocene times (Figure 13; Figure 29).

In the south, the thickness of the Triassic Unit 1 is similar within the Penguin Ridge and the Makrell Horst (Figure 29). Correlation into the Penguin Half-Graben is difficult due to lack of well data and poorly constrained Triassic reflectivity. In the north, Unit 0 and older units are interpreted with similar thickness in the Makrell Horst, Penguin Ridge and the Marulk Basin (Figure 15). Correlation of pre-Cretaceous units into the Magnus Basin is generally difficult. The Lower Jurassic interval (Unit 2) is generally thicker in the Penguin Half-Graben compared to the Penguin Ridge. The large displacement along the West Penguin Fault accommodates a thick Middle-Upper Jurassic succession (Unit 3), with well-developed wedge-geometry. This contrasts to the Penguin Ridge, where the same succession is very thin/absent due to truncation by the Near Top Heather reflector and the BCU (Figure 30). The uppermost Jurassic succession (Unit 4) thickens within the Penguin Half-Graben but thins towards the West Penguin Fault (Figure 29), and on the Penguin ridge, only a thin layer of Unit 4 is preserved (Figure 30). In the northernmost areas however, where the relief of the Mort Horst is interpreted to be controlled by the Magnus Fault and the Penguin Ridge 2 Fault, large Upper Jurassic wedge geometries have developed in both the eastern and western hanging walls (Figure 22).

Well 33/5-1, situated on the crest of the Makrell Horst, encountered 20 metres of the uppermost Cromer Knoll Group (Rødby Formation) (Unit 5), similar to the thickness range as found in the wells on the Mort Horst and Snorre Fault Block. Seismic mapping of the Cromer Knoll Group is challenging due to its low thickness in the area. However, the interpretation reveals that Unit 5 is present on the Penguin Ridge and increases in thickness away from the East Penguin Fault (Figure 29). The thickness of Unit 5 is thin and below seismic resolution in the Penguin Half-graben. In the Magnus Basin, however, significant subsidence along the Magnus Fault accommodates a thick Lower Cretaceous succession (Figure 15). The lower part of the Shetland Group (Unit 6) onlap the fault plane of the East Penguin Fault and the West Penguin Fault (Figure 29). The upper part of Unit 6 is divided into three sub-units (1, 2 and 3, Figure 29). Sub-unit 1 shows approximately equal thickness above and to each side of the Makrell Horst. This contrasts to sub-units 2 and 3 which show markedly thinning above the Makrell Horst. Similar thinning is also seen in the Rogaland Group (Unit 7).

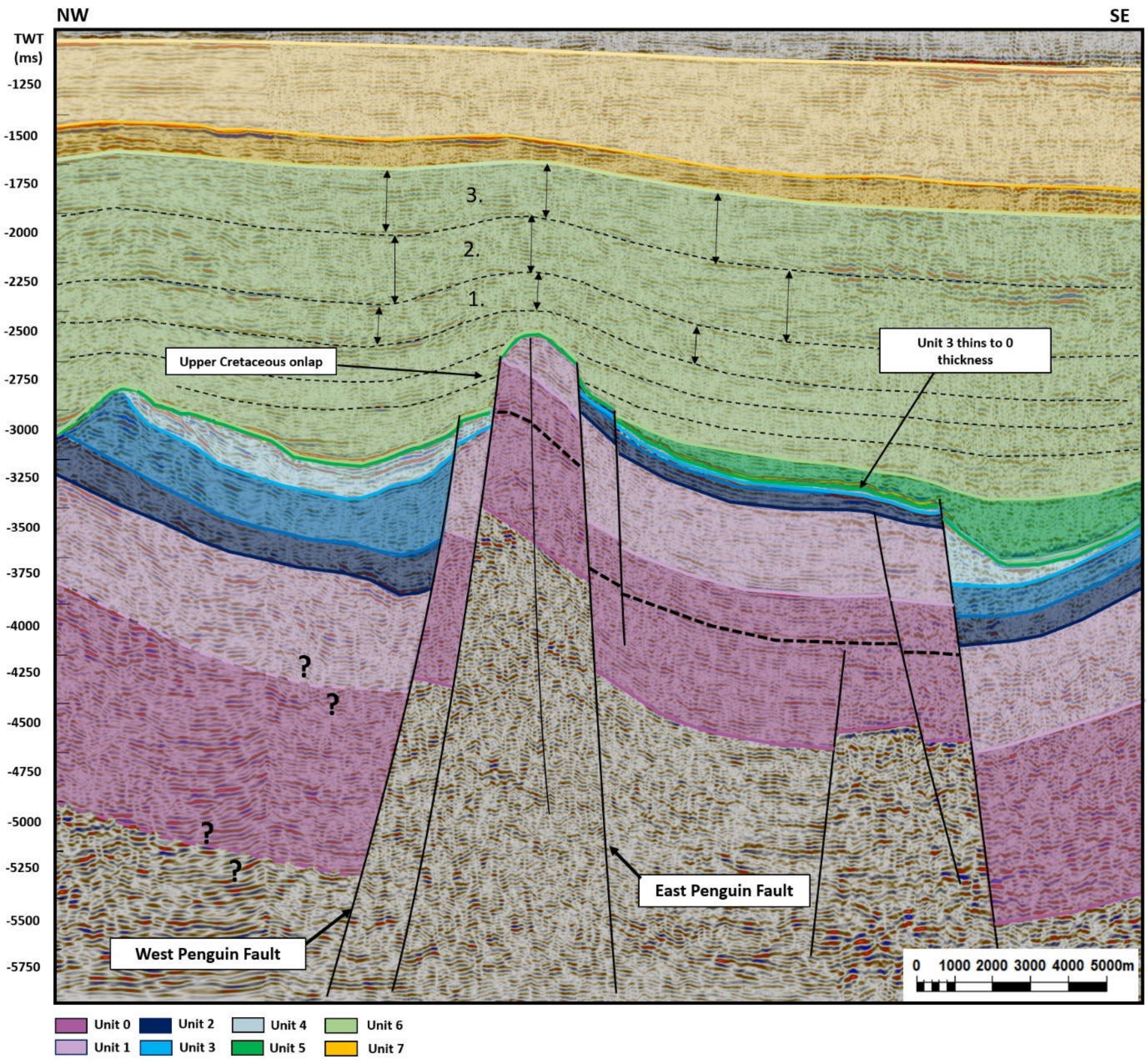

Figure 29: NW-SE seismic section from the Penguin Half-Graben in the west, ascross the Makrell Hors and Penguin Ridge, into the southern end of the Marulk Basin. Location of the seismic line is indicated in Figure 24.

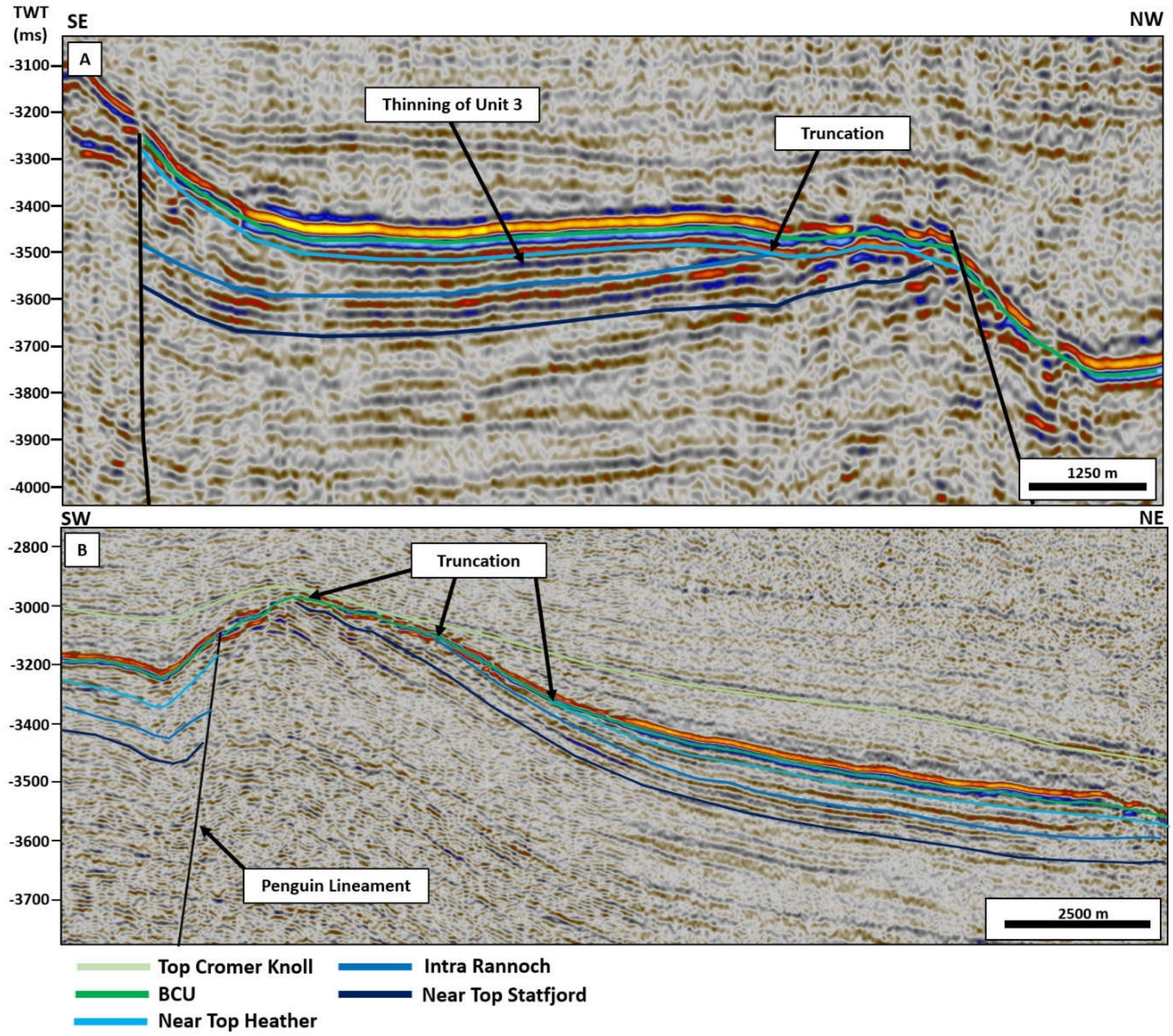

Figure 30: Seismic sections across the Penguin ridge showing (A) SW-NE thinning of Unit 3 and related truncation of reflectors at the eastern crest of the fault block, and (B) the southwestern margin of the Penguin Ridge defined by the SW dipping fault of the Penguin Lineament, and truncation of intra-Jurassic reflectors. Location of the seismic lines is indicated in Figure 24,

4.3.4 Penguin Ridge

In map view, the Penguin Ridge appears as an elongated structural high with a general deepening towards the north (Figure 31). At the shallowest, the ridge is encountered at -3000 ms on BCU level, while the deepest part is encountered approximately 1000 ms deeper. Its relief is controlled by faults of four different structural trends. Displacement on the East Penguin Fault defines a rotated half-graben structure where internal reflectors dip gently to the WNW (Figure 14). The eastern crest of the half-graben is defined by the Penguin Ridge 1 and Penguin Ridge 2 Faults (Figure 11). In the southwest, the ridge is limited by the Penguin Lineament (Figure 30B). In the south, the Penguin Ridge is bounded by the southern expression of the Penguin Ridge 1 Fault in the east, and opposite dipping normal faults in the west, defining a horst-like structural high where internal reflectors are sub-horizontal to gently east dipping (Figure 32).

Along the Penguin Ridge 1 Fault, the thickness of the Triassic successions (Unit 0 and 1) is less on the Penguin Ridge than on the Marulk Basin (Figure 14; Figure 29). Along the Penguin Ridge 2 Fault, however, no significant loss in thickness of these units is observed from the Marulk Basin into the Penguin Ridge (Figure 15). Both faults show increased thickness for the Middle-Upper Jurassic succession (Unit 3) in their respective hanging walls, but this unit thins both southward and eastward, and is truncated against the Near Top Heather reflector on the Penguin Ridge as described above (Figure 30). Similarly, uppermost Jurassic (Unit 4) wedge development is seen in the hanging walls of the Penguin Ridge 1 and Penguin Ridge 2 Faults (Figure 22; Figure 29), while only a thin layer of this unit is preserved on the ridge. Finally, the thickness of the Lower Cretaceous Cromer Knoll Group (Unit 5) is significantly reduced from the Marulk Basin into the Penguin Ridge. This is obvious both along the Penguin Ridge 1 Fault (Figure 29; Figure 32) and the Penguin Ridge 2 Faults (Figure 13; Figure 22).

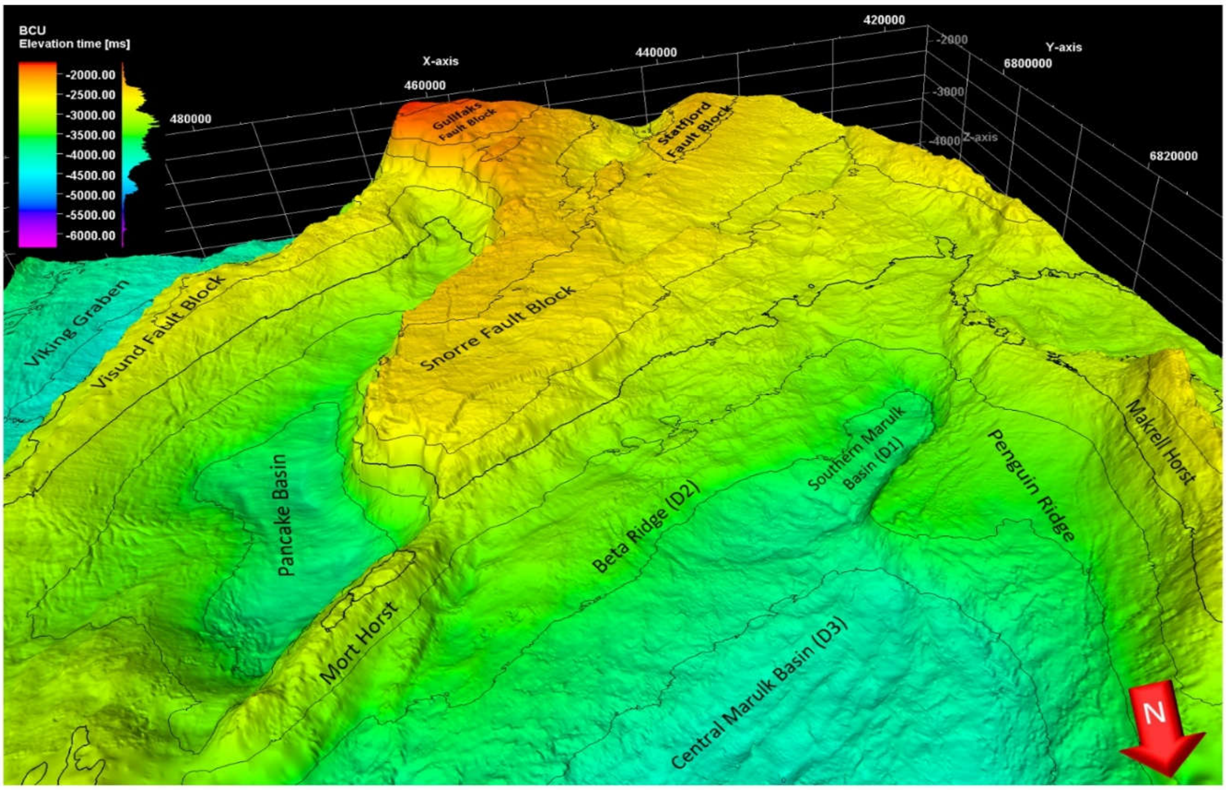

Figure 31: 3D map view of the BCU showing the southern and central areas of the Marulk Basin with adjacent basins and highs.

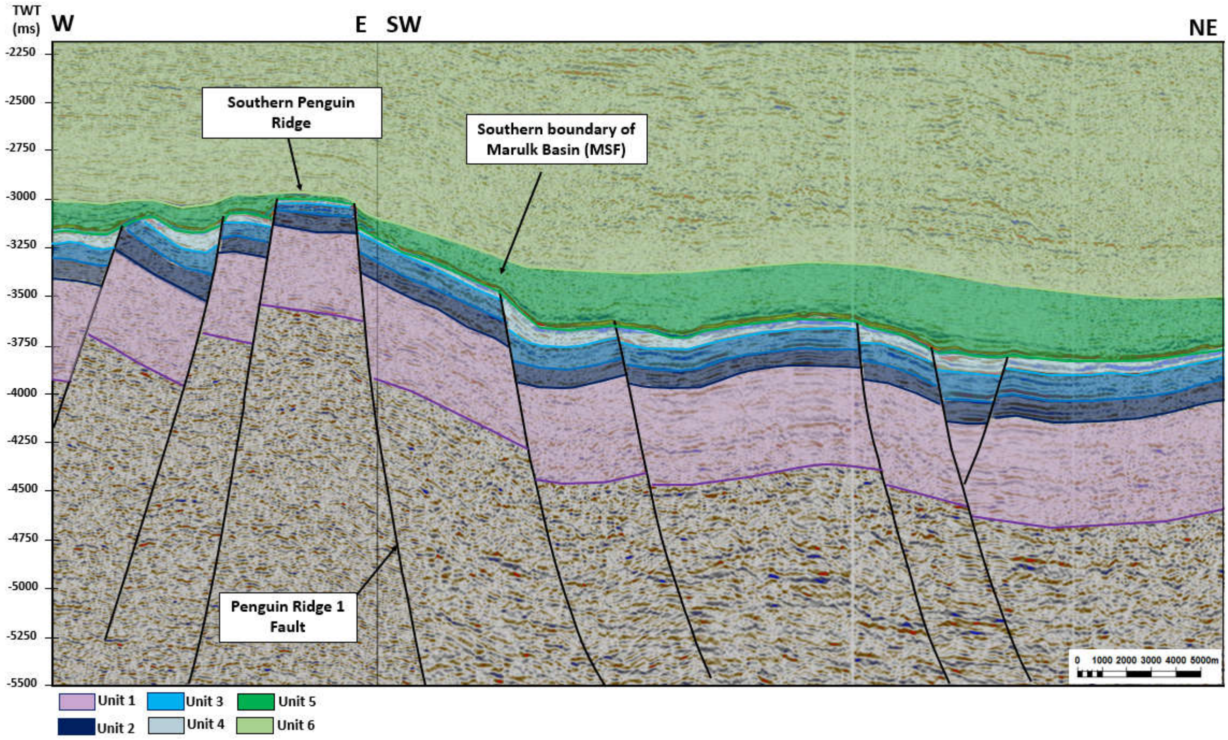

Figure 32: Seismic section crossing W-E across the southern Penguin Ridge and northeastward into the Marulk Basin. Location of the seismic line is indicated in Figure 24.

4.3.5 Marulk Basin

In map view, the Maruk Basin is a lense shaped elongated feature. The outer shape is defined by the major basin bounding structures as previously described. The internal basin geometries also show a wide range of structural configurations. In order to describe the different internal trends and structures, the greater Marulk Basin is divided into four separated structural domains covering the southern, central and northern areas of the basin (see Figure 11).

Domain 1: Southern termination of Marulk Basin

The southern end of the Marulk Basin is defined by the Penguin Ridge 1 Fault in the west, the Western Snorre 2 Fault in the east and the ENE-dipping Marulk South Fault in the southwest (Figure 11). The Marulk South Fault belongs to a series of NNW-SSE trending faults interpreted within the southern Marulk Basin (Figure 32). These faults are generally steeply dipping with and offset from BCU down to the Triassic stratigraphy. Throw is generally below 200 ms. Slight increased thickness of the Middle to Upper Jurassic successions (Unit 3 and Unit 4) is seen towards some of these faults, while Triassic and Lower Jurassic successions (Unit 1 and 2) show no change in thickness (Figure 32). The Marulk South Fault seems to play the most important control on Middle Jurassic to Lower Cretaceous thickness accumulation.

This is suggested by the thickening of the Upper Jurassic succession (Unit 4) in the hanging wall of this fault, and the thinning of the Cromer Knoll Group (Unit 5) above (Figure 32).

Domain 2: Beta Ridge

A low relief anticline trending parallel to the Western Snorre Fault Zone extends for about 21 kilometres along the hanging wall of the Western Snorre 2 Fault. This anticline is identified on the BCU and top Cromer Knoll level and defines the crest of the Beta Ridge (Figure 31). On the post-Cretaceous structure maps (Figure 13), the ridge is defined by a series of normal faults antithetic to the Western Snorre 2 Fault, creating tilted fault blocks with northwestward increase in rotation (Figure 33). The faults show similar offset in the Jurassic and Triassic reflectors. To the west of the Beta Ridge, the Middle to Upper Jurassic successions (Unit 3 and 4) gradually loose thickness (Figure 14; Figure 33) towards the ridge where the Near Top Heather reflector truncates against the BCU (Figure 34). The SW dipping faults define a graben structure towards the Western Snorre 2 Fault. The thickness of Unit 3 is preserved within the graben area which also displays an Upper Jurassic (Unit 4) wedge.

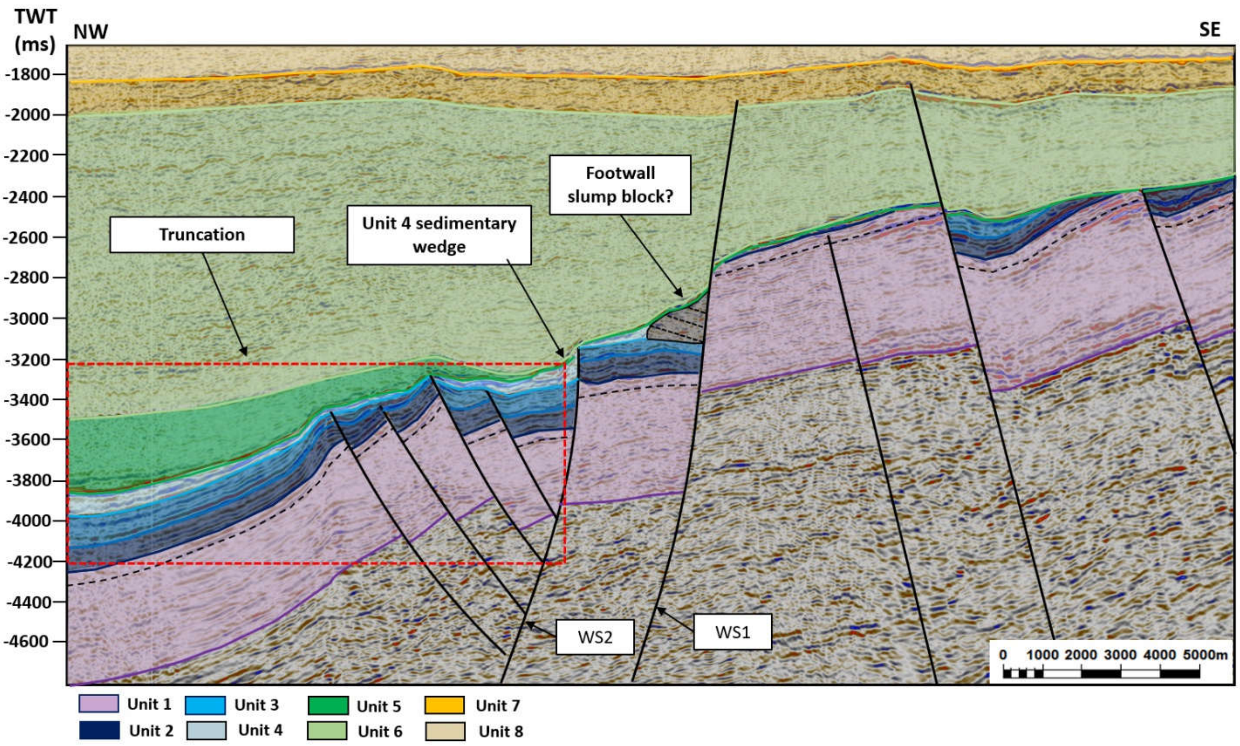

Figure 33: NW-SE seismic section crossing the Beta Eidge and into the Snorre Fault Block. The red box indicates the outline of Figure 34. Location of the seismic line is indicated in Figure 24.

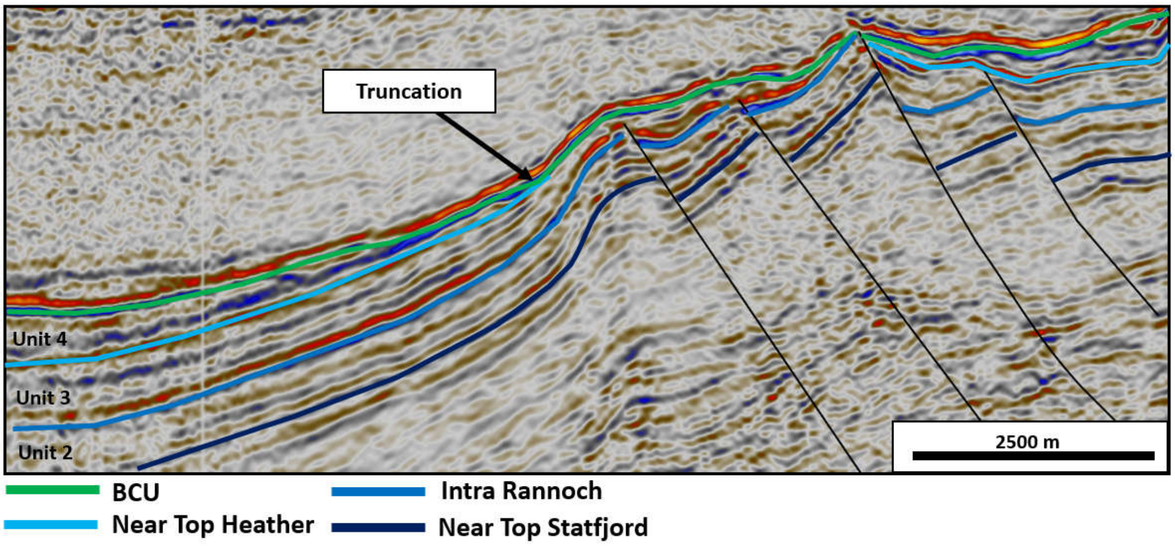

Figure 34: Zoom in of seismic west of the Beta Ridge as indicated in figure 33, showing the progressive eastward thinning of Unit 2 and 3 and related truncation of the Near Top Heather and older reflectors.

Domain 3: Central Basin area

The Marulk Basin appears as a lens-shaped structural low measuring up to 34 kilometres from the Magnus Fault in the NW to the Mort West Fault in the SE (Figure 11). On the post-Cretaceous structural maps, a general deepening trend is seen from the Mort West Fault to the Penguin Ridge 2 Fault (Figure 13). East of the Penguin Ridge 2 Fault, an area of opposite dipping faults defines a graben structure with NE-SW axial trend (Figure 11), offsetting Jurassic and Triassic layers with throw in the range of 100-300 ms. The faults east of the graben axis is steeper than the faults west of the graben axis, which shows westward increase in rotation (Figure 15).

Domain 4: Northern Expression

As previously mentioned, the major NW dipping Marulk North Fault defines the deepest part of the Marulk Basin in the north (Figure 23). The axis of this deep basin trends approximately NE-SW, like the graben of Domain 3. The northeastward deepening of the basin from Domain 3 to Domain 4, as seen on the BCU structure map, is controlled by several NE-dipping normal faults trending perpendicular to the two major fault zones in the north, defining a gradual stepping into the northernmost basin area (Figure 35). The normal faults mainly offset pre-Cretaceous successions, but seismic correlation and detailed fault mapping into this area is limited by the poor seismic quality and lack of well control. The resulting basin subsidence accommodated a thick succession of the Lower Cretaceous Cromer Knoll Group (Figure 17 and 35). In addition, a Lower Cretaceous wedge t is recognized within the deep Marulk Basin with layers thickening towards the Mort East Fault (Figure 36).

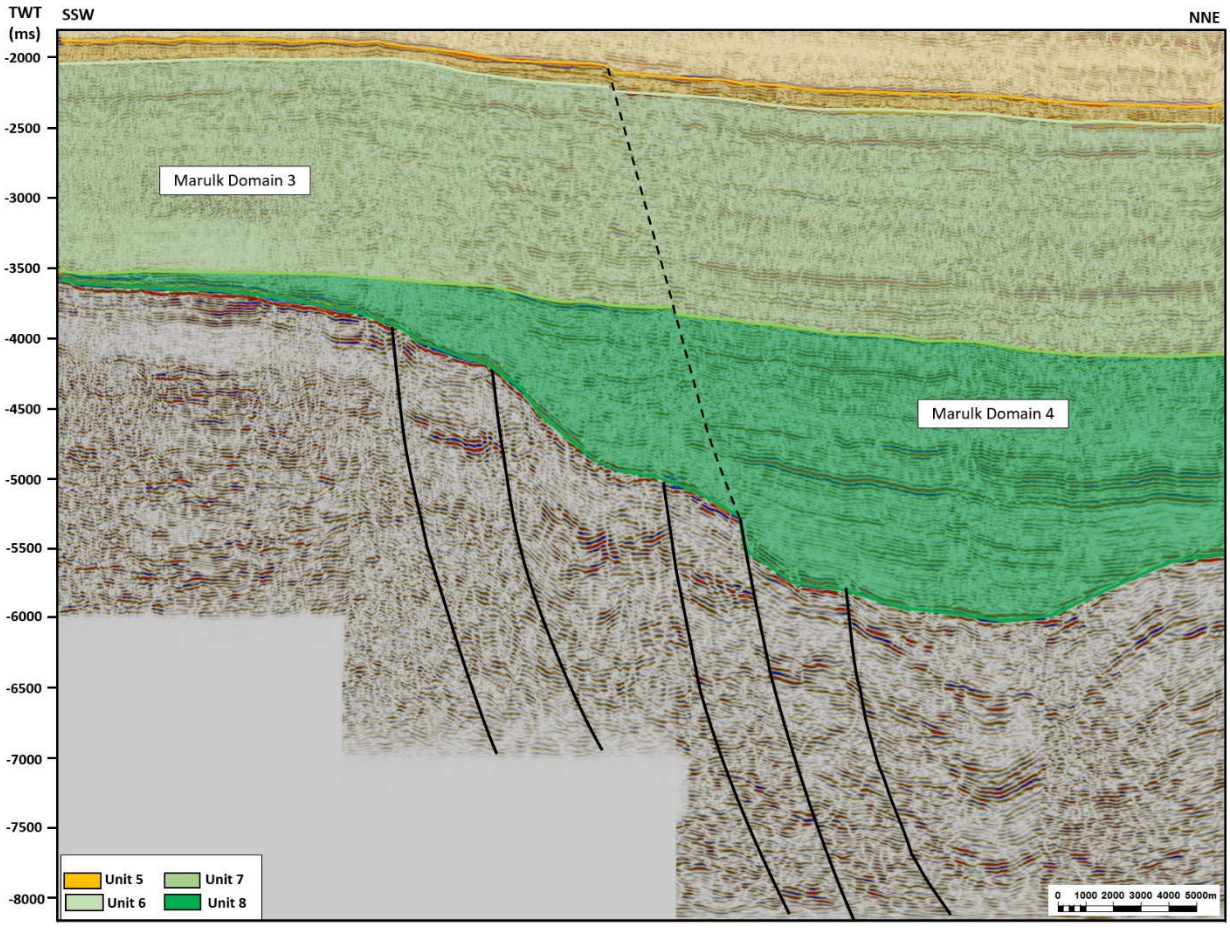

Figure 35: SSW-NNW seismic transect displaying the transition from the Central Domain 3 of the Marulk Basin, down to the deep northern basin of Domain 4. Location of the seismic line is indicated in Figure 24.

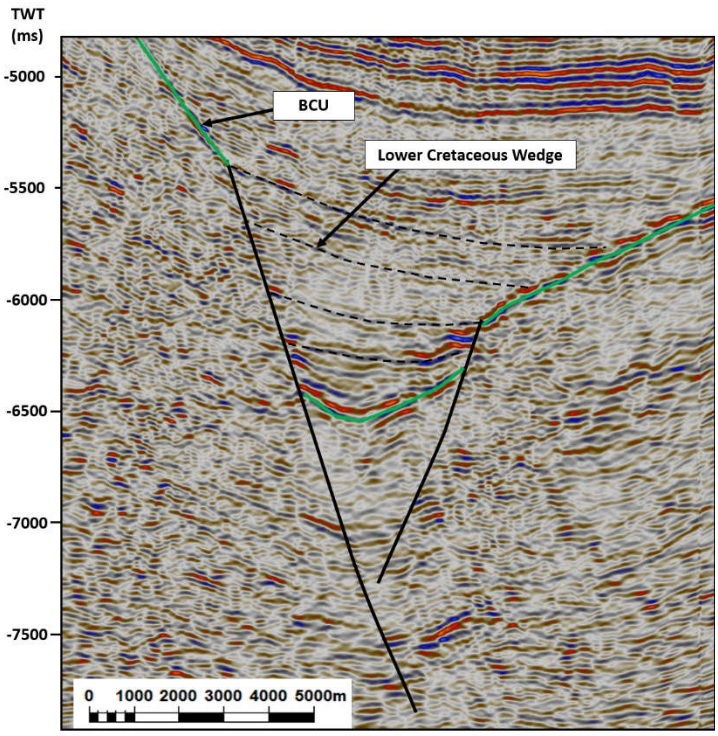

Figure 36: Lower Cretaceous sedimentary wedge in hanging wall of the Magnus North Fault. Location of the seismic line is indicated in Figure 24.

4.4 Structural evolution

The following chapter describes the general thickness trends within the area of interest as indicated by the isochron maps to identify the temporal variability in accommodation space within the study area. Isochron maps are provided for the 3D interpreted Jurassic and Cretaceous intervals (Unit 2 – Unit 6) (Figure 37). The Triassic is not described in this chapter.

4.4.1 Lower Jurassic

The Lower Jurassic isochron map represents the thickness of Unit 2 (Figure 37A). The succession is not present on the Makrell Horst and is observed to be truncated by the BCU resulting in zero thickness in the northern area of the Snorre Fault Block. The thickness displayed in the area of Mort Horst is measured from the BCU to the Intra Mort Fault plane, representing the combined thickness of the successions preserved within the fault blocks detaching along the Intra Mort Fault. In the hanging wall of the Mort West Fault, thickness is measured from the downthrown Intra Mort Fault to the Near Top Heather reflector, explaining the thickness anomalies seen in this area.

A general southeastward increase in thickness is observed for the Lower Jurassic succession, with largest accumulation within the hanging wall of the Snorre Fault. Within the southern and central areas of the Marulk Basin, the thickness is uniform. On the Penguin Ridge, the thickness is larger in the central and northern areas towards the East Penguin Fault, decreasing towards the footwall highs of the Penguin Ridge 1 and Penguin Ridge 2 faults.

4.4.2 Middle Jurassic – Upper Jurassic

The Middle to Upper Jurassic interval is represented by the thickness of Unit 3 (Figure 37B). As with Unit 2, this interval is absent on the Makrell Horst and the northern end of the Snorre Fault block. In addition, thickness below resolution is recorded in the crestal and southwestern areas of the Penguin Ridge. The area of the Mort Horst is highlighted with interrogation marks. This is because in this area, the interval is encountered within the fault blocks detaching along the Intra Mort Fault, such that determining thickness would requires detailed interpretation of each individual sliding block. Similarly, there is high uncertainty regarding what is preserved above the Intra Mort Fault in the downthrown hanging wall block of Mort West Fault, as explained in section 4.3.2.

Elsewhere, Unit 3 shows variation in thickness. The largest accumulation is documented in the hanging walls at the northern end of the Snorre Fault and the southern end of the Mort East Fault. Within the Marulk Basin, slightly increased thickness is observed towards the Marulk South Fault and Penguin Ridge 1 Fault in the southern end of the basin (Domain 1), towards the Penguin Ridge 2 Fault, and in the graben area in the central part of the basin (Domain 3). This defines a general southeastward thinning within the Marulk Basin. Unit 3 is present within the central and southern areas of the Penguin Ridge. Elsewhere it is truncated by the Near Top Heather Reflector and/or the BCU, as explained in section 4.3.4

4.4.3 Upper Jurassic – Lower Cretaceous

The Upper Jurassic to Lower Cretaceous isochron map represents the thickness of Unit 4 (Figure 37C). Based on observed trends within the area, Unit 4 can be divided into three different areas: (1) areas of zero thickness or thickness below seismic resolution , (2) areas with significant increase in thickness, and (3) areas where a thin layer is present with thickness <100 ms.

Areas with Class 1 are mainly related to the structural highs including Makrell Horst, Mort Horst and the Snorre Fault Block. In addition, zero thickness is observed in the elevated southeastern end of the Penguin Ridge. Class 2 is observed as thickness increase in the hanging wall block of major faults, defining wedge-geometries. This is most prominent in the Pancake Basin with increased thickness towards the Snorre Fault and the Mort East Fault, but also clearly defined towards the Penguin Ridge 2 and the Western Snorre 2 faults. In addition, increased thickness is observed in the graben area of the Marulk Basin (Domain 3), in the Penguin Half-Graben, and towards the Penguin Ridge 1 and Marulk South faults in the southern end of the Marulk Basin (Domain 1). Class 3 is observed in the hanging wall of the West Penguin Fault, on the Penguin Ridge, and in in the central area of Marulk basin between the Beta Ridge (Domain 2) and the graben area (Domain 3).

4.4.4 Lower Cretaceous

The Lower Cretaceous succession is defined between the BCU and the Top Cromer Knoll marker horizons (Figure 37D). As previously described, a thin layer of the upper Cromer Knoll Group is recognized above the structural highs but with thickness below seismic resolution. This is the case in the areas with a constant red colour. Lower Cretaceous thickness has developed mainly within the Viking Graben, Pancake Basin, Marulk Basin and Magnus Basin, with thickest accumulation in the northern area of the Marulk Basin (Domain 4).

An overall southwestward thinning of the Cromer Knoll Group is evident within the Marulk Basin. In Domain 1, the thickness of this unit is controlled by the Penguin Ridge 1 and Marulk South faults marking the southern boundaries of the Penguin Ridge, where significant thinning is seen. Within Domain 3, increased thickness is recognized in the graben area and towards the Penguin Ridge 2 Fault. In the north, the major thickness variation is controlled by the Marulk North Fault, defining a deep early Cretaceous basin with thick accumulation of the Cromer Knoll Group. The thickness of this unit within the Pancake Basin is generally low compared to the Marulk Basin and the Viking Graben.

4.4.5 Upper Cretaceous

The Upper Cretaceous isochron map is defined by the Top Cromer Knoll and Top Shetland horizons (Figure 37E), which show a general N to NW increase in thickness. Significant thinning is evident above the Makrell Horst and Mort Horst, in addition to the Snorre, Gullfaks and Visund fault blocks.

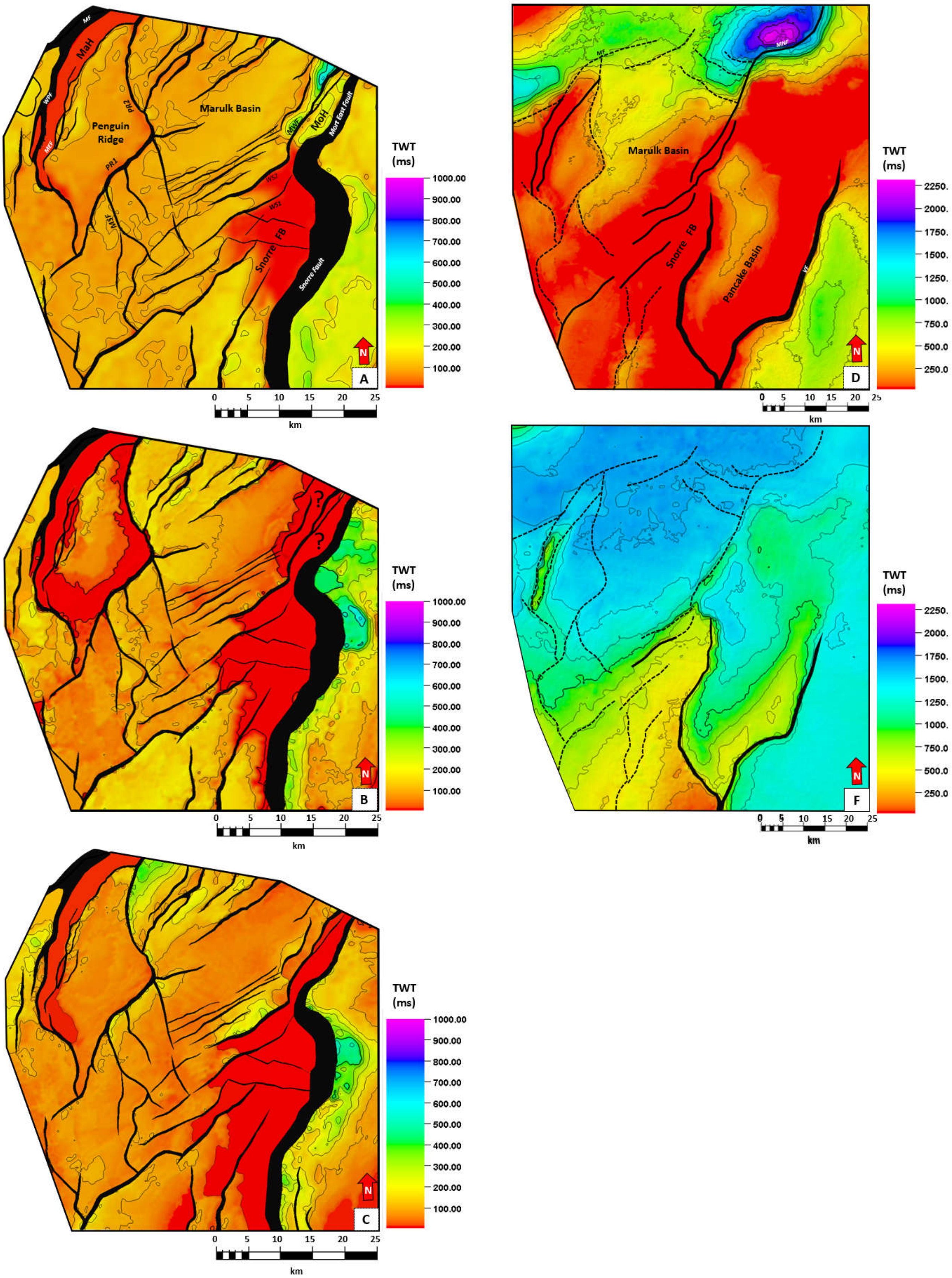

Figure 37: Isochron maps of (A) Lower Jurassic Unit 2, (B) Middle-Upper Jurassic Unit 3, (C) Upper Jurassic to Lower Cretaceous Unit 4, (D) Lower Cretaceous Unit 5 and Upper Cretaceous Unit 6. The pre-Cretaceous isochron maps have the same time thickness scale and same contour interval of 100 ms, and the Cretaceous isochrone maps have the same time thickness scale and contour interval of 200 ms.

6. Discussion

The focus of this study, as introduced in chapter 1, is to assess the structural evolution of the Marulk Basin and adjacent highs, and how this evolution relates to the general rift evolution of the Northern North Sea. The study aims to accomplish this by incorporating 3D seismic interpretation and interpretation of individual 2D lines with publications and established models of the adjacent areas. In the following section, the results and observations will be discussed with focus on how the Marulk Basin relates to the rift evolution of the Northern North Sea (section 6.1), and the evolution of fault systems and structural elements (section 6.2).

6.1 Rift Evolution

Within the northern North Sea the Permo-Triassic rift basin is generally recognized to have developed under an E-W extensional regime, with mainly S-N trending faults (Badley et al., 1988; Færseth, 1996). This is in contrasts to the Permo-Triassic evolution of the Møre Margin, which is defined by a NW-SE extensional regime (Gabrielsen et al., 1999). During the middle Jurassic – early Cretaceous rifting event, the northern North Sea and the Møre Margin were affected by NW-SE extension, although with significant difference in timing (Færseth, 1996; Gabrielsen et al., 1999). Jurassic rifting is generally accepted to have ended by the early Cretaceous. In the Møre Basin, on the other hand, rifting continued episodically within the mid Cretaceous and Paleocene (Grunnaleite and Gabrielsen, 1995).

Based on the structural maps, thickness maps and interpreted cross-sections (e.g. Figure 13; Figure 14; Figure 15; Figure 37), it is clear that the structural configuration of the Marulk Basin and the adjacent highs is influenced by extensional events of different timing and orientation. The trend of the northern and central part of the Marulk Basin and the Magnus Basin coincides with the trend recognized for the Møre-Trøndelag Fault Complex and the axis of the Møre Basin. This suggests that these basins were developed within the same NW-SE extensional regime. The Viking Graben and Pancake Basin, on the other hand, show structural trends more similar to the Sogn Graben, which coincide with the E-W extensional regime accounting for the Permo-Triassic rift event, with later Jurassic fault reactivation (Figure 38). The resultant northwesterly change in orientation of basins and intrabasinal highs suggests a differentiation between structures of Permo-Triassic origin, and basins developed mainly as a result of the late Jurassic extension. Suggesting that the Magnus and Marulk basins originate from Permo-

Triassic extension implies that these basins developed as an extension of the Møre Margin. However, it is clear that the Marulk Basin is located in a marginal position to what is normally differentiated as the North-Sea rift system and the Mid-Norwegian rift system, suggesting a complex structural setting.

The general trend as represented by the thickness maps shows a northwestward shift in accommodation space from early Jurassic to late Cretaceous. Thickness variations suggest that the Pancake Basin had established as a depocenter already in the early Jurassic and continued to be a main depocenter for sediment accumulation throughout the Jurassic. The Marulk Basin shows a different evolution with the development of local depocenters within individual fault blocks from the middle Jurassic, accelerating into late Jurassic. However, the central and southern segments of the basin did not develop as a part of the greater Marulk Basin until the early Cretaceous (Figure 37D). At this time, the Marulk Basin replaced the Pancake Basin and northern Viking Graben as the major depocenter. Thus, looking at the Jurassic and Cretaceous development of the northern Viking Graben and the Møre Basin as a whole, it can be argued that the Marulk Basin acts as a step in a progressive northwestward development of the rift system.

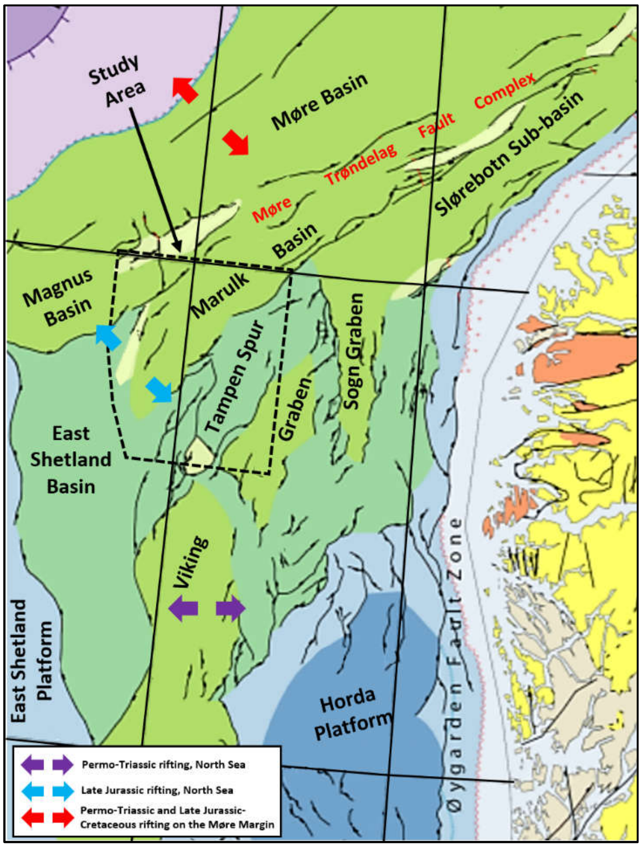

Figure 38: Marulk Basin is located at a marginal position to both the North Sea Rift System the Møre Margin. Modified from Brekke et.al (2008).

6.2 Structural Evolution

6.2.1 Triassic

A complete assessment of the Triassic basin evolution is outside the scope of this thesis, primarily due to the lack of high quality deep seismic data and deeply penetrating wells within the basinal areas. Interpretation of the 2D seismic lines provides some information of the Triassic rift basin configuration within the study area but this is limited to the upper part of the Triassic succession.

The general eastward increase in thickness of the Middle to Upper Triassic successions (Unit 0 and Unit 1) as seen within the Snorre Fault Block (Figure 25), indicates eastward increase in accommodation space during deposition. This may imply activity along faults during the Triassic, effecting the sediment accumulation in the Snorre Fault Block area. Similar observations are reported by Dahl and Solli (1993), who interpret increased thickness towards west-dipping Permo-Triassic faults trending N-S within the Snorre Fault Block. Furthermore, the Penguin Ridge 1 Fault is observed to control the thickness of the Middle to Upper Triassic successions based on the thickness decrease of these units from the southern Marulk Basin into the Penguin Ridge (Figure 14). Thickness variation combined with interpretation of upward decrease in displacement, suggests that offset on the Penguin Ridge 1 Fault was established already during the Permo-Triassic rift phase, with continued subsidence throughout the Triassic. In the central area of the Marulk Basin (Domain 3), on the other hand, the Middle to Upper Triassic successions (Unit 0 and Unit 1) are equally thick from the Makrell Horst in the west to the Mort Horst in the east, providing no evidence of Triassic fault activity (Figure 14). Thus, evidence of Triassic fault activity is limited to the southern end of the Marulk Basin.

Periods of increased subsidence during middle Triassic to early Jurassic constitute control on megasequence development in the northern North Sea (Steel, 1993) and differential subsidence across Permo-Triassic rift structures is recognized during this time (Steel and Ryseth, 1990). In addition, local development of syn-rift geometries and fault block rotation points towards minor phases of renewed extension, and thus, Ravnås et al. (2000) refer to this period as an inter-rift stage rather than post-rift basin development. The interpreted trend of the Middle to Upper Triassic successions within the study area may therefore indicate that the southern Marulk Basin and the Tampen Spur are more proximal to the Permo-Triassic rift basin, compared to the central and northern areas of the Marulk Basin.

Increased thickness of the Lower Jurassic Unit 2 is evident within the Pancake Basin, although more pronounced in the hanging wall of the Snorre Fault compared to the Mort East Fault. This may result from early onset of the late Jurassic rifting phase or movement along older fault systems. The latter assumes a Permo-Triassic origin of the Snorre Fault and Mort East Fault, with continued subsidence throughout the Triassic and early Jurassic periods. A Permo-Triassic origin of the Snorre Fault and Mort East Fault is supported by observed trends and magnitude of the fault displacement.

The Makrell Horst is generally accepted as a Triassic structural high (Domínguez, 2007; Thomas and Coward, 1995). This partly coincides with the observations of this study. The easterly dip of the Triassic reflectors within the Makrell Horst may have two explanations: (1) Faulting along the West Penguin Fault and East Penguin Fault occurred simultaneously to define the horst, with later eastward tilting, (2) The West Penguin Fault developed offset during the Permo-Triassic rifting, defining an easterly tilted fault block, which were later cut by the East Penguin Fault to define the present horst structure. Observations in this study points towards the latter. This is supported by (i) the significant difference in offset between the West Penguin Fault and the East Penguin Fault, and (ii) similar thickness of the intra-Triassic successions on the Penguin Ridge and the Makrell Horst.

Permo-Triassic rifting is documented by syn-rift wedge geometries within the Magnus Basin (Christiansson et al., 2000). The trend of the Magnus Fault differs from the N-S trend generally recognized for the Permo-Triassic rifting within the North Sea. If the Magnus Fault has a Triassic origin, the Triassic evolution of the Magnus Basin must be seen in context with the Møre Basin, with NW-SE extension direction during Permo-Triassic rifting (Gabrielsen et al., 1999). However, the age of the Magnus Fault within the area of interest is hard to determine due to poor control on the Triassic succession within the Magnus Basin.

6.2.2 Jurassic

In general, the Lower Jurassic succession (Unit 2) belongs to the inter-rift stage of relative tectonic quiescence. The thickness trends within this succession are mainly the result of large-scale depositional trends and differential subsidence. Local variations can also be due to erosion or minor fault movements along Permo-Triassic faults. The general southeastward thickening of this unit may be related to proximity to the Permo-Triassic rift basin (Figure

37A). As previously discussed, the Upper Triassic successions shows an eastward increase in thickness within the Snorre Fault Block, while further north no such trends are observed. The trend recognized for Unit 2 may be related to the same mechanisms, reflecting subsidence across older fault systems in the southeast. The thickness of Unit 2 within the central and southern Marulk Basin gives little indication of fault activity during this period. Increased thickness is seen towards the East Penguin Fault within the Penguin Half-Graben. The observed thickening is more an effect of thinning towards the footwall crest of Penguin Ridge 1 and Penguin Ridge 2 faults, due to later erosion.

The NNW-SSE trend defined for the Penguin Ridge 2 Fault, can be traced through the Marulk Basin and Snorre Fault Block, is similar to the trend recognized at the southern termination of the Snorre Fault, defining the northern boundary of the Gullfaks Fault Block (Figure 11). This trend also coincides with the ENE dipping faults within the southern domain of the Marulk Basin (Domain 1) (Figure 32). The origin of these faults is uncertain, but structural maps, thickness maps and interpreted seismic sections indicate activity during deposition of Unit 3 and Unit 4. This is most evident with development of syn-rift geometries along the Penguin Ridge 2 Fault (Figure 13; Figure 22) and slight thickening towards the Marulk South Fault (Figure 32; Figure 37). The cause of this fault trend is not clear, but some possibilities can be presented: (1) the NNW-SSE fault trend is a result of inherited structural grain, (2) the trend may represent an oblique shear component of the main extensional direction, or (3) the trend represents cross-faults between major fault systems.

Precambrian NNW-SSE to subordinate NW-SE structural grains are recognized beneath the northern Viking Graben (Gabrielsen et al., 1999). Domínguez (2007) suggest that the major change in structural trend at the southern end of the Makrell Horst (the NW-SE trending Penguin Lineament) resulted from a basement lineament possibly inherited from a Caledonian basements shear zone. Thus, it is possible that the NNW-SSE to NW-SE fault trends are inherited from deeper structural heterogeneities. A NW-SE fault trend is also recognized in the terrace leading down to the northern domain of the Marulk Basin (Domain 4) (Figure 11; Figure 35). These faults may either act as the southwestward continuation of the Magnus North Fault, link faults in the overlap zone between the Mort West Fault and the Magnus Fault, or a combination of these two possibilities. This is however uncertain and requires further investigation.

Snorre Fault Block

Fault movement along the Snorre Fault and the Mort East Fault reached maximum activity during the late Jurassic to earliest Cretaceous rift phase as indicated by the thickness maps, showing increased thickness and growth geometries for both Unit 3 and Unit 4 (Figure 37). The interpreted link between the Snorre Fault and the Mort East Fault resembles a breached relay ramp (Figure 16). Berger and Roberts (1999) suggested a hard link transfer zone between the synthetic approaching faults, arguing that the two major faults do not overlap. This thesis provides evidence that a zone of overlap between the Mort East Fault and the Snorre Fault does exist, linked by WNW-ESE cross fault. The interpreted pattern of breaching may be a combination of tip breach with propagation of the hanging wall fault (Mort East Fault) and mid-ramp breach with secondary link faults (Childs et al., 1995; Fossen and Rotevatn, 2016). Thus, it is possible that the synthetic overlapping Snorre Fault and Mort East Fault defined a relay ramp following the Permo-Triassic rifting phase, with final breaching during the Jurassic rifting. However, fully understanding of this would require detailed reconstruction of the overlapping fault zone.

Uplift and rotation of the Snorre Fault Block is assumed to occur during the middle to late Jurassic extensional phase, and modelling suggests erosion of up to 1500 meters of Jurassic and uppermost Triassic rocks (Berger and Roberts, 1999; Dahl and Solli, 1993). Fault activity on the westernmost part of the Snorre Fault Block (WS1 and WS2) is associated with fault growth only within Unit 4 (Figure 25; Figure 37), indicating younger age of the western margin compared to the eastern margin of the Snorre Fault Block. No evidence of Triassic activity along the Western Snorre Fault Zone is found in this study, and a late Jurassic origin of the Western Snorre Fault Zone coincides with the observed NE-SW fault trend, defined by the NW-SE extensional regime of the late Jurassic rifting phase. The westerly tilt of the Snorre Fault Block is observed westward into the Marulk Basin, suggesting that the Snorre Fault Block initially extended westward, and were later cut by the Western Snorre Fault zone separating the fault block from the Marulk Basin.

Makrell Horst and Penguin Ridge

Jurassic activity along the West Penguin Fault was initiated during deposition of Unit 3 (Figure 39C), supported by the pronounced thickening and wedge development of Unit 3 within the Penguin Half-Graben (Figure 29). The Intra-Rannoch reflector truncate against the Near Top Heather reflector on the Penguin Ridge (Figure 30) suggesting that the Penguin Ridge was subaerially exposed and eroded during the initial stage of Unit 4 deposition (late Oxfordian – early Cretaceous). These interpretations imply increased offset along the West Penguin Fault from the late Oxfordian leading to block tilting, subaerial exposure and erosion at the initial stage of Unit 4 deposition (Figure 39D). The large westerly tilted fault block was later faulted by the East Penguin Fault to separate the Makrell Horst from the Penguin Ridge (Figure 39E).

Fault block evolution with late Jurassic footwall uplift and rotation is common on the Tampen Spur, primarily seen on westerly tilting fault blocks. The cause of uplift is a subject of debate and several models try to explain this phenomenon. These include rigid body models (domino models) (Jackson and McKenzie, 1983; Yielding and Roberts, 1992), and flexural/isostatic models (Kusznir et al., 1991; Yielding and Roberts, 1992). On Tampen Spur and in the northern North Sea in general, significant effort is put into understanding the relationship between footwall uplift, tilting and erosion, in order to predict syn-rift deposition (Færseth et al., 1995; Nøttvedt et al., 2000; Ravnås et al., 2000). It is possible that the Makrell Horst experienced a similar evolution to other fault blocks on the Tampen Spur, but it was later cut by the East Penguin Fault to define a horst structure, and thus, differ from the more common structural style of westerly rotated fault blocks. A similar evolution can be applied to the Mort Horst, as will be further discussed.

The sub-parallel internal reflectors in the northern area of the Makrell Horst (Figure 22), contrast greatly to the eastward dip described farther south, indicating a difference in the evolution of the Makrell Horst along strike. A possible explanation could be that the northern part of the Makrell Horst developed at a later stage with contemporaneous faulting of the East Penguin Fault and the Magnus Fault. However, in the northernmost 2D line across Makrell Horst Jurassic fault activity on both the Magnus Fault and the Penguin Ridge 2 Fault is proven by the presence of upper Jurassic syn-rift wedges (Figure 22). Thus, the northern end of the Makrell Horst was defined at the onset of the Cretaceous, contrasting to the mid-Cretaceous evolution of this region suggested by Grunnaleite and Gabrielsen (1995).

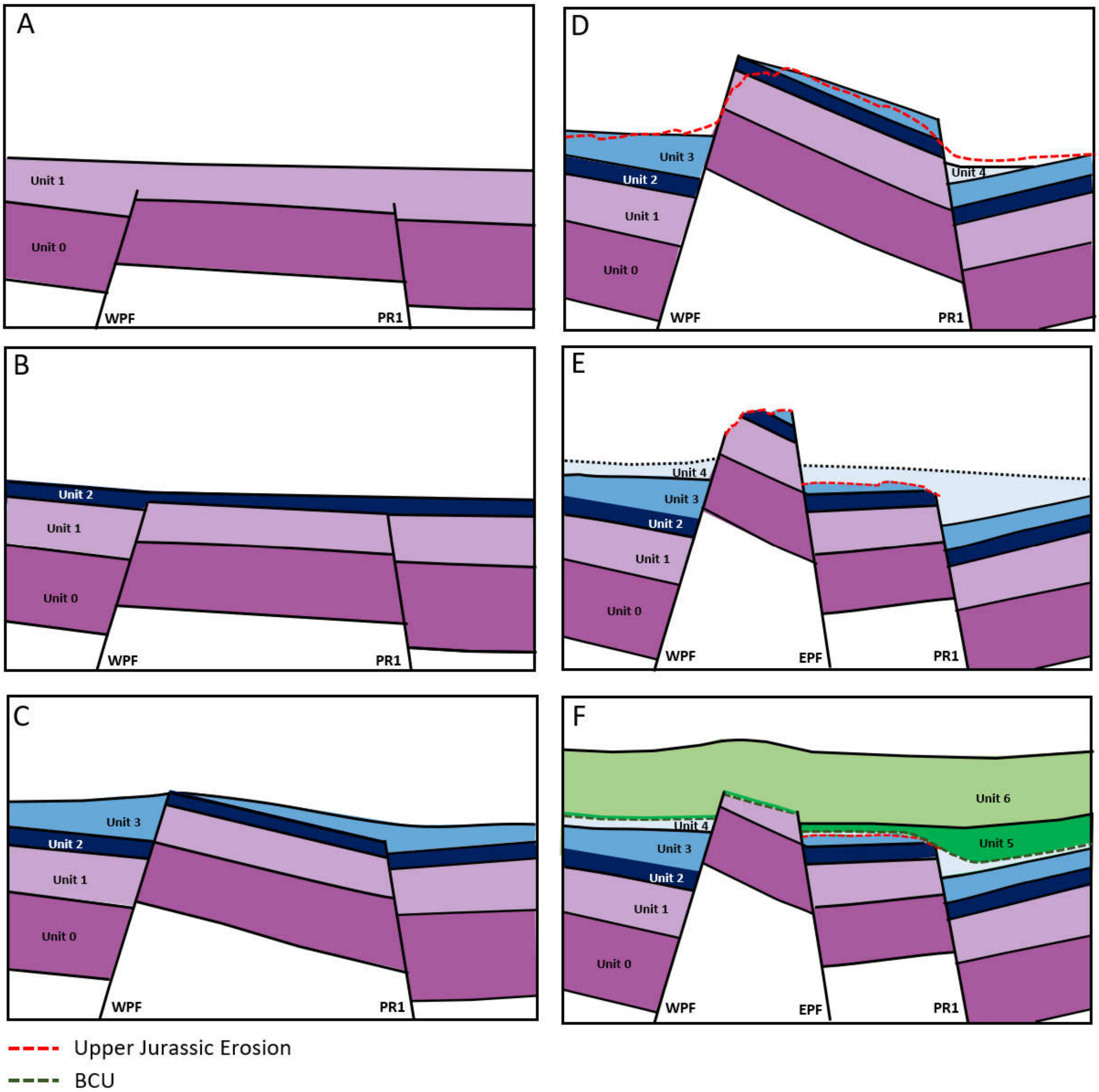

Figure 39: Conceptual model of the middle to late Triassic and Jurassic evolution in the southern end of the Makrell Horst.

Mort Horst

The deformation described within the Mort Horst is similar to gravitational collapse structures as described in footwall blocks to the main boundary faults of several fields within the Tampen Spur area (Figure 40) (Coutts et al., 1996; Hesthammer and Fossen, 1999). The reason for slope failure may be attributed to different causes such as rapid sedimentation, slope steepening, pore-pressure and/or seismic shocks (Hesthammer and Fossen, 1999). The observations in this thesis indicate that the Mort Horst and the area to the west were part of the same sub-aerially exposed fault block at onset of activity along the Intra Mort Fault. This suggests that significant amounts of offset had taken place along the Mort East Fault with accommodation rates exceeding the sedimentation rates, causing movement along the Intra Mort Fault, similar to the evolution of the eastern crest of the Statfjord Fault Block (Figure 40). Subsequent to the development of the Intra Mort Fault, the Mort West Fault became active as indicated by the presence of Intra Mort Fault in the downfaulted hanging wall block (Figure 26; Figure 27).

The Mort East Fault thus predates the Mort West Fault, which is supported by i) the thick accumulation of Unit 3 and 4 in the Pancake Basin compared to the thin development of this unit in the Marulk Basin, ii) truncation of Unit 3 reflectors against the Near Top Heather reflector suggesting late Jurassic erosion similar to the previously discussed evolution on the Penguin Ridge (Figure 39), iii) the relative truncation of the Mort East Fault by a younger fault system related to the Mort West Fault marking the northern end of the Mort Horst (Figure 18). Berger and Roberts (1999) suggest accelerating activity on the Mort East Fault (their Inner Snorre Fault) during late Oxfordian – early Kimmeridgian with subsequent faulting on the Mort West Fault during Kimmeridgian/Tithonian times. This coincides broadly with the observations in this study. Seismic interpretation in this study suggests that fault activity along the Mort East Fault ended before the Mort West Fault where faulting continued in the early Cretaceous.

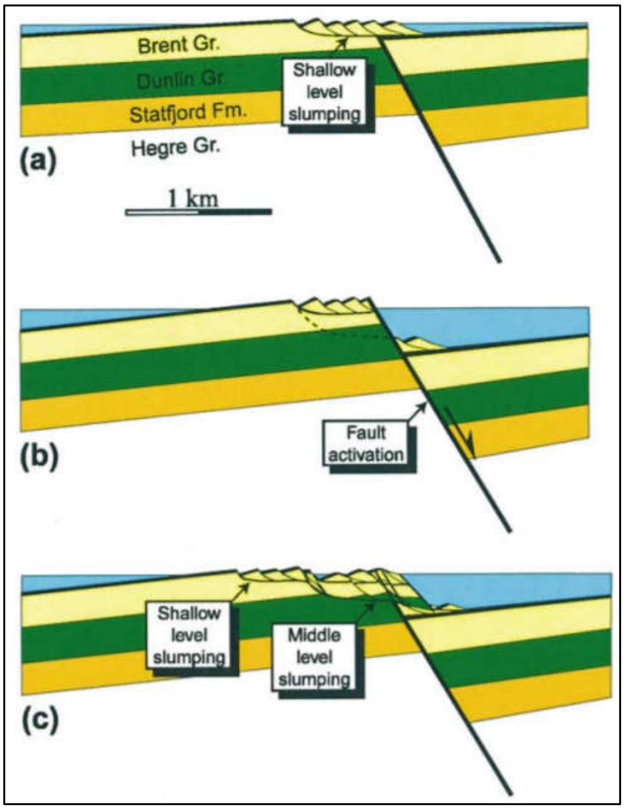

Figure 40: Early evolution of gravitational slide complex at the eastern crest of the Statfjord Fault Block. Modified from Hesthammer and Fossen (1999).

Fault Families

The faults within the study area can be subdivided into four main fault families (Figure 41). Fault family 1 represents NE and NNE trending faults formed mainly during deposition of Unit 4 (late Oxfordian – early Cretaceous). Fault family 2 represents Jurassic faults of NE to NNE trends with fault movement initiated during Unit 3 deposition (~ Bajocian – early Oxfordian). Fault Family 1 and 2 are likely related to the two main rift stages generally recognized for the middle Jurassic to early Cretaceous rifting phase, namely the middle Bathonian – early Oxfordian rift stage and the late Oxfordian – early Cretaceous rift stage (Nøttvedt et al., 2000). Fault family 3 represents faults trending NNW-SSE, possibly originating from basement heterogeneities. Finally, fault family 4 represents faults of Triassic origin, reactivated during the Jurassic rifting phase. This interpretation suggests that fault family 1 dominates in the northern areas, while fault family 2 and 3 are more common in the south. This coincide with the trend observed on the thickness map, suggesting that the Marulk Basin is developed at a later stage (~late Oxfordian – early Cretaceous) compared to the Viking Graben and the adjacent Pancake Basin.

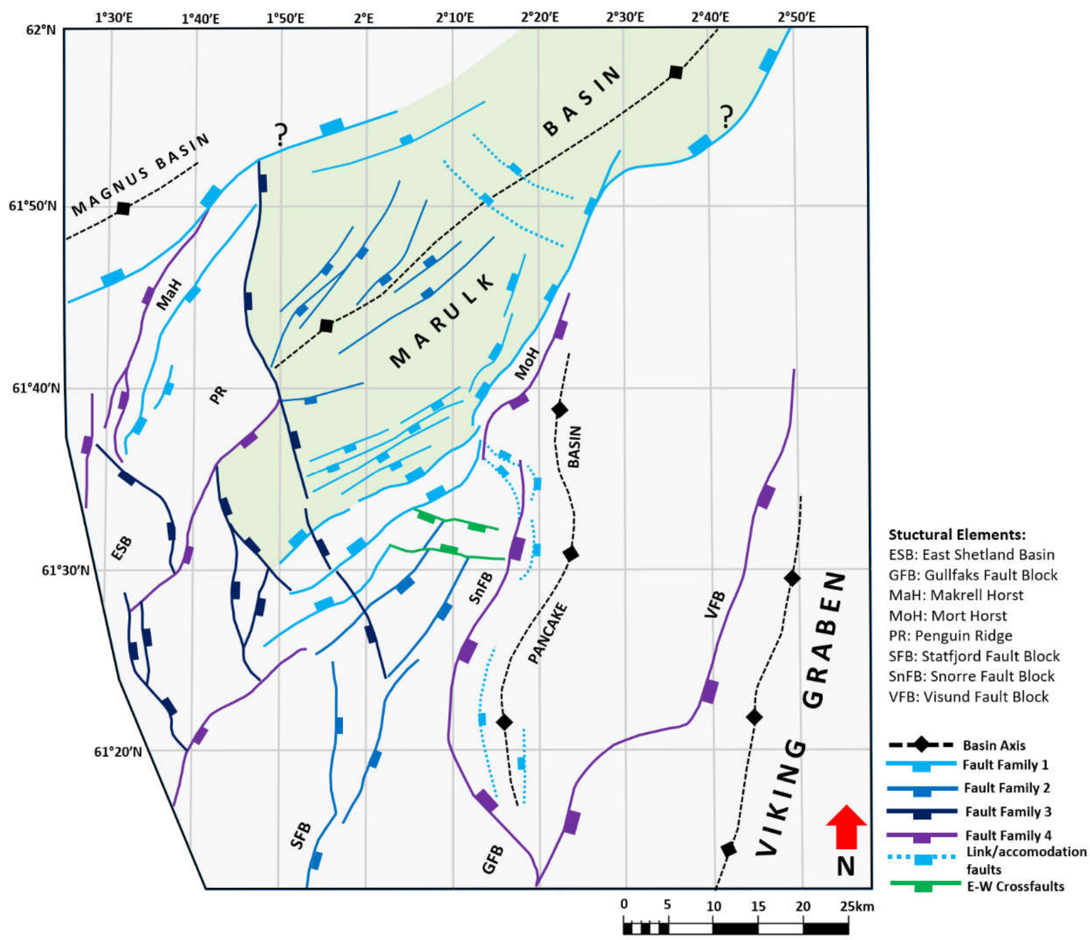

Figure 41: Suggested subdivision of fault families within the study area.

6.2.3 Cretaceous

Extension within the Møre Basin continued into Cretaceous times, which is supported by the presence of syn-rift geometries towards the NE-SW trending faults of the Møre-Trøndelag fault complex (Grunnaleite and Gabrielsen, 1995). Similarly, the Lower Cretaceous sedimentary wedge that developed within the hanging wall of the Marulk North Fault shows indications of syn-rift growth geometry (Figure 36). Thus, activity along the Marulk North Fault is likely to have continued into early Cretaceous times. Similar growth geometries within the Lower Cretaceous successions are not recognized within the central and southern end of the Marulk Basin, neither in the Pancake Basin. Rather, progressive onlap of the Lower Cretaceous Cromer Knoll Group is defined within these areas.

As recorded from the Snorre Fault Block, Makrell Horst and Mort Horst, a thin layer of the uppermost Cromer Knoll Group covers the structural highs, indicating flooding of these structures during early Cretaceous times (Figure 41B). Offset of the Top Cromer Knoll Group indicates reactivation of faults at the boundary between the Lower and Upper Cretaceous successions (Figure 41C). The cause of fault reactivation is uncertain. Dahl and Solli (1993) suggests that continued movement along faults is the results of differential compaction within the Cretaceous basins. However, fault reactivation is evident along several of the major faults within the area, including West Penguin Fault, East Penguin Fault, the Western Snorre Fault Zone, the Snorre Fault and the Mort West Fault, suggesting a more regional reactivation pattern. Thus, a minor phase of renewed extension may be suggested, possibly related to the continued extension recorded in the Møre Margin.

The late Cretaceous evolution of the horst structures can be discussed by identifying thickness variations above the horst. Decrease in layer thickness can either result from differential loading in the adjacent basins or tectonic uplift of the horst structure itself. The late Cretaceous evolution of the Mort Horst is suggested by a conceptual model (Figure 41). Decrease in thickness is interpreted within all successions above the horst, into Paleocene times (Figure 27 and 41). A mechanism causing this continuity in layer-thinning above the horst may be differential loading. For the Makrell Horst, the layer immediately above the horst show equal thickness to the sides and above the horst, possibly indicating a period of inactivity with neither differential subsidence nor tectonic uplift (Figure 31). However, layer thinning is evident in the upper interval of the Upper Cretaceous succession, suggesting onset of differential loading or tectonic uplift at a later stage in the late Cretaceous evolution of the Makrell Horst. The cause of layer thinning remains subject for debate, and better understanding of the Cretaceous evolution of the Mort Horst and Makrell Horst may be achieved by performing structural restoration.

Minor reverse movements along faults within the Beta Ridge during the early Cretaceous is suggested to account for the anomalous relief seen on the BCU and Top Cromer Knoll horizons within this area (Figure 31). Compressional features are commonly described within the Tampen Spur and East Shetland Basin (Booth et al., 1992; Dahl and Solli, 1993; Domínguez, 2007; Hesthammer et al., 1999; Thomas and Coward, 1995). However, no regional indication of early Cretaceous basin inversion is indicated by this study, suggesting that the compressional feature as recorded from the Beta Ridge is only local. Finally, fault reactivation post-dating Cretaceous is evident with offset on the Top Shetland Reflector. This is observed on the Snorre Fault (Figure 14), the Western Snorre 2 Fault (Figure 20B), and the Marulk North Fault (Figure 35). Based on the described and discussed observation it is evident that the Cretaceous evolution is complex. To further improve understanding of the Cretaceous evolution, detailed analysis of this succession is required

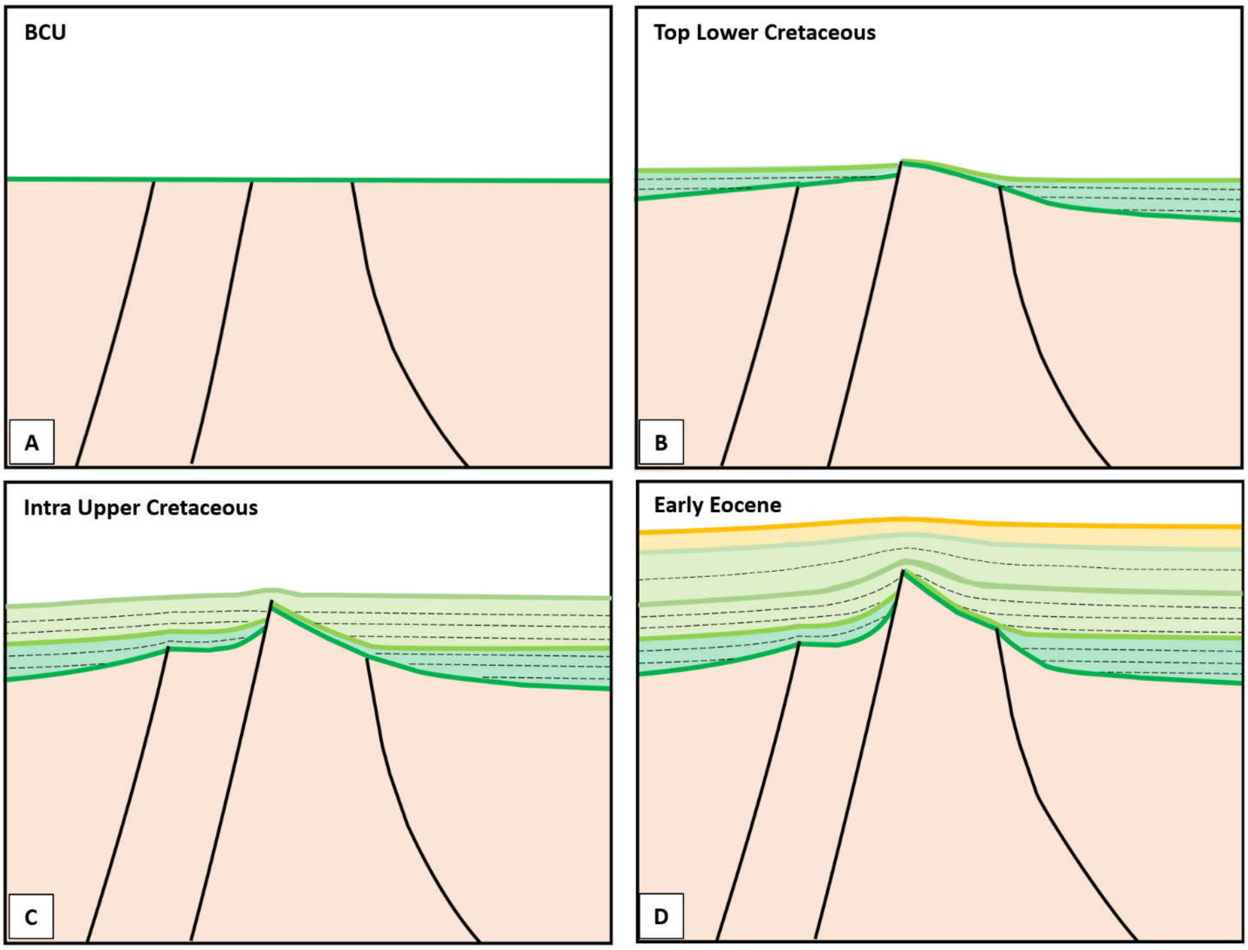

Figure 42: Conceptual model suggesting the Cretaceous evolution of the Mort Horst.

7. Conclusion

The Marulk Basin is located at a marginal position to both the North-Sea rift system and the Møre Margin, resulting in a complex structural picture. The structural evolution of the Marulk Basin and adjacent highs can be divided into two main tectonic events: (1) The Permo-Triassic extensional event and (2) the middle Jurassic-early Cretaceous extensional event. The latter can be further subdivided into two stages based on observed fault activity: (1) The middle Bathonian to early Oxfordian rift stage and (2) late Oxfordian – early Cretaceous rift stage.

Permo-Triassic rifting affected the southern end of the Marulk Basin, western margin of the Makrell Horst and the Tampen Spur, with subsequent fault-controlled subsidence throughout late Triassic-early Jurassic times. The middle Bathonian- early Oxfordian rift stage caused reactivation along the older Permo-Triassic rift structures, movement along NNW-SSE trending normal faults, and defined new sets of NE-SW trending faults recognized by syn-rift sedimentary wedges. The late Oxfordian – early Cretaceous rift stage defined new sets of NE to NNE trending normal faults, also identified by the presence of syn-rift sedimentary wedges.

The Marulk Basin is younger than the Jurassic basins to the east. This is recognized by a northwestward shift of depocenter from the early Jurassic to early Cretaceous times. The basin-bounding faults also become progressively younger in the same direction, and the northern end of the Marulk Basin show fault activity into the early Cretaceous. This implies that the evolution of the Marulk Basin cannot be explained solely by the North Sea rift system, but must also be seen in context with the evolution of the Møre Basin.

The Snorre Fault Block, Mort Horst, Penguin Ridge and Makrell Horst are all defined by faults that show activity from Permo-Triassic times. The late Oxfordian-early Cretaceous rift stage caused footwall uplift recognised by upper Jurassic erosion. Horst and half-graben structures were then developed by subsequent onset of faulting. These structures contrast to the general structural style of rotated half-grabens within the Tampen Spur. To better understand the relation between fault timing, basin subsidence and footwall uplift, the results of this study can be further tested by performing structural restoration of key seismic sections. This would also help unravel the Cretaceous evolution of the structural highs within the study area.

8. References

Badley, M. E., Price, J. D., Rambech Dahl, C., and Agdestein, T., 1988, The structural evolution of the northern Viking Graben and its bearing upon extensional modes of basin formation: Journal of the Geological Society, v. 145, no. 3, p. 455-472.

Berger, M., and Roberts, A. M., 1999, The Zeta Structure: a footwall degradation complex formed by gravity sliding on the western margin of the Tampen Spur, Northern North Sea: Geological Society, London, Petroleum Geology Conference series, v. 5, no. 1, p. 107-116.

Booth, A., Stockley, F. J., and Robbins, J. A., 1992, Late Jurassic Structural Inversion in the North Viking Graben and East Shetland Basin, UK North Sea: Energy Exploration & Exploitation, v. 10, no. 4/5, p. 281-299.

Bukovics, C., and Ziegler, P. A., 1985, Tectonic development of the Mid-Norway continental margin: Marine and Petroleum Geology, v. 2, no. 1, p. 2-22.

Brekke, H., Williams, R.W., and Magnus., C., 2008, The Geology of the Norwegian Sea Continental Margin and Probable Similarities with the Jan Mayen Ridge (slide 5) Retrieved from: https://orkustofnun.is/media/radstefnur/Harald_Brekke_IEC_2008.pdf

Childs, C., Watterson, J., and Walsh, J. J., 1995, Fault overlap zones within developing normal fault systems: Journal of the Geological Society, v. 152, no. 3, p. 535.

Christiansson, P., Faleide, J. I., and Berge, A. M., 2000, Crustal structure in the northern North Sea: an integrated geophysical study: Geological Society, London, Special Publications, v. 167, no. 1, p. 15.

Coutts, S. D., Larsson, S. Y., and Rosman, R., 1996, Development of the slumped crestal area of the Brent reservoir, Brent Field; an integrated approach: Petroleum Geoscience, v. 2, no. 3, p. 219.

Dahl, N., and Solli, T., 1993, The structural evolution of the Snorre Field and surrounding areas: Geological Society, London, Petroleum Geology Conference series, v. 4, no. 1, p. 1159-1166.

Domínguez, R., 2007, Structural evolution of the Penguins Cluster, UK northern North Sea: Geological Society, London, Special Publications, v. 292, no. 1, p. 25.

Færseth, R. B., 1996, Interaction of Permo-Triassic and Jurassic extensional fault-blocks during the development of the northern North Sea: Journal of the Geological Society, v. 153, no. 6, p. 931-944.

Færseth, R. B., Sjøblom, T. S., Steel, R. J., Liljedahl, T., Sauar, B. E., and Tjelland, T., 1995, Tectonic controls on bathonian-volgian syn-rift successions on the visund fault block, northern north sea, *in* Steel, R. J., Felt, V. L., Johannessen, E. P., and Mathieu, C., eds., Norwegian Petroleum Society Special Publications, Volume 5, Elsevier, p. 325-346.

Fazlikhani, H., Fossen, H., Gawthorpe, R. L., Faleide, J. I., and Bell, R. E., 2017, Basement structure and its influence on the structural configuration of the northern North Sea rift: Tectonics, v. 36, no. 6, p. 1151-1177.

Fjellanger, E., Olsen, T. R., and Rubino, J. L., 1996, Sequence stratigraphy and palaeogeography of the Middle Jurassic Brent and Vestland deltaic systems, Northern North Sea: Norsk Geologisk Tidsskrift, v. 76, p. 75-106.

Fossen, H., and Rotevatn, A., 2016, Fault linkage and relay structures in extensional settings-A review: Earth-Science Reviews, v. 154, no. C, p. 14-28.

Gabrielsen, R. H., Foerseth, R., Hamar, G., and Rønnevik, H., Nomenclature of the main structural features on the Norwegian Continental Shelf north of the 62nd parallel, *in* Proceedings Petroleum Geology of the North European Margin, Dordrecht, 1984// 1984, Springer Netherlands, p. 41-60.

Gabrielsen, R. H., Odinsen, T., and Grunnaleite, I., 1999, Structuring of the Northern Viking Graben and the Møre Basin; the influence of basement structural grain, and the particular role of the Møre-Trøndelag Fault Complex: Marine and Petroleum Geology, v. 16, no. 5, p. 443-465.

Grunnaleite, I., and Gabrielsen, R. H., 1995, Structure of the Møre basin, mid-Norway continental margin: Tectonophysics, v. 252, no. 1, p. 221-251.

Helland-Hansen, W., Ashton, M., Lomo, L., and Steel, R., 1992, Advance and retreat of the Brent delta: Recent contributions to the depositional model: Geological Society, London, Special Publications, v. 61, p. 109-127.

Hesthammer, J., and Fossen, H., 1999, Evolution and geometries of gravitational collapse structures with examples from the StatfJord Field, northern North Sea: Marine and Petroleum Geology, v. 16, no. 3, p. 259-281.

Hesthammer, J., Jourdan, C., E. Nielsen, P., E. Ekern, T., and Gibbons, K. A., 1999, A tectonostratigraphic framework for the Statfjord Field, northern North Sea: Petroleum Geoscience, v. 5, no. 3, p. 241-256.

Isaksen, D., and Tonstad, K., 1989, A Revised Cretaceous and Tertiary lithostratigraphic nomenclature for the Norwegian North Sea, Volume no. 5: Stavanger, Oljedirektoratet, p. 59.

Jackson, J., and McKenzie, D., 1983, The geometrical evolution of normal fault systems: Journal of Structural Geology, v. 5, no. 5, p. 471-482.

Johannessen, E. R., Mjøs, R., Renshaw, D., Dalland, A., and Jacobsen, T., 1995, Northern limit of the “Brent delta” at the Tampen Spur —a sequence stratigraphic approach for sandstone prediction, *in* Steel, R. J., Felt, V. L., Johannessen, E. P., and Mathieu, C., eds., Norwegian Petroleum Society Special Publications, Volume 5, Elsevier, p. 213-256.

Kirk, R. H., 1980, Statfjord Field - A North Sea giant: AAPG Memoir, v. 30, p. 95-116.

Kusznir, N. J., Marsden, G., and Egan, S. S., 1991, A flexural-cantilever simple-shear/pure-shear model of continental lithosphere extension: applications to the Jeanne d'Arc Basin, Grand Banks and Viking Graben, North Sea: Geological Society, London, Special Publications, v. 56, no. 1, p. 41.

Lervik, K. S., Spencer, A. M., and Warrington, G., Outline of Triassic stratigraphy and structure in the central and northern North Sea, *in* Proceedings Correlation in Hydrocarbon Exploration, Dordrecht, 1989// 1989, Springer Netherlands, p. 173-189.

Nøttvedt, A., Gabrielsen, R. H., and Steel, R. J., 1995, Tectonostratigraphy and sedimentary architecture of rift basins, with reference to the northern North Sea: Marine and Petroleum Geology, v. 12, no. 8, p. 881-901.

Nøttvedt, A., M. Berge, A., Dawers, N., B. Faerseth, R., O. Hager, K., Mangerud, G., and Puigdefabregas, C., 2000, Syn-rift evolution and resulting play models in the Snorre-H area, northern North Sea: Geological Society, London, Special Publications, v. 167, p. 179-218.

Nybakken, S., and Bäckstrøm, S. A., Shetland Group: stratigraphic subdivision and regional correlation in the Norwegian North Sea, *in* Proceedings Correlation in Hydrocarbon Exploration, Dordrecht, 1989// 1989, Springer Netherlands, p. 253-269.

Nystuen, J. P., and Fält, L.-M., 1995, Upper Triassic-Lower Jurassic reservoir rocks in the Tampen Spur area, Norwegian North Sea, *in* Hanslien, S., ed., Norwegian Petroleum Society Special Publications, Volume 4, Elsevier, p. 135-179.

Nystuen, J. P., Knarud, R., Jorde, K., and Stanley, K. O., Correlation of Triassic to Lower Jurassic sequences, Snorre Field and adjacent areas, northern North Sea, *in* Proceedings Correlation in Hydrocarbon Exploration, Dordrecht, 1989// 1989, Springer Netherlands, p. 273-289.

Odinsen, T., Christiansson, P., Gabrielsen, R. H., Faleide, J. I., and Berge, A. M., 2000, The geometries and deep structure of the northern North Sea rift system: Geological Society, London, Special Publications, v. 167, no. 1, p. 41-57.

Ravnås, R., Nøttvedt, A., Steel, R. J., and Windelstad, J., 2000, Syn-rift sedimentary architectures in the Northern North Sea: Geological Society, London, Special Publications, v. 167, no. 1, p. 133-177.

Røe, S. L., and Steel, R., 1985, Sedimentation, Sea-Level Rise and Tectonics at the Triassic-Jurassic Boundary (statfjord Formation), Tampen Spur, Northern North Sea: Journal of Petroleum Geology, v. 8, no. 2, p. 163-186.

Sheriff, R. E., 2002, Encyclopedic Dictionary of Applied Geophysics, Fourth edition, Society of Exploration Geophysicists, Geophysical References Series, 442 p.

Steel, R., and Ryseth, A., 1990, The Triassic — early Jurassic succession in the northern North Sea: megasequence stratigraphy and intra-Triassic tectonics: Geological Society, London, Special Publications, v. 55, no. 1, p. 139-168.

Steel, R. J., 1993, Triassic–Jurassic megasequence stratigraphy in the Northern North Sea: rift to post-rift evolution: Geological Society, London, Petroleum Geology Conference series, v. 4, no. 1, p. 299.

Thomas, D. W., and Coward, M. P., 1995, Late Jurassic-Early Cretaceous inversion of the northern East Shetland Basin, northern North Sea: Geological Society, London, Special Publications, v. 88, no. 1, p. 275.

Vollset, J., and Doré, A. G., 1984, A Revised Triassic and Jurassic lithostratigraphic nomenclature for the Norwegian North Sea, NPD-bulletin, Volume no. 3: Stavanger, Oljedirektoratet, p. 52.

Wood, R., and Barton, P., 1983, Crustal thinning and subsidence in the North Sea: Nature, v. 302, p. 134-136.

Yielding, G., and Roberts, A., 1992, Footwall uplift during normal faulting - implications for structural geometries in the North Sea, *in* Larsen, R. M., Brekke, H., Larsen, B. T., and Talleraas, E., eds., Structural and Tectonic Modelling and its Application to Petroleum Geology, Volume 1: Amsterdam, Elsevier, p. 289-304.

Ziegler, P. A., 1975, Geologic Evolution of North Sea and Its Tectonic Framework: AAPG Bulletin, v. 59, p. 1073-1097.